AD-A035 735 VIRGINIA POLYTECHNIC INST AND STATE UNIV BLACKSBURG --ETC F/G 6/16
PREDICTION OF MODULATION DETECTABILITY THRESHOLDS FOR LINE-SCAN--ETC(U)
DEC 76 R L KEESEE F33615-71-C-1739

UNCLASSIFIED AMRL-TR-76-38 NL

1 OF 2
AD-A
035 735

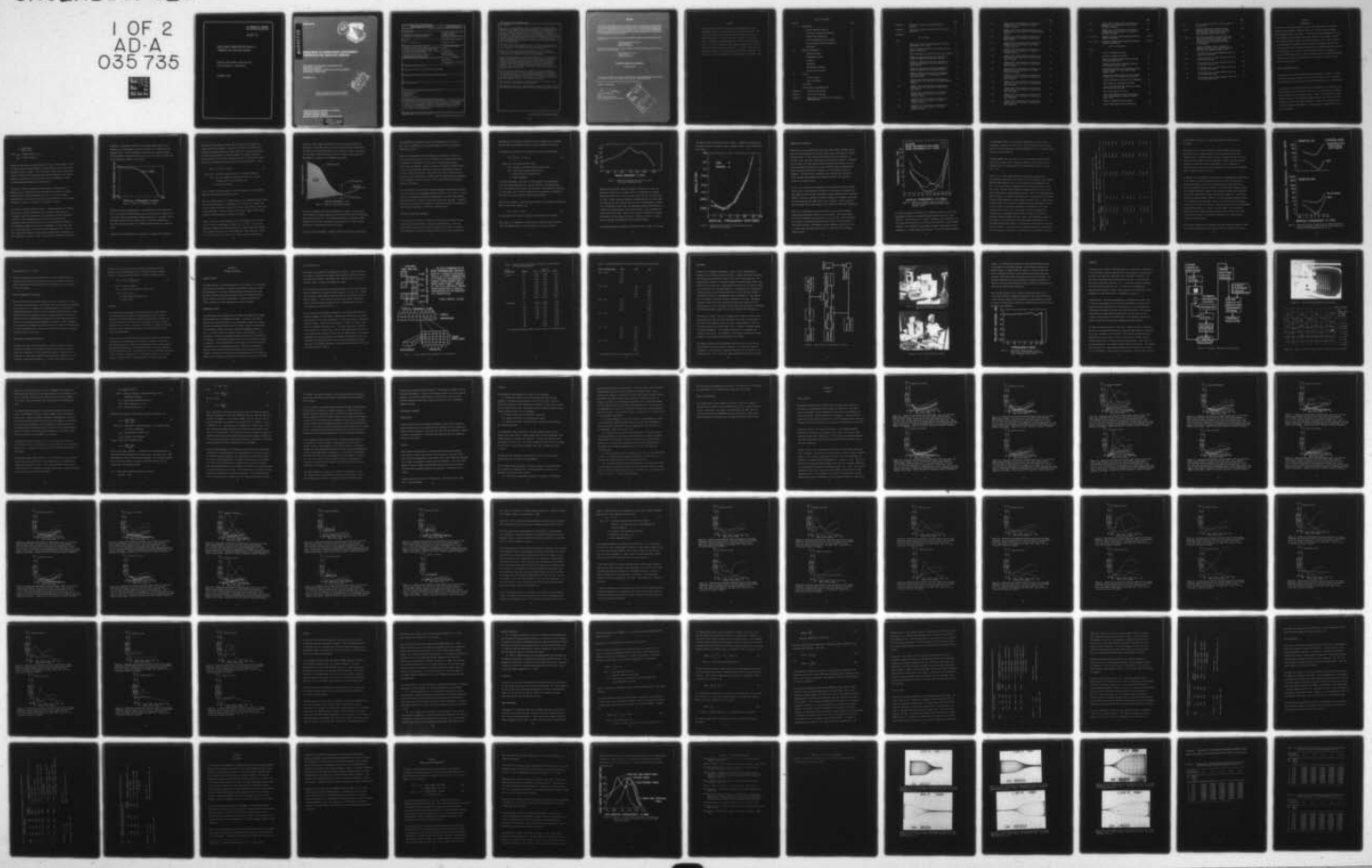

PREDICTION OF MODULATION DETECTABILITY THRESHOLDS FOR LINE-SCAN DISPLAYS

VIRGINIA POLYTECHNIC INSTITUTE AND
STATE UNIVERSITY, BLACKSBURG

DECEMBER 1976

AMRL-TR-76-38

PREDICTION OF MODULATION DETECTABILITY THRESHOLDS FOR LINE-SCAN DISPLAYS

DEPARTMENT OF INDUSTRIAL ENGINEERING AND
OPERATIONS RESEARCH
VIRGINIA POLYTECHNIC INSTITUTE AND STATE UNIVERSITY
BLACKSBURG, VIRGINIA 24061

DECEMBER 1976

AEROSPACE MEDICAL RESEARCH LABORATORY
AEROSPACE MEDICAL DIVISION
AIR FORCE SYSTEMS COMMAND
WRIGHT-PATTERSON AIR FORCE BASE, OHIO 45433

SECURITY CLASSIFICATION OF THIS PAGE *(When Data Entered)*

REPORT DOCUMENTATION PAGE		READ INSTRUCTIONS BEFORE COMPLETING FORM
1. REPORT NUMBER AMRL-TR-76-38	2. GOVT ACCESSION NO.	3. RECIPIENT'S CATALOG NUMBER
4. TITLE *(and Subtitle)* PREDICTION OF MODULATION DETECTABILITY THRESHOLDS FOR LINE-SCAN DISPLAYS		5. TYPE OF REPORT & PERIOD COVERED TECHNICAL REPORT 9/15/73 - 11/15/75 6. PERFORMING ORG. REPORT NUMBER
7. AUTHOR(s) Robin L. Keesee, Ph.D.		8. CONTRACT OR GRANT NUMBER(s) F33615-71-C-1739
9. PERFORMING ORGANIZATION NAME AND ADDRESS Department of Industrial Engineering & Operations Research, Virginia Polytechnic Institute and State University, Blacksburg, Virginia 24061		10. PROGRAM ELEMENT, PROJECT, TASK AREA & WORK UNIT NUMBERS 61102F 2313-V1-04
11. CONTROLLING OFFICE NAME AND ADDRESS Aerospace Medical Research Laboratory Aerospace Medical Division, AFSC Wright-Patterson AFB, OH 45433		12. REPORT DATE December 1976 13. NUMBER OF PAGES 120
14. MONITORING AGENCY NAME & ADDRESS*(if different from Controlling Office)*		15. SECURITY CLASS. *(of this report)* Unclassified 15a. DECLASSIFICATION/DOWNGRADING SCHEDULE
16. DISTRIBUTION STATEMENT *(of this Report)* Approved for public release; distribution unlimited.		
17. DISTRIBUTION STATEMENT *(of the abstract entered in Block 20, if different from Report)*		
18. SUPPLEMENTARY NOTES		
19. KEY WORDS *(Continue on reverse side if necessary and identify by block number)* Human engineering Image quality Television Contrast thresholds		
20. ABSTRACT *(Continue on reverse side if necessary and identify by block number)* Determination of the modulation detectability threshold for sinusoidal gratings is a prerequisite to several measures of image quality for line-scan imaging systems. To develop predictive models for these thresholds, an experiment was conducted to determine the modulation detectability threshold functions for a range of system parameters typical of medium- to high-resolution low-light-level television systems.		

DD FORM 1 JAN 73 1473 EDITION OF 1 NOV 65 IS OBSOLETE

SECURITY CLASSIFICATION OF THIS PAGE *(When Data Entered)*

20. Abstract.

Specifically, the psychophysical method of adjustments with target grating modulation as the dependent variable was employed in an experiment where, at each of 10 combinations of video line rate and video noise passband, each of 7 subjects received 2 replications at every combination of 10 spatial frequencies, 2 target orientations, and 5 noise amplitudes. Line rates were 525, 945, and 1225 lines per frame; the spatial frequencies were between 1 and 20 c/deg; and the gratings were oriented vertically (perpendicular to the video raster) and horizontally (parallel to the raster). As the three highest spatial frequencies were not used at the 525 line rate, horizontal orientation, there were 13,160 trials.

The target gratings were displayed in a 16.2 cm square center portion of a 25.4 cm by 35.6 cm video monitor with both the grating and surround having a mean luminance of 51.4 cd/m^2. Viewing distance was 101.6 cm.

Using a step-wise multiple regression technique to evaluate candidate variables, a model predicting the modulation threshold as a function of the other variables was developed for each grating orientation.

In the vertical orientation, a correlation coefficient of .77 was achieved between the experimental data and a three-variable equation consisting of a variable representing the integration of noise power from zero spatial frequency to the grating spatial frequency, the value of the modulation threshold determined by DePalma and Lowry (1962) at the grating spatial frequency, and a variable representing the noise power in the spatial frequency region of the grating. The addition of twenty-two other variables increased the correlation to .82.

For the horizontal orientation, a correlation of .74 was obtained with a three-variable equation including the variable representing an integration of noise power from zero to the grating spatial frequency, the inverse of the raster spatial frequency, and a shaping variable equal to the square of the grating spatial frequency minus 9 c/deg. The inclusion of twenty-three additional variables yielded a .81 correlation coefficient.

The correlation coefficients are between the models and the complete data sets, not means across subjects and replications.

These models are useful in the application of the modulation transfer function area (MTFA) and other spatial frequency-based line-scan image quality metrics.

NOTICES

When US Government drawings, specifications, or other data are used for any purpose other than a definitely related Government procurement operation, the Government thereby incurs no responsibility nor any obligation whatsoever, and the fact that the Government may have formulated, furnished, or in any way supplied the said drawings, specifications, or other data, is not to be regarded by implication or otherwise, as in any manner licensing the holder or any other person or corporation, or conveying any rights or permission to manufacture, use, or sell any patented invention that may in any way be related thereto.

Please do not request copies of this report from Aerospace Medical Research Laboratory. Additional copies may be purchased from:

National Technical Information Service
5285 Port Royal Road
Springfield, Virginia 22161

Federal Government agencies and their contractors registered with Defense Documentation Center should direct requests for copies of this report to:

Defense Documentation Center
Cameron Station
Alexandria, Virginia 22314

TECHNICAL REVIEW AND APPROVAL

AMRL-TR-76-38

This report has been reviewed by the Information Office (OI) and is releasable to the National Technical Information Service (NTIS). At NTIS, it will be available to the general public, including foreign nations.

This technical report has been reviewed and is approved for publication.

FOR THE COMMANDER

CHARLES BATES, JR.
Chief
Human Engineering Division
Aerospace Medical Research Laboratory

AIR FORCE - 4 FEBRUARY 77 - 200

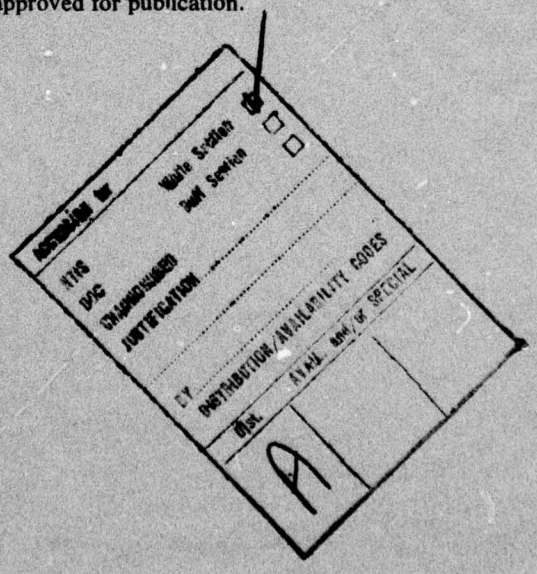

PREFACE

This study was initiated by the Visual Display Systems Branch, Human Engineering Division, of the Aerospace Medical Research Laboratory. The research was conducted by the Department of Industrial Engineering and Operations Research, of Virginia Polytechnic Institute and State University of Blacksburg, Virginia 24061, under Air Force contract F33615-71-C-1739. Dr. Harry L. Snyder was the principal investigator for Virginia Polytechnic Institute and State University. Mr. James L. Porterfield was the Technical Monitor for the Aerospace Medical Research Laboratory. The report covers research performed between September 1973 and November 1975.

TABLE OF CONTENTS

LIST OF TABLES

LIST OF ILLUSTRATIONS

SECTION I

INTRODUCTION

The need for a single quantitative index of the image quality of line-scan display systems has been stated by Snyder (1973), Snyder, Keesee, Beamon, and Aschenbach (1974), and others. Of several alternative candidates for the role, the modulation transfer function area (MTFA) has been shown to be the most promising summary measure yet proposed (Snyder, *et al.*, 1974). However, one disadvantage of the MTFA is that it requires knowledge of the observers' modulation detectability threshold function for the intended display conditions of the imaging system. Thus, at least prototype hardware is required to obtain the threshold functions. This research has been directed toward developing models that predict these functions as they depend on system line rate and noise power spectra.

SPATIAL FREQUENCY ANALYSIS

To some extent, any sampled imagery system reproduces the contrast of large detail more accurately than the contrast of small detail. This is because the sampling spot of the raster is not infinitely small but has a finite size.

In the camera, the information given by the sampling spot or aperture is the mean luminance over its area; the camera gives no information about details that are smaller than this sampling spot. Detail, in two-dimensional, monochromatic scenes, is best described quantitatively by its contrast and the inverse of its size, its spatial frequency. Rather than use contrast with its several algebraic definitions, a related quantity, modulation, is used and is defined as:

$$m = \frac{L_{max} - L_{min}}{L_{max} + L_{min}} \qquad (1)$$

where L_{max} = maximum luminance, and

L_{min} = minimum luminance.

Target size describes one target element as having a certain number of units of length; spatial frequency defines a certain number of equal-sized target elements per unit of length. Thus, for periodic objects such as black-and-white bar patterns and sine-wave gratings, spatial frequency is in terms of bars/inch, cycles/inch, or, as will be used here, cycles/degree (c/deg) of subtended angle measured at the system input.

The extent to which an imaging system can reproduce the modulation of image detail of varying sizes can be described by the modulation transfer function (MTF). Defined photometrically, MTF is the ratio of signal modulation out of the system to the input signal modulation over all spatial frequencies. Figure 1 is an MTF for a hypothetical system.

For an MTF to describe validly a system or a system component, the transfer function must represent performance with a sine-wave input (Scott and Frauenhofer, 1971); the response of the system must be uniform throughout the field of view (homogeneous) and in all directions (isotropic) (Cornsweet, 1970); and the ratio of output to input modulation, known as the modulation transfer factor, must be independent of input levels, that is, it must depend only on spatial frequency (Cornsweet, 1970). The MTF has a very useful property if these linear systems analysis conditions are met. The MTF of a system is equal to the product of the MTFs of the system

components. Using MTFs, the effect of a proposed design change in one component on the performance of the total system can be computed from the component MTFs. If these conditions are not met, the resulting analysis may have somewhat restricted utility, but may still be useful in predicting system performance (Snyder, *et al.*, 1974).

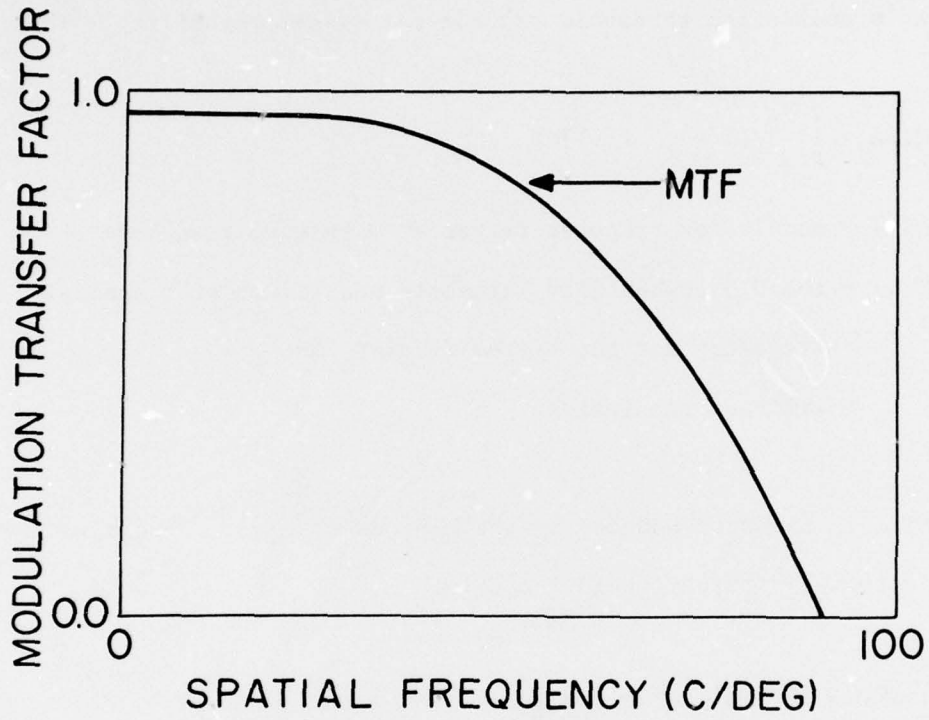

Figure 1. MTF for a Hypothetical System.

Television systems approximate all of the assumptions for MTF analysis but one: the continuous sampling along a scan line and discrete sampling across a line make video system displays decidedly anisotropic. This means that an MTF measured parallel to the raster and an MTF measured perpendicular to the raster are both required for a complete MTF description of a line-scan system.

Charman and Olin (1965) improved on the MTF as an image quality measure by

developing for photographic systems what is now known as the modulation transfer function area (MTFA). Illustrated in figure 2, the MTFA is the integrated difference between the system capability to transmit modulation (the MTF) and the observer's contrast threshold for spatial frequencies varying from zero to the system limiting resolution, the point beyond which the observer's modulation threshold exceeds the system capability. Thus,

$$\text{MTFA} = \int_{0}^{\nu_o} [M(\nu) - T(\nu)]d\nu \qquad (2)$$

where $M(\nu)$ = modulation transfer factor at ν spatial frequency,

$T(\nu)$ = the 0.5 probability threshold modulation at ν spatial frequency for the system display, and

ν_o = limiting resolution.

Thus, the MTFA is the area bounded by the MTF and what will be called the modulation detectability threshold function.

MTFA as a summary measure of TV image quality, a use proposed by Snyder (1973), has several advantages and a disadvantage. In its favor, it includes the effects of many variables affecting the displayed image quality: sensor and display bandwidth, line rate, signal-to-noise ratio, gamma, contrast, mean luminance, edge enhancement, and spatial filtering.

Further, the worth of MTFA assessment of TV system image quality has been shown in a pair of experiments by Snyder, *et al.*, (1974). In the first experiment, dynamic air-to-ground imagery was viewed through five simulated LLLTV systems differing only in noise amplitude. MTFA values had a 0.965 correlation ($p<.01$) with proportion of targets correctly recognized by

observers. These computations differed from the correct procedure for measurement of the MTFA, however, in that both the MTF and the modulation detectability threshold were measured for square-wave inputs. Essentially this experiment tested the ability of MTFA to predict target acquisition performance as a function of increasing noise levels.

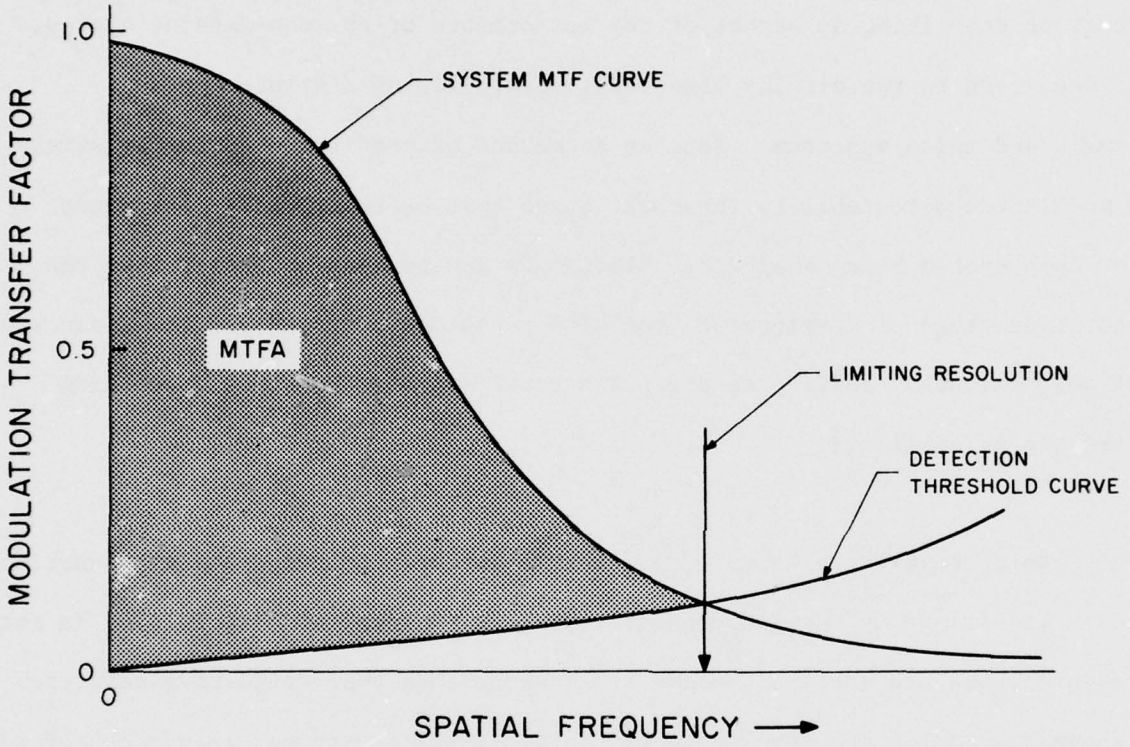

Figure 2. MTFA for a Hypothetical System.

The second experiment used facial photographs as stimuli. The faces were viewed through TV systems simulating three different MTFs with five different noise levels for each MTF. The correlation between the logarithm of MTFA computed as in the first experiment and the proportion of faces correctly identified in a matching task was 0.87 ($p<.01$).

In both of these experiments, the MTFs, modulation detectability thresholds,

and the MTFAs were measured only with bars perpendicular to the raster. Here, then, the MTFAs gave the system performance only in one direction--along the scan lines.

MTFA has the disadvantage that the modulation detectability function, a function describing an aspect of the performance of the man-machine system, is dependent on the display line rate, size, viewing distance, noise level, and noise spectrum. Because no method of prediction currently exists, a modulation detectability threshold curve must be empirically determined for each system being analyzed. Since this can be done no sooner than the prototype stage of development, the MTFA cannot be computed and the advantages of the designers' ability to predict a total system MTF before assembling hardware is nullified.

Only one attempt has been made to determine modulation detectability functions for a wide range of the independent variables (Snyder, *et al.*, 1974). In that research, the appropriate photometric measurements that would have permitted generalization of the results to many other systems were not made. Therefore, the need still exists for a procedure for predicting a modulation detectability threshold given knowledge of the display characteristics.

FLAT-FIELD, NOISE-FREE THRESHOLDS

Of many studies of contrast or modulation detectability thresholds for the flat-field, noise-free image, two papers are representative. Lowry and DePalma (1961) had the concern that, although the use of MTFs as a measure of the goodness of an optical system was growing, there was no satisfactory

determination of the human eye MTF that could be compared with or cascaded with the optical system MTF to obtain the total man-machine system MTF.

To determine this visual MTF, they applied the convolution expression,

$$I(x) = \int_{-\infty}^{\infty} A(x' - x)\, O(x)\, dx \tag{3}$$

where $A(x)$ = line spread function (MTF),

$I(x)$ = observer's perceived luminance distribution,

$O(x)$ = object space luminance distribution,

x = projected object coordinate, and

x' = image coordinate,

to the Mach phenomenon. The white-to-black gradient of the phenomenon, $O(x)$, was measured photometrically and the observer's matching response, $I(x')$, was measured with a visual slit photometer. This photometer consisted of a very small slit of variable luminance that was matched in luminance by the observer to points along the white-to-black gradient.

The sine-wave response, or MTF, was then obtained by converting the expression above by the Fourier integral into

$$I\#(\nu) = A\#(\nu) \cdot O\#(\nu) \tag{4}$$

and solving for $A\#(\nu)$ where # indicates the complex Fourier transform.

Their results, a combination of data from three gradients having different slopes and perhaps based on only one observer, are given in figure 3.

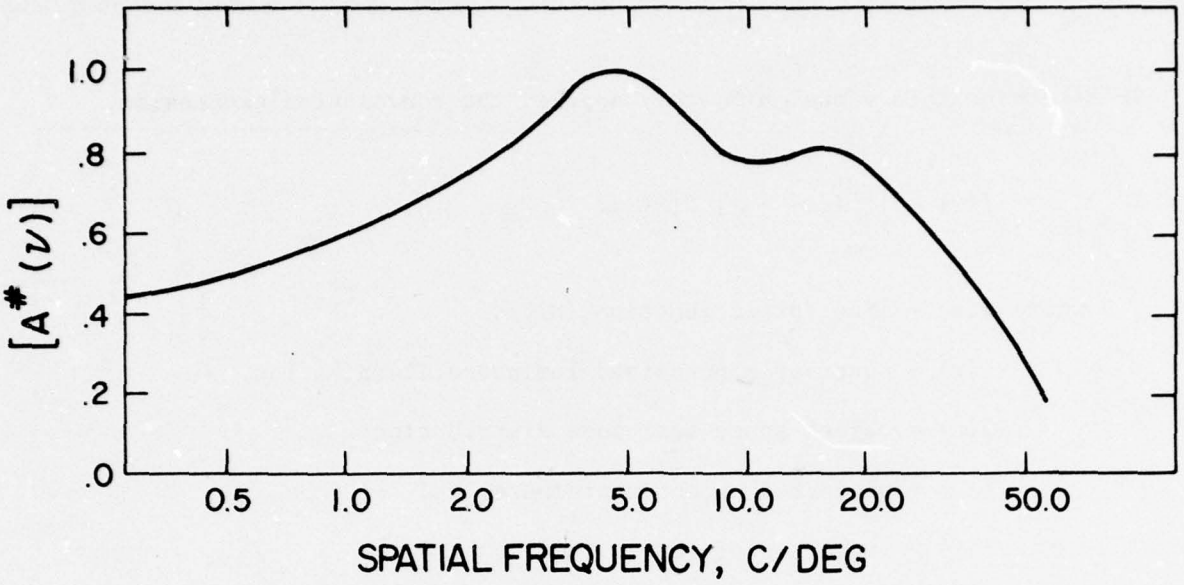

Figure 3. Modulation Transfer Function for the Eye, from Lowry and DePalma (1961).

DePalma and Lowry (1962) found detectability thresholds for sine- and square-wave targets over a range of 0.30 to 30 c/deg, for four viewing distances from 25.4 cm to 142.2 cm at 68.5 cd/m^2, and with a visual angle of 6 deg. Another luminance condition, viewing distance, and visual angle were used but were not factorial with the rest of the experiment. Figure 4 is a replotting of their sine- and square-wave modulation thresholds for the 88.9 cm viewing distance, the distance closest to that at which most video displays are viewed. Again in this study, no inferential statistics and possible only one subject were used. Threshold contrast at a given spatial frequency increases with closer viewing distances.

The minimum modulation threshold is reached at about 3 c/deg in both Lowry

and DePalma (1961) and DePalma and Lowry (1962). Thresholds for square-wave gratings have also been found to reach a minimum at about 3 c/deg (Schober and Hilz, 1965).

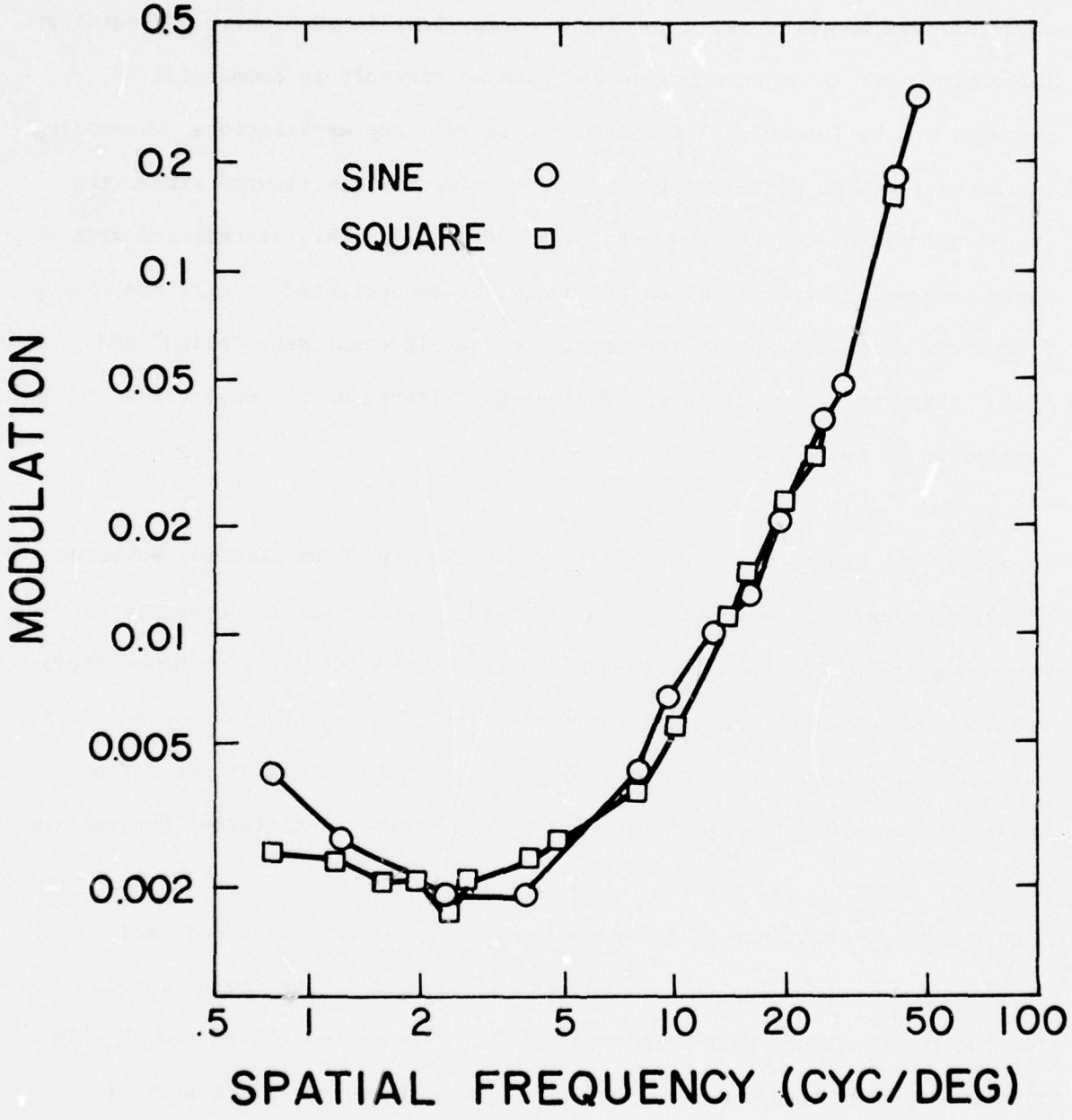

Figure 4. Modulation Detectability Threshold Functions from DePalma and Lowry (1962).

DYNAMIC NOISE THRESHOLDS

Dynamic noise can be generated by line-scan electro-optical imaging systems when they are operating with low input energy levels, when there are outside influences such as other stations and passing aircraft in commercial TV systems, and by intentional interference in military applications. Depending on the source, the noise amplitude may be uniformly distributed across the system bandwidth, distributed over just a few MHz or KHz, distributed with power inversely proportional to frequency, or concentrated at only one frequency. Different noise frequencies cause different size "blips" and "blip" patterns having different detrimental effects on the observer's perception of target objects.

In one of the two recent investigations of *noise spectrum effects*, Eckhardt (1969) used an 8 MHz bandwidth, 525 line, 43.2 cm monitor to determine sine-wave modulation detectability thresholds for twelve different noise conditions. Besides a zero-noise condition, the twelve included two broadband conditions, one medium passband, and eight narrow noise passbands. All of the narrow noise passbands had the same shape but were centered at different frequencies.

Figure 5 is a comparison of the no-noise and two narrow noise passband modulation detectability thresholds for one subject. Here, noise levels for the two passbands were both equal to $5.5 \pm .4$ mV rms. Even though this plot consists of single data points from one subject, there are several interesting features. The minimum, no-noise threshold signal is at 0.8 to 3.2 c/deg, which generally agrees with the 3 c/deg from the non-sampled imagery studies.

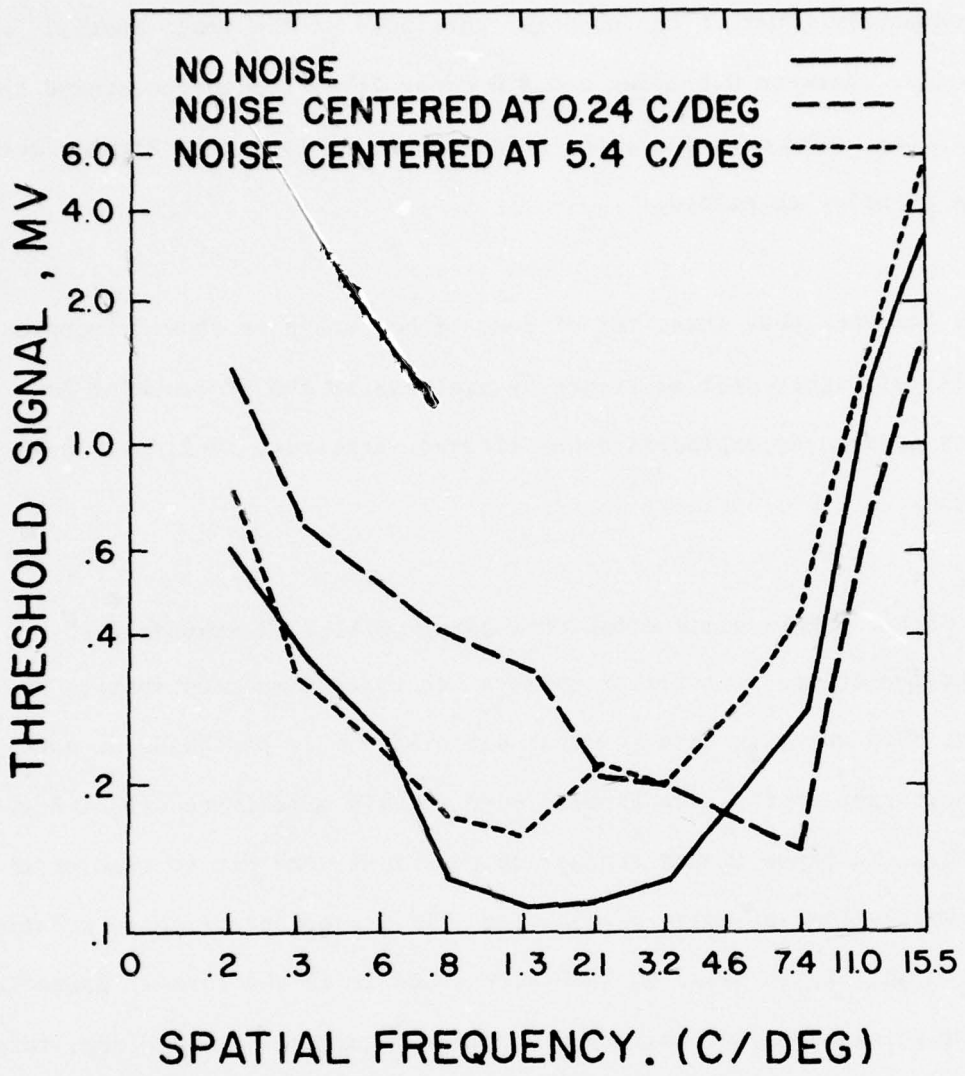

Figure 5. Modulation and Noise Limited Thresholds for One Subject Viewing a 525-Line Display, after Eckhardt (1969).

The lowest frequency narrow-band noise condition, centered at 0.24 c/deg, approximately doubles the threshold signal compared to the zero noise condition. This is true up to 3 c/deg. Thereafter, the threshold for the 0.24 c/deg noise condition is a little more than half that of the no-noise threshold. The threshold for the highest frequency noise condition, that centered at 5.4 c/deg, appears more rational. This noise-limited threshold

is approximately equal to the no-noise threshold at the lower spatial frequencies. Between 0.8 c/deg and 8.0 c/deg (the frequencies around the center of the noise spectrum), the noise threshold is 1.5 to 2 times greater than the no-noise threshold.

Eckhardt comments that three out of four of her subjects showed improved visibility of higher spatial frequency gratings in the presence of low frequency noise. No explanation was offered (Eckhardt, 1969, pp. 38-40 and p. 45).

Snyder, *et al.* (1974) found modulation detectability thresholds for noise-limited square-wave tribar targets for three simulated systems having different MTFs and with three or four different noise passbands at each MTF. The target spatial frequencies used in this experiment were 1.8 to 22.5 c/deg. Multiple linear regression equations were fit to each of the eleven combinations of noise passband and MTF. Each one of these equations, listed in table 1, is based on 1680 points and is in the form of noise level in rms mV being dependent on target spatial frequency (SF) in c/deg, target modulation (M), and an intercept. Although there was significant lack-of-fit in at least one equation, correlation coefficients for all eleven equations were at least 0.90. This range of spatial frequencies is equivalent to the ascending portion of the threshold curves found by Eckhardt (1969) and DePalma and Lowry (1962). The substantial changes in the values of the coefficients as one moves among the equations for a particular MTF show the effects of varying noise spectrum shape on detectability thresholds. In part because of inadequate photometric measurement of the noise spectra, the analysis of the data was not continued to the point

Table 1. Noise Limited Modulation Detectability Thresholds, from Snyder, *et al.* (1974)

Bandwidth/Line Rate (MHz/lines)	Noise Passband (c/deg)	Correlation Coefficient	Least Squares Multiple Regression Equations Noise (rms mV) = _____ (SF)(c/deg) + _____ (M) + _____		
32/1225	0 -27.1	.92	-.157	235.6	34.8
	0 - 6.8	.94	-.112	127.2	22.8
	4.9- 6.8	.93	-.112	225.8	20.1
	4.9-13.6	.93	-.168	343.5	31.5
16/945	0 - 8.8	.95	-.168	136.9	29.3
	0 -17.6	.90	-.189	184.9	33.3
	6.3- 8.8	.94	-.150	237.9	23.7
	6.3-17.6	.91	-.202	370.0	30.0
8/525	0 -15.8	.91	-.196	190.0	41.0
	6.0-15.8	.91	-.297	325.5	44.1
	11.4-15.8	.91	-.408	337.5	62.6

of predicting the effects of a noise power spectrum on detectability thresholds.

Both Snyder, *et al.* (1974) and Eckhardt (1969) reached the qualitative conclusion that low frequency noise is more detrimental than is high frequency noise. Eckhardt offers the tentative explanation that due to the frame-to-frame incoherence of noise compared to signal, "the low frequency components of the noise would be less subject to the attenuation of inhibition than the signal and would consequently be a more potent degrading factor" (Eckhardt, 1969, pp. 45-46).

An analogy, not an explanation, may be found in an experimental determination of the effects of variable exposure time on the contrast sensitivity of square-wave gratings. This work by Schober and Hilz (1965) shows that, while the luminance difference threshold rose with shortened exposure times, the luminance difference threshold versus spatial frequency curve flattened at the lower frequencies for short exposure times (figure 6). The interval between the longest exposure, 1000 msec, and an interpolated exposure similar to the length of one video frame, 30 msec, at the lowest spatial frequency used, about 0.12 c/deg, is only half as great as the interval at the approximate minimum threshold point, 1.2 c/deg. The data suggest that the relative detriment of noise centered around 0.12 c/deg with a target of 0.12 c/deg will be twice as great as the relative detriment of 1.2 c/deg noise to a target of that frequency.

For the high frequencies, the luminance difference threshold curves for 1000 msec and the interpolated 30 msec exposure time are almost parallel above

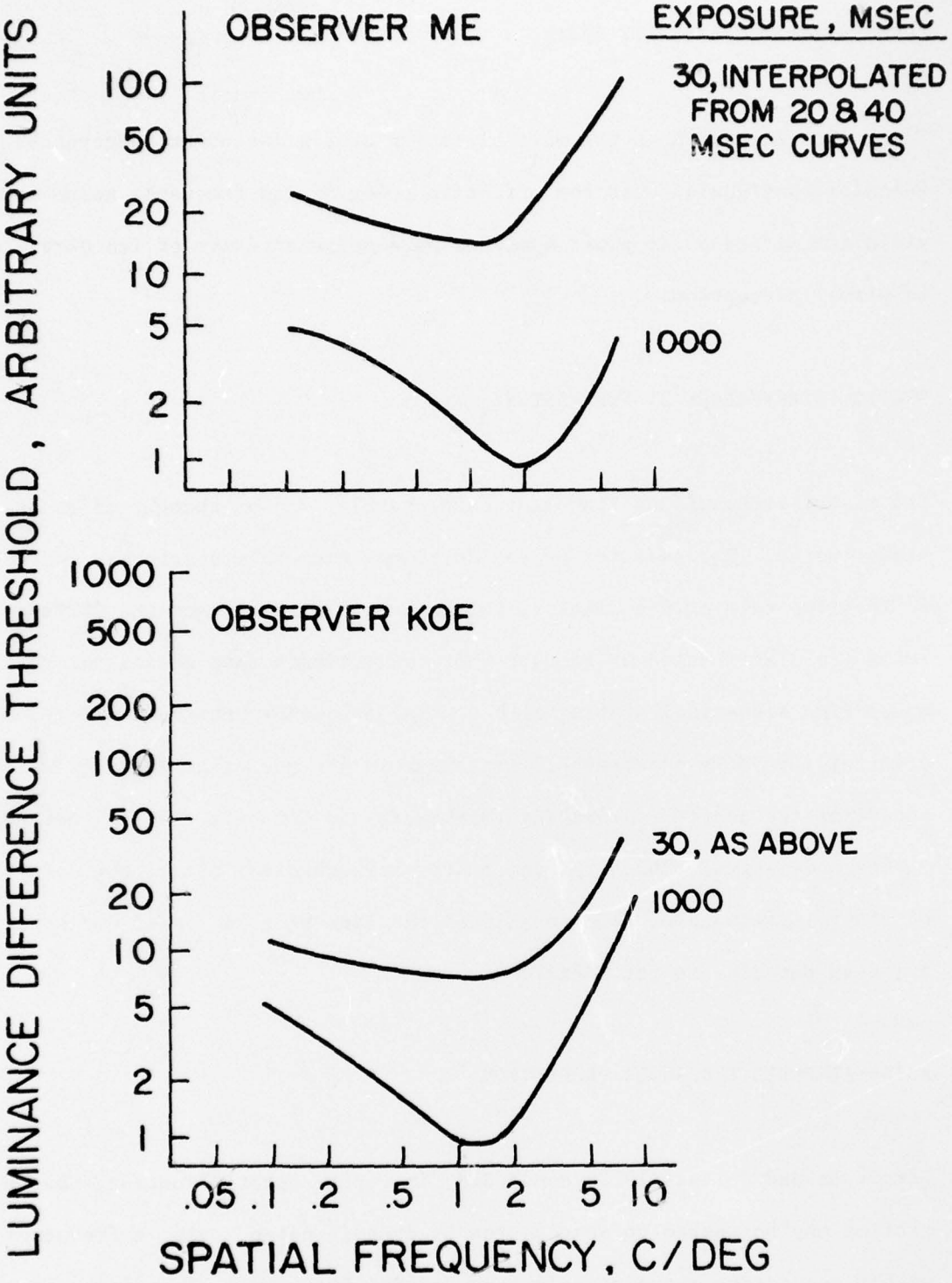

Figure 6. Square-wave Contrast Sensitivity for Different Exposure Times, from Schober and Hilz (1965). Mean Luminance was 107.8 cd/m^2 and Viewing Distance was 1 m.

the minimum level at 1.2 c/deg.

These data suggest that the multiplication of a noise power spectrum by a function that would boost the effective power of low frequency noise would yield a modified noise power spectrum more representative of its detriment to visual perception.

STATIC INTERFERENCE BY THE RASTER

The raster structure of line-scan displays also can be thought of as static visual noise. The severity of the detriment from this stationary noise depends on the line rate of the display, the interlace pattern, and the CRT spot luminance distribution or focus. There is evidence that adaptation to a high modulation sinusoidal grating with spatial frequency between 3 c/deg and 14 c/deg will raise the detectability threshold for any other gratings within an octave of the adaptation grating (Blakemore and Campbell, 1969). Depending on its modulation, therefore, the raster structure may affect the detectability of spatial frequencies down to half of the line rate, at least for a grating oriented parallel to the raster.

NOISE-AFFECTED THRESHOLD PREDICTION

Stromeyer and Julesz (1972) concluded, in a non-raster situation, that a grating may be masked to some degree by dynamic noise having a frequency within one octave above or below the grating frequency. Therefore, it is reasonable to expect that the modulation detectability threshold, $D(\nu)$, for a grating at some spatial frequency, ν_i, is some inverse function of the

product of the effective noise power at spatial frequencies around the frequency of the grating weighted by the difference in spatial frequency between the grating and the noise power. A possible expression would be:

$$D(\nu_i) = f[k \int_0^\infty \frac{N(\nu)}{1 + (\nu-\nu_i)^2} d\nu] \quad (5)$$

where ν = spatial frequency,

$D(\nu_i)$ = modulation detectability threshold at ν_i

$N(\nu)$ = noise power at ν,

ν_i = grating spatial frequency, and

k = some constant

OBJECTIVES

Using these results as background, the overall objective of this research is to develop models that predict the modulation detectability threshold functions for sinusoidal gratings oriented both perpendicular (vertical) and parallel (horizontal) to the raster for the important mid-range of spatial frequencies (0 - 20 c/deg). The models should predict the effects on threshold functions of noise spectra and power likely to be encountered in airborne line-scan imaging systems.

Specific goals are that the models should predict the modulation detectability threshold function sufficiently well to permit the continued investigation, and limited application, of MTFA as an image quality measure witbout requiring experimental determination of the threshold function for each new combination of noise power and line rate. The simplifying, and thus constraining, limitation is that the models be developed for but one viewing situation, *i.e.*, one combination of viewing distance, display luminance, and ambient illuminance.

SECTION II

RESEARCH METHODOLOGY

RESEARCH STRATEGY

To maximize utility of the data generated in this research, it is desirable that the predictive models of modulation detectability functions include all combinations of line rate, system bandwidth, noise amplitude, noise frequency passband, and target orientation, where the modulation detectability function describes the dependence of threshold modulation on spatial frequency for each combination of the other variables.

EXPERIMENTAL DESIGN

The experimental method employed was the method of adjustments with target grating modulation as the dependent variable. In general, this method requires that after presentation of the experimental stimulus, the subject decreases the dependent variable until he ceases to perceive the stimulus. The experimenter records this value, reduces the dependent variable to zero or a level far below the threshold region, and the subject is then permitted to increase the dependent variable level until he just perceives the stimulus. This dependent variable level is also recorded and one trial is completed. The trial threshold is the average of the first and second recorded levels of the dependent variables. This method is appealing because the two scores theoretically bracket the true threshold and the average is assumed to be nearer the actual threshold than if the subject is asked to set the dependent variable at the point where he feels the stimulus

is half perceptible.

The design of the experiment is summarized in figure 7. Three line rates were chosen to represent the medium-to-high resolution video system typical of airborne applications. The nominal rates used were 525, 945, and 1225 lines per frame. All were at 30 frames per second.

It was desired in the selection of noise passbands to have a broad passband and some combination of narrow and medium bands at each line rate. Nominal noise frequency ranges (between 3-dB down points) in electrical units are given in figure 7. Later figures show noise power spectra described in terms of spatial frequency computed using a viewing distance of 101.6 cm to a display that was 25.4 by 35.6 cm.

At each line rate-noise passband combination, a factorial experiment was executed composed of ten grating or target spatial frequencies, two target orientations, and five noise amplitudes. The ten target spatial frequencies, listed in table 2, ranged from the medium-low 1 c/deg to 20 c/deg, a point near the reasonable resolution limit. The target gratings were oriented either vertically or horizontally. The five noise amplitudes used for each noise passband were selected to insure that the target image at the greatest modulation was severely degraded at the highest noise amplitude, with the remaining noise amplitude values spaced at pseudo-logarithmic intervals from zero to the highest amplitude. Specific noise amplitudes at each noise passband are given in table 3.

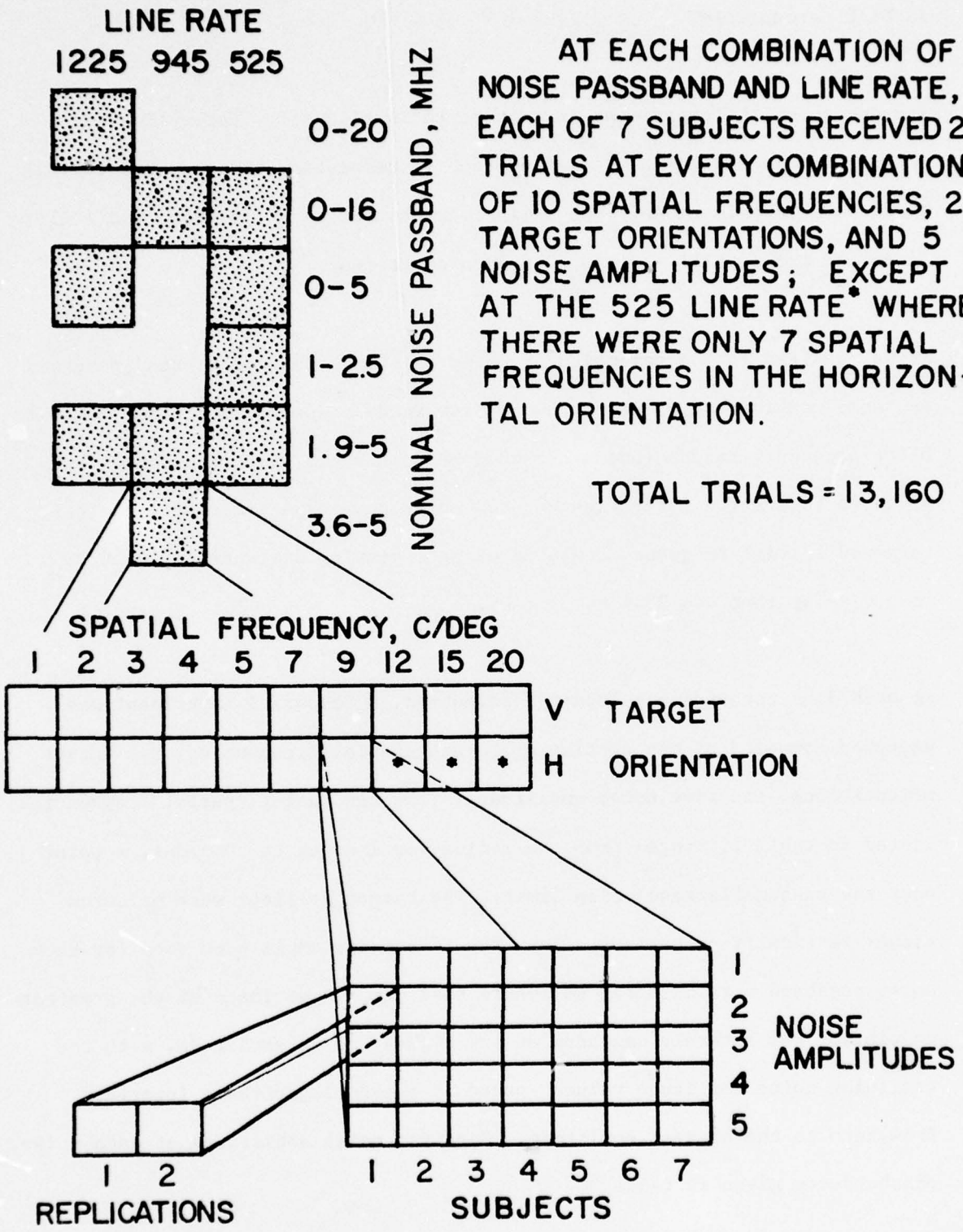

Figure 7. Diagram Summarizing the Design of the Experiment.

Table 2. Specific Spatial Frequencies (c/deg) at each Line Rate and Grating Orientation

Target Orientation	Target	Line Rate 525	945	1225
Vertical	1V	(1.00)	(1.00)	(1.00)
	2V	1.99	1.99	1.99
	3V	3.01	3.01	3.01
	4V	3.99	3.99	3.99
	5V	5.00	5.00	5.00
	6V	6.74	6.74	6.91
	7V	8.96	8.96	9.05
	8V	11.96	11.45	11.96
	9V	14.48	14.94	14.94
	10V	20.12	18.10	19.08
Horizontal	1H	(1.00)	(1.00)	(1.00)
	2H	2.02	1.99	1.99
	3H	3.01	3.01	3.01
	4H	3.99	3.99	3.99
	5H	5.00	5.00	5.00
	6H	6.91	6.91	6.91
	7H	8.96	7.17	8.96
	8H		9.96	11.96
	9H		13.07	14.34
	10H		16.29	17.92

( ) Indicates an estimate rather than the result of the PWRSPC program.

Table 3. Noise Amplitudes (rms mV) at each Line Rate and Noise Passband

Noise Passband (MHz)	1225	945	525
0.0* - 20.0	0.0		
	2.3		
	4.2		
	10.9		
	22.5		
0.0* - 16.0		0.0	0.0
		1.8	5.0
		3.4	10.0
		8.9	20.0
		18.3	30.0
0.0* - 5.0	0.0		0.0
	1.0		2.0
	2.0		4.0
	5.0		10.0
	10.0		20.0
1.0 - 2.5			0.0
			1.0
			2.4
			7.4
			15.3
1.9 - 5.0	0.0	0.0	0.0
	2.0	3.5	2.0
	4.0	8.5	4.0
	8.0	16.0	8.0
	15.0	40.0	15.0
3.6 - 5.0		0.0	
		2.7	
		6.8	
		12.7	
		33.3	

* The lower limit of the noise spectra is 20 Hz.

EQUIPMENT

Central to the equipment diagrammed in figure 8 is the image generator designed in the VPI Human Factors Laboratory. Through appropriate triggering and blanking of the sinusoidal output of the Wavetek signal generator, the image generator produces a sinusoidal grating of variable height, width, and position in the video image. Frequency and orientation of the target grating are controllable from the signal generator. The modulation of the grating is varied through a five-turn potentiometer that controls the gain voltage to an amplifier within the image generator and is connected by a long cable so that the subject can hold the control conveniently on his lap. Modulation settings of this control were recorded by noting the voltage across this potentiometer for later conversion to modulation using photometric measurements. Descriptions and model numbers for the other equipment are in Appendix A.

As pictured in figures 9 and 10, the subjects were seated in a dental chair and positioned so that they were comfortable, had a line of sight normal to the center of the display surface, and had a viewing distance of 101.6 cm. The display monitor was a Conrac RQA-17 with a standard P4 phosphor having a blue-gray appearance. The sinusoidal grating was 16.2 cm square and centered in the screen. The luminance of the grating surround and the mean luminance of the grating were maintained at 51.4 cd/m^2.

The exposed portion of the CRT faceplate was 25.4 cm by 35.6 cm with the long dimension vertical as shown in figure 9. The raster had a vertical orientation. All references to grating orientation use the monitor as the reference plane. Thus a "vertical" target grating was vertical to the video

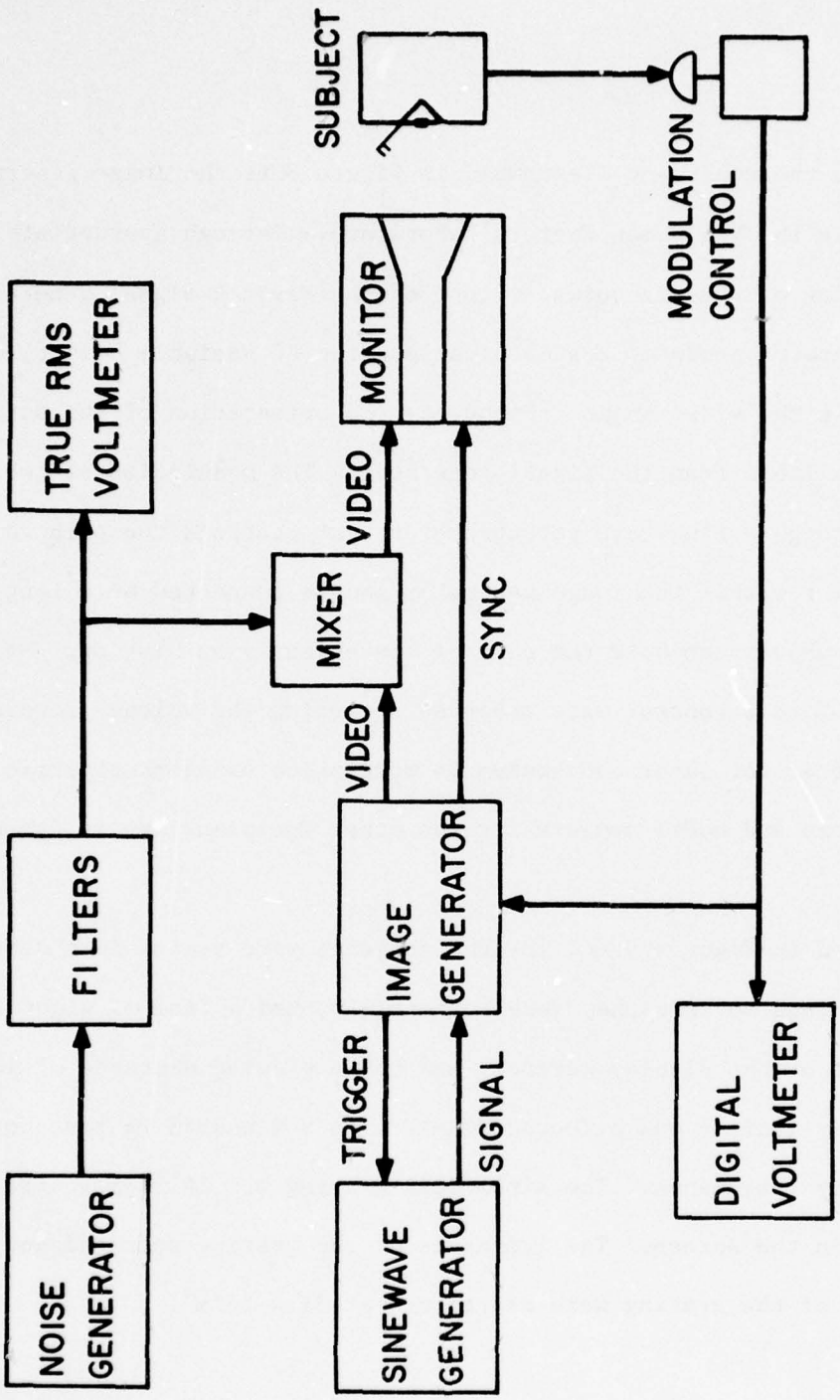

Figure 8. Block Diagram of Experimental Equipment.

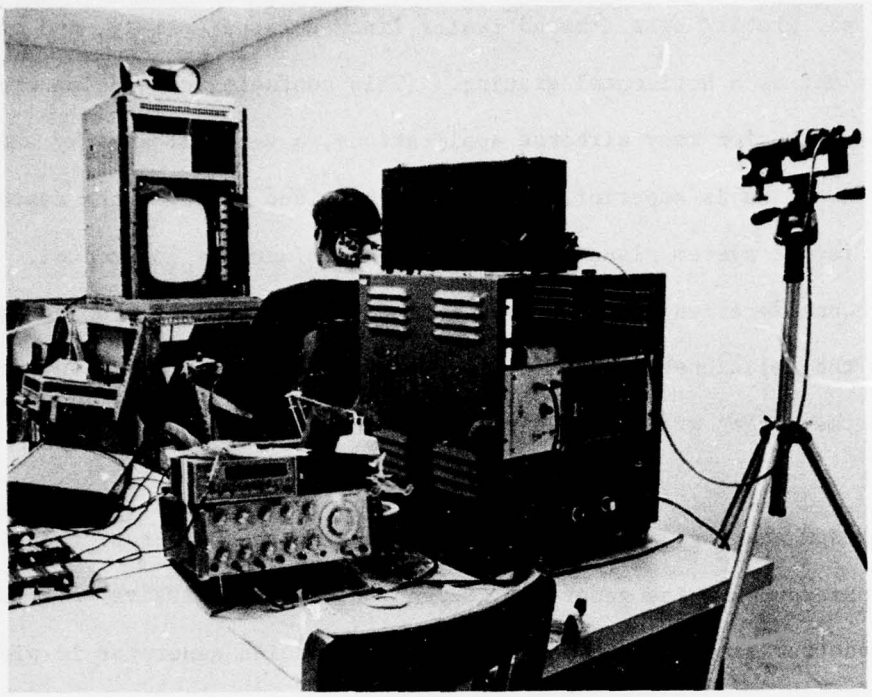

Figure 9. View of the Experiment Room Showing the Display and the Subject's Position.

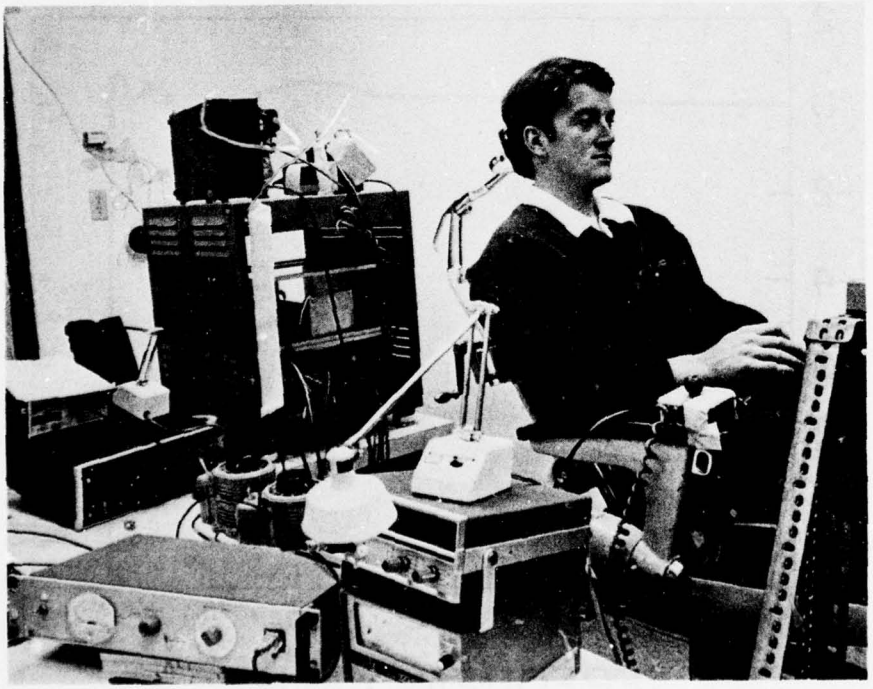

Figure 10. View of the Subject's Position.

system, *i.e.*, grating bars crossed raster lines perpendicularly, and seen by the subject as a horizontal grating. (This confusing convention was adopted because, for many airborne applications, a vertical display and raster orientation is superior, but in general video systems, the raster direction is the system plane of reference and is usually horizontal. The important consideration in this investigation of grating orientation is to determine the relationship between the raster interference at different line rates and the target grating orientation.)

Noise spectrum shaping, if any, is done by passing the output of the 20 Hz-20 MHz random noise generator through one or more passive RF filters. A noise spectrum similar to that produced by the noise generator is plotted in figure 11 (General Radio, 1969) and the passband shapes of the filter combinations are in Appendix B.

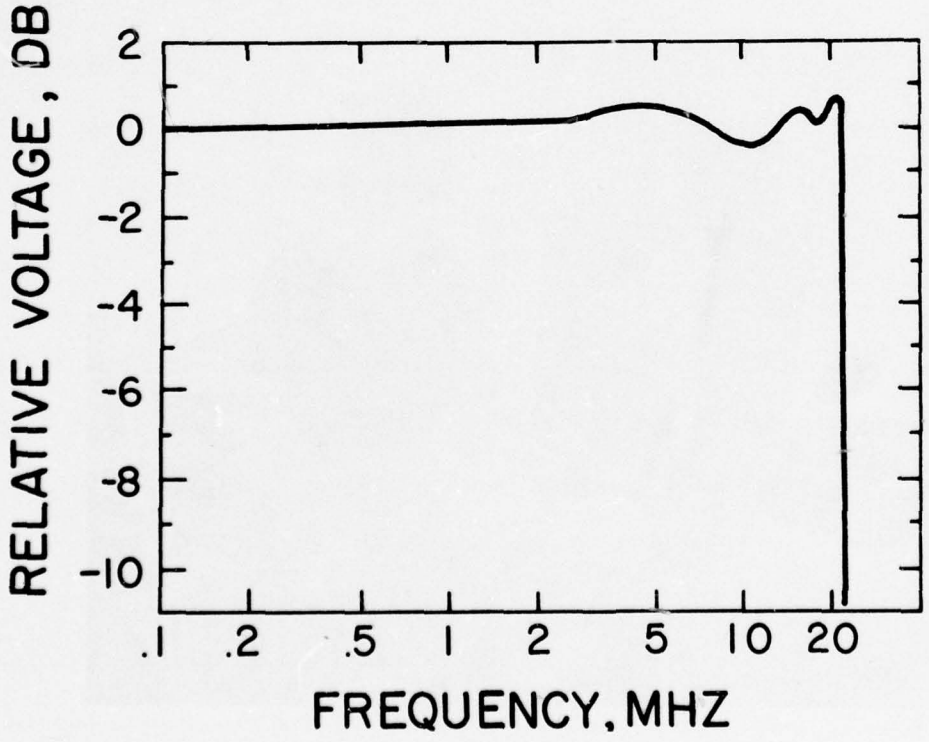

Figure 11. Noise Output Spectrum Typical of the General Radio 1383 Random-Noise Generator (curve from General Radio, 1969).

PHOTOMETRY

To determine the conversion from image generator voltage gain to modulation, it was necessary to measure photometrically the modulation of gratings over as much of the modulation range used in the experiment as possible. As the voltage gain-modulation relationship was nonlinear, the measurements were made at each input frequency, *i.e.*, at each grating spatial frequency, grating orientation, and line rate. At each of these combinations, modulation was measured at eight voltage settings of the modulation control. Equipment for these measurements is diagrammed in figure 12.

Although direct, peak-to-peak measurements of modulation are usually made of stimuli in experiments of this type, it was intended to avoid in this study the several opportunities for subjective error in that procedure by determining the modulation through power spectrum analysis of the gratings. Transforming the image luminance distribution from the spatial to the frequency domain permits the determination of the modulation amplitude at specific frequencies including the fundamental grating frequency.

To begin the analysis charted in figure 12, a central portion of the monitor CRT surface was scanned photometrically using the Gamma Scientific photometer with optics configured as a microscope. The scan was accomplished with a scanning-slit eyepiece shown in figure 13 having a 25μ by 2500μ aperture moving through 10 mm in the image plane of the microscope. Thus, with a 1X microscope objective, the eyepiece scanned 10 mm on the CRT face. The eyepiece slit was driven by a small battery-powered motor with 60 to 80 sec required for a 10 mm traverse. Output was on an X-Y plotter. Data for power spectrum

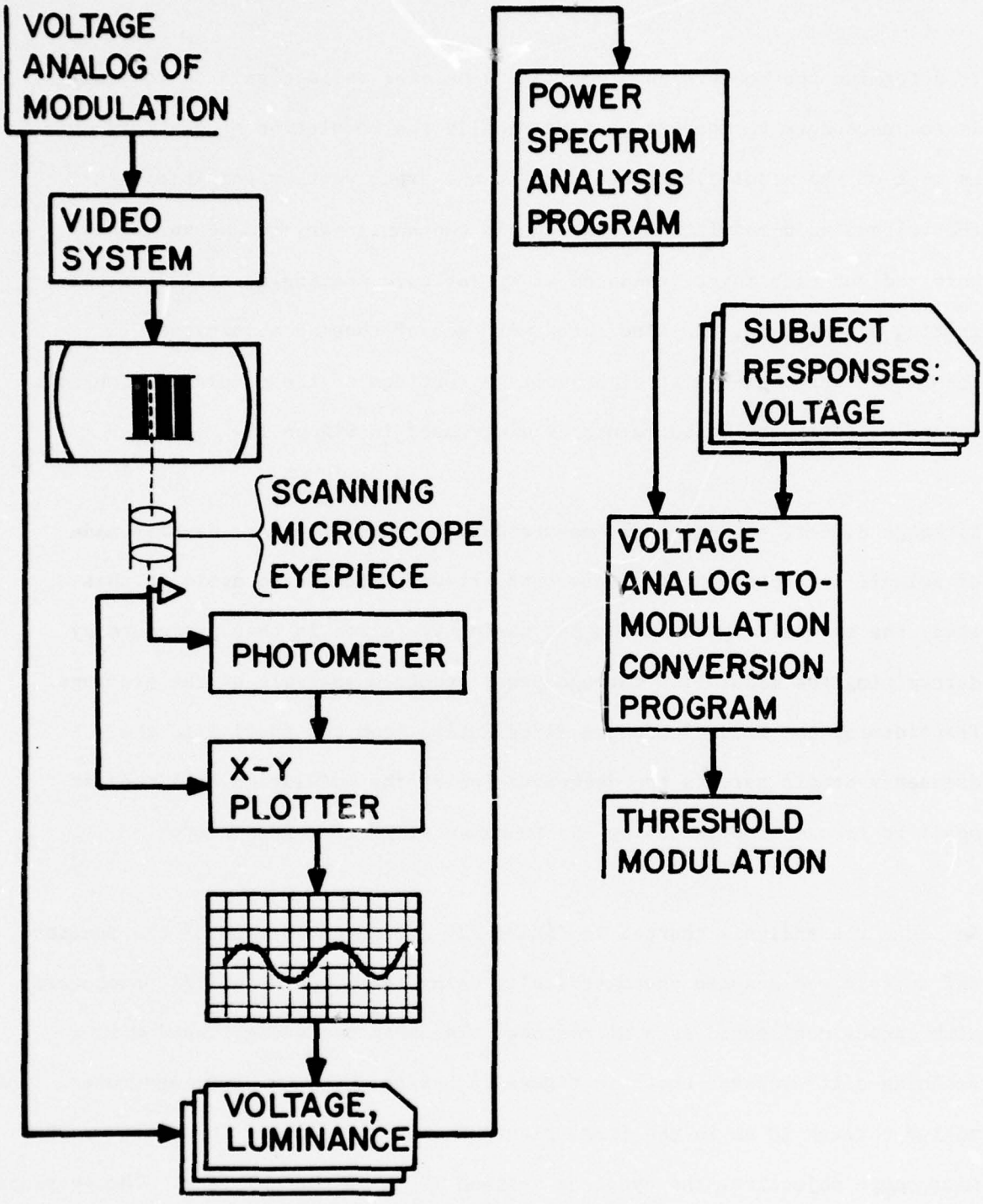

Figure 12. Diagram of Photometry Data Processing.

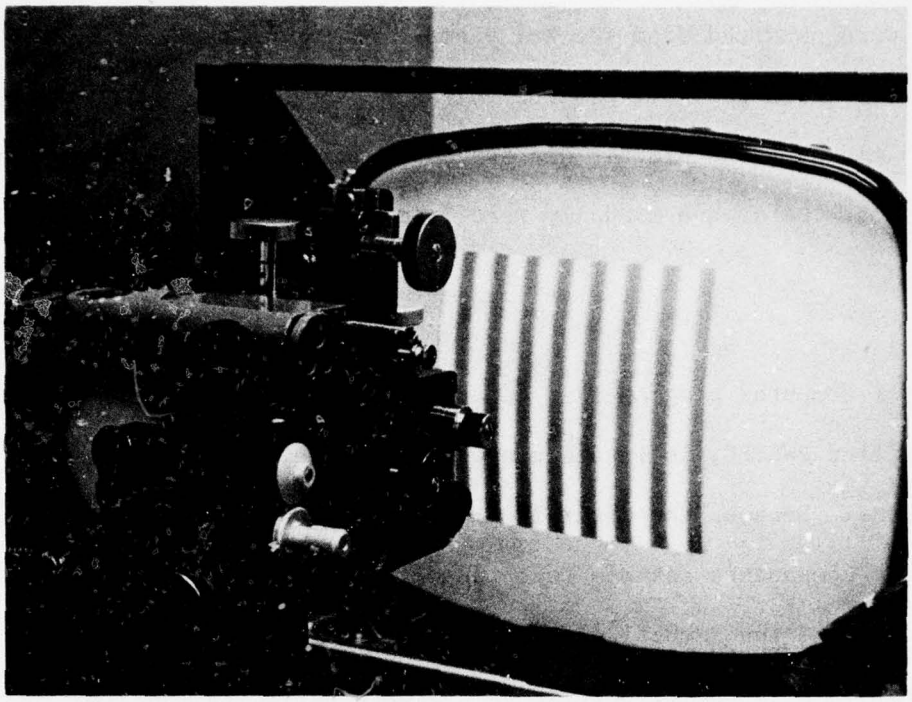

Figure 13. View of Photometer Microscope and Display.

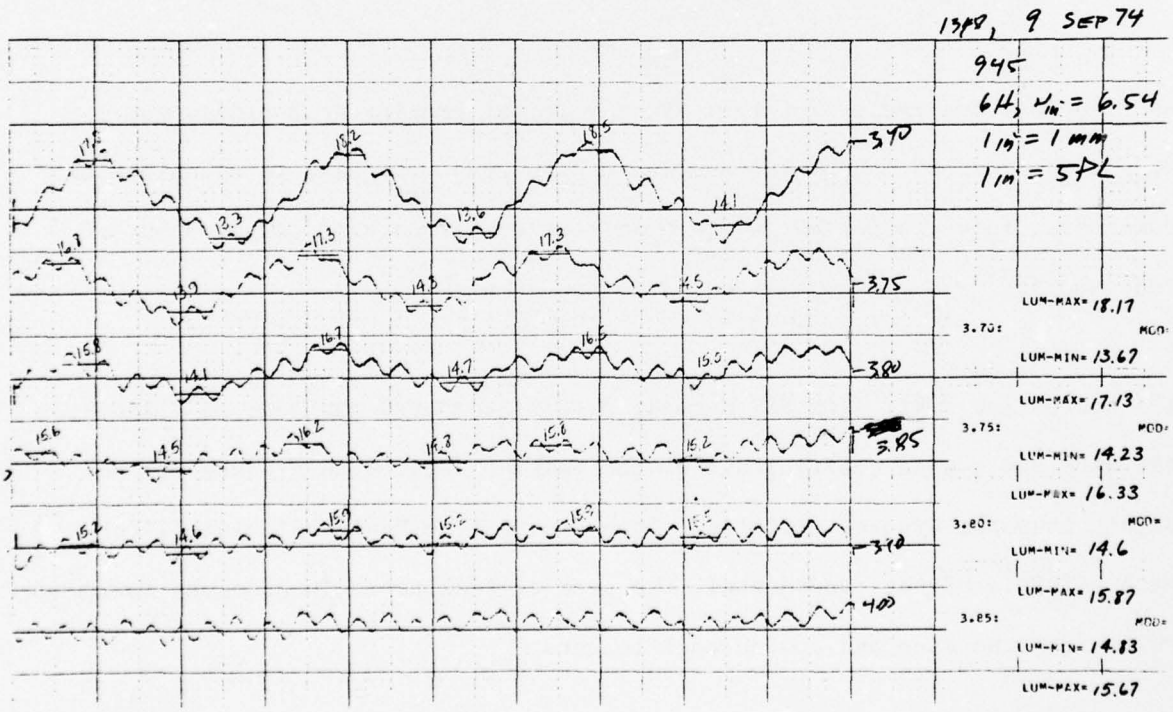

Figure 14. Copy of a Portion of the X-Y Plot for Target 6H, 945 Line Rate.

analysis were obtained from the X-Y plots. (Examples are in figure 14). Maximum resolution possible was 100 points per scan, or one luminance value every 2.5 mm where the plotter was scaled so that a 10 mm scan equaled a 25.4 cm plot. Data were manually read from the plots and punched on IBM cards.

The digital computer program that calculated the power spectrum for each target, titled PWRSPC, is listed elsewhere (Keesee, 1976) and described briefly here. Because the digital computation subprogram that calculated the Fourier components assumes that the data vector passed to it represents one cycle of the fundamental, it was necessary to calculate and input to the program as data the proportion of a scan equal to the largest integral number of cycles of the nominal spatial frequency for the target scanned. This vector length is called SCNSTP in the program.

As examples, one cycle of target 2V, a vertical grating at 2 c/deg, was 8.9 mm long, so 89 out of 100 samples of the scan were used to calculate the power spectrum. Target 4V, 4 c/deg, must also be analyzed using 89 out of 100 samples.

The subroutine FORIT (IBM SSP Manual, p. 275) computed the vectors *A* and *B*, the sine and cosine coefficients of the sampled data, with frequencies no higher than the Nyquist criteria. Then, subroutine POWER calculated, for each multiple of the fundamental, the peak-to-peak power in absolute luminance units from the sine and cosine coefficients:

$$P(\nu) = \sqrt{A(\nu)^2 + B(\nu)^2} \tag{6}$$

where ν = spatial frequency in integer multiples of the fundamental frequency,

$P(\nu)$ = peak-to-peak luminance power at ν,

$A(\nu)$ = sine coefficient at ν, and

$B(\nu)$ = cosine coefficient at ν.

Modulation of a grating or other target at spatial frequency ν is:

$$m(\nu) = \frac{L_{max} - L_{min}}{L_{max} + L_{min}} \tag{7}$$

where $m(\nu)$ = modulation at spatial frequency ν, an integer multiple of the scan fundamental,

L_{max} = maximum target luminance, and

L_{min} = minimum target luminance.

If L_{mean} = mean target luminance, then

$$m(\nu) = \frac{L_{max} - L_{min}}{2\ L_{mean}}. \tag{8}$$

The sine and cosine coefficients are defined to be the amplitudes of the sinusoidal waveform measured from the mean value to the peak value. Then, this amplitude is half of peak-to-peak amplitude. By calculating luminance power in the above manner, it becomes an amplitude measure, half of peak-to-peak, that disregards phase.

If ΔL = peak-to-peak luminance difference at spatial frequency ν, then

$$\Delta L = L_{max} - L_{min}$$

and

$$m(\nu) = \frac{\Delta L}{2\ L_{mean}} . \tag{9}$$

But $\Delta L = 2\ P(\nu)$

so

$$m(\nu) = \frac{P(\nu)}{L_{mean}} . \tag{10}$$

After computation of the modulation power spectrum, the program determined whether the proportion of the total photometric scan was less than 100 out of the 100 total samples. If this number, SCNSTP, was less than 100, then the above calculations were repeated for the sample from 2 to SCNSTP + 1, then 3 to SCNSTP + 2, etc. This iteration is performed 100 - SCNSTP times. After each iteration the modulation spectra were summed and then averaged at the end of the last iteration. This iterative process is necessary to obtain the greatest utilization possible from the relatively small number of samples per scan, and thereby generate a modulation estimate less influenced by occasional system transients and minor irregularities in the phosphor.

Since the initial length of the photometric scan used in these calculations was based on an assumed nominal spatial frequency that may be only close to the displayed spatial frequency, some adjustment was occasionally necessary. To find the required adjustment, the length of the photometric scan sample used initially was shortened by one sample and the process was repeated. This resulting modulation for the frequency of interest, the grating frequency, was compared with the first result. If the modulation was increased, the scan length was shortened until a maximum was reached. If the modulation after the first comparison was decreased, the scan length was increased in search

of a maximum. The spatial frequency of the target grating used in subsequent analyses was found from the scan length at the maximum modulation determined for each target.

It was not possible to determine through this described power spectrum analysis the modulation of targets with a spatial frequency of 1 c/deg because the eyepiece limited the photometric scan to 10 mm and this length included less than one complete cycle of the target. However, direct modulation measurements from the X-Y plots were taken from the photometric scans of all of the targets. The error trend in the direct measures compared with power spectrum results was applied as a correction to directly measured modulation estimates for the 1 c/deg targets. Direct measurement modulation estimates were also used to reconcile anomalies from the power spectrum analyses for the other spatial frequencies.

While the general procedure employed here to determine displayed modulation is believed to be sound, the specific implementation is uncertain at two extremes. First, a single sampling of one or more cycles of a low frequency grating gives little subjective confidence that these cycles are representative. Second, for the higher spatial frequencies, up to nine cycles of the grating were sampled but this results in approximately only ten samples of luminance per cycle. Doubt exists in this case when the grating is horizontal and imposed upon a raster where the sampling rate is little more than twice the fundamental raster frequency.

Two summary comments may be made on the conduct of the photometry. First, the original intent to use digital tape recording of the photometric scans with a sampling rate of 8000 or more samples per scan would probably have

produced more reliable modulation measures. Unfortunately, equipment failures precluded this approach. Second, the estimates produced by the power spectrum analysis, even with the limited samples, are much better than the direct modulation measures because they eliminate subjective error in determining maxima and minima.

EXPERIMENTAL PROCEDURE

Randomization

Within each line rate-noise passband combination, target spatial frequency, target orientation, and noise amplitude were randomized with the random order unique for each combination of subject, line rate, and noise passband. Further, the order of presentation of line rate-noise passband blocks was random and unique for each subject.

Subjects

Eight subjects were selected with the criteria that they have binocular visual acuity of 20/20, near and far, with correction if necessary, and at least 20/23 corrected monocular acuity and no other vision anomalies, including color vision, as measured by a Bausch and Lomb Orthorator. One of the eight subjects failed to complete the experiment and her data have been deleted. Five males and two females completed the experiment. The author was not a subject.

Subjects were paid at the rate of $3.00 per hr. Each subject spent about 20 hr. in the experiment.

Procedure

Several general rules governed the conduct of the experiment:

(1) During the operation of the experimental equipment, the mean luminance of the monitor was maintained at 51.4 to 52.4 cd/m^2. This was insured by checking the spot luminance of the monitor at least every 2 hr and at every change of line rate. Experience with more frequent luminance checks showed adjustment every 2 hr to be adequate.

(2) Subjects worked for no more than 2 hr per day.

(3) Subjects were given a 5 min break every 30 min.

(4) Subjects were given sufficient time to dark adapt when starting each experiment session.

The experimental room was kept dark. The only luminance sources in the room were the video monitor, a small reading lamp for each experimenter, and digital displays on counters and voltmeters. Just the video monitor was in the subject's field of view. The surfaces within the field of view surrounding the CRT, that is, the walls and equipment rack, had a luminance less than 3.1 cd/m^2.

Each subject had a minimum of 5 hr experience in this type of threshold determination task in earlier pilot experiments.

Once the subject was dark adapted, comfortably seated, and positioned with eyes centered on the monitor and at a viewing distance of 101.6 cm, the following trial procedure was executed:

(1) The assistant experimenter adjusted the frequency of the Wavetek

signal generator to the value necessary to create the target spatial frequency and orientation called for in the experiment program/data sheet. Input frequency was adjusted to an accuracy of three digits using a digital counter. With proper adjustment attained, the assistant experimenter informed the subject to proceed. As the assistant experimenter had to remove the trigger from the image generator to the Wavetek signal generator for the duration of his adjustment, it was only at the command to proceed that a grating appeared before the subject. This adjustment usually took less than 2 sec with practice by the assistant experimenter.

(2) During adjustment of the input frequency, the experimenter recorded on the program/data sheet the modulation of the second half (ascending) of the previous trial and adjusted the noise amplitude for the level given in the program/data sheet for the next trial.

(3) Starting from a position of high modulation, the subject reduced the grating modulation to the point where he/she could no longer distinguish separate bars in the grating. The subject was permitted to make control reversals as necessary until satisfied that he/she had reached this point. The subject then informed the experimenter that he/she had reached the criterion point.

(4) The experimenter noted the modulation (actually the gain-controlling voltage of the image generator modulation amplifier), told the subject to proceed, and recorded the value on the program/data sheet.

(5) The subject quickly turned the modulation to the near-zero position and then began to increase the modulation to the point where he/she was first able to visually distinguish separate bars in the grating. Upon reaching this point, the subject so informed the experimenter.

The steps above were repeated for each trial. The average trial cycle length was approximately 1 min although 40-sec trials were not unusual.

INITIAL DATA REDUCTION

The threshold data in the original form of gain voltage as an analog of modulation were converted to actual modulation values by a digital computer program. Essentially, the product of the photometry and power spectrum analysis described under PHOTOMETRY above was the basis for linear interpolation between the photometrically determined equivalence scale values.

SECTION III

RESULTS

INITIAL RESULTS

The modulation detectability threshold data, averaged across subjects and iterations, are shown graphically in figures 15 through 34. Each figure plots the thresholds for one combination of line rate, noise passband, and target orientation. Means are tabulated in Appendix C. Plotted with the means are the noise power functions at each noise amplitude and the modulation threshold curve for the 88.9 cm viewing distance from DePalma and Lowry (1962).

The general trends of the means are reasonable. The minimum modulation detectability threshold occurs between 4 and 9 c/deg. The narrower noise passbands produce higher thresholds. For the broad noise passband conditions, lower noise amplitudes produce modulation thresholds little different from zero noise conditions.

However, there are some incongruities within three of the target orientation-line rate groups. The plots for the 1225 line rate, vertical target orientation (figures 15-17) show the thresholds at 2 c/deg for all noise amplitudes and passbands to be greater than the thresholds at 1 c/deg or 3 c/deg. Within the 945 line rate (figures 28-30) horizontal data, there is an apparent depression of the modulation detectability thresholds between 4 and 7 c/deg. Part of this appearance may be due to elevation of the modulation thresholds below these frequencies; part of the appearance is also due to the uncertainty from the PWRSPC program results concerning the actual spatial frequency of target 7H at

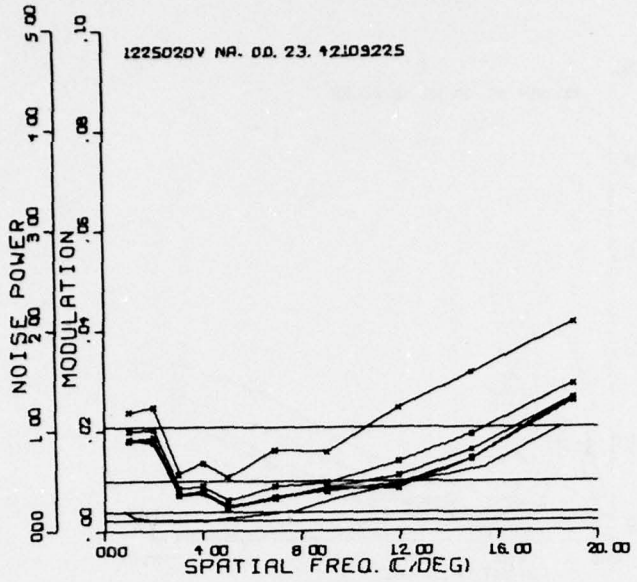

Figure 15. Modulation detectability threshold means (with x's) and noise power curves (without x's) for the line rate (1225), noise passband (0.0-20.0 MHz), target orientation (V), and noise amplitudes (0.0, 2.3, 4.2, 10.9, and 22.5 mV, rms) given in the legend in the upper left. Both sets of curves are generally in ascending order of noise amplitude with zero noise at the bottom. A modulation threshold function from DePalma and Lowry (1962) is also shown. Noise is in mV as a function of spatial frequency.

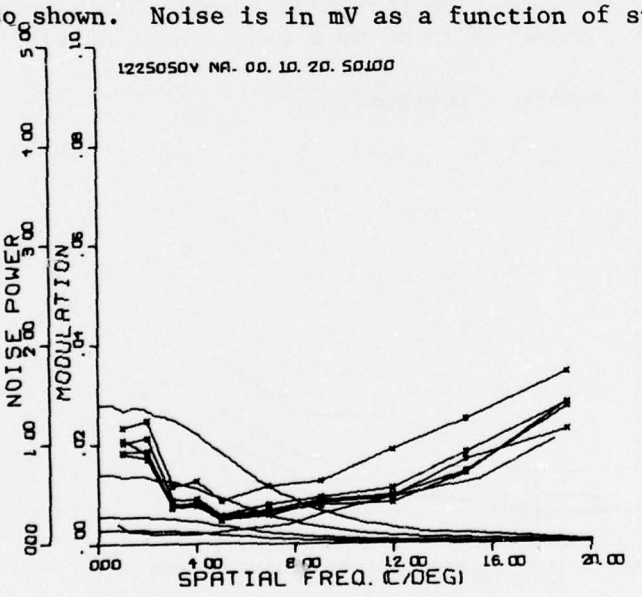

Figure 16. Modulation detectability threshold means (with x's) and noise power curves (without x's) for the line rate (1225), noise passband (0.0-5.0 MHz), target orientation (V), and noise amplitudes (0.0, 1.0, 2.0, 5.0, 10.0 mV, rms) given in the legend in the upper left. Both sets of curves are generally in ascending order of noise amplitude with zero noise at the bottom. A modulation threshold function from DePalma and Lowry (1962) is also shown. Noise is in mV as a function of spatial frequency.

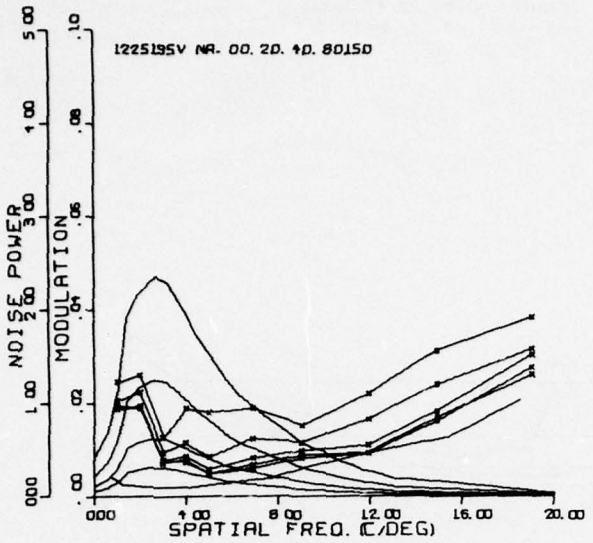

Figure 17. Modulation detectability threshold means (with x's) and noise power curves (without x's) for the line rate (1225), noise passband (1.9-5.0 MHz), target orientation (V), and noise amplitudes (0.0, 2.0, 4.0, 8.0, 15.0 mV, rms) given in the legend in the upper left. Both sets of curves are generally in ascending order of noise amplitude with zero noise at the bottom. A modulation threshold function from DePalma and Lowry (1962) is also shown. Noise is in mV as a function of spatial frequency.

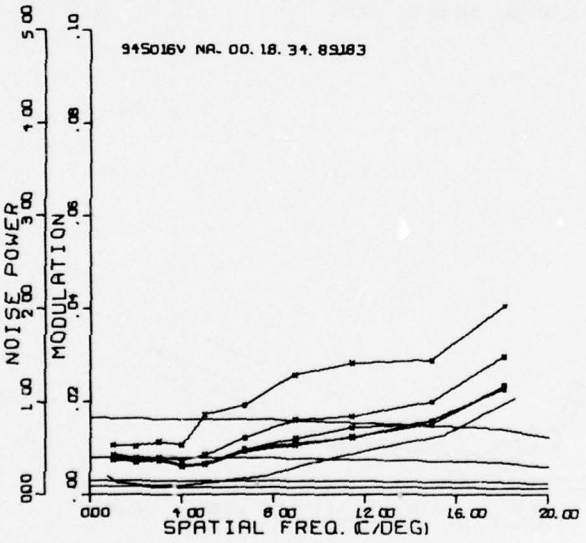

Figure 18. Modulation detectability threshold means (with x's) and noise power curves (without x's) for the line rate (945), noise passband (0.0-16.0 MHz), target orientation (V), and noise amplitudes (0.0, 1.8, 3.4, 8.9, 18.3 mV, rms) given in the legend in the upper left. Both sets of curves are generally in ascending order of noise amplitude with zero noise at the bottom. A modulation threshold function from DePalma and Lowry (1962) is also shown. Noise is in mV as a function of spatial frequency.

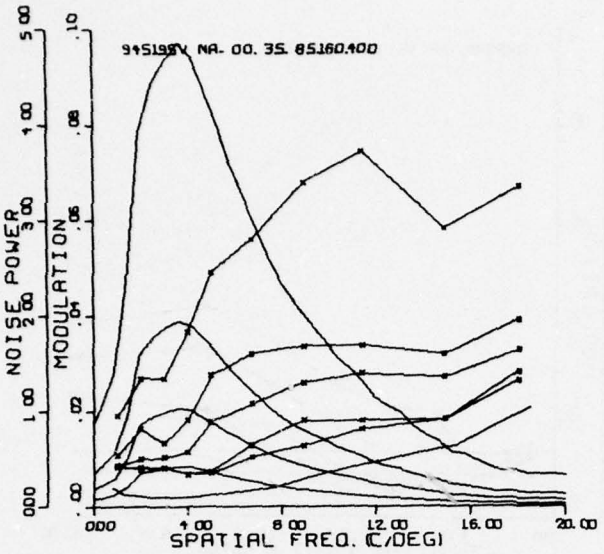

Figure 19. Modulation detectability threshold means (with x's) and noise power curves (without x's) for the line rate (945), noise passband (1.9-5.0 MHz), target orientation (V), and noise amplitudes (0.0, 3.5, 8.5, 16.0, 40.0 mV, rms) given in the legend in the upper left. Both sets of curves are generally in ascending order of noise amplitude with zero noise at the bottom. A modulation threshold function from DePalma and Lowry (1962) is also shown. Noise is in mV as a function of spatial frequency.

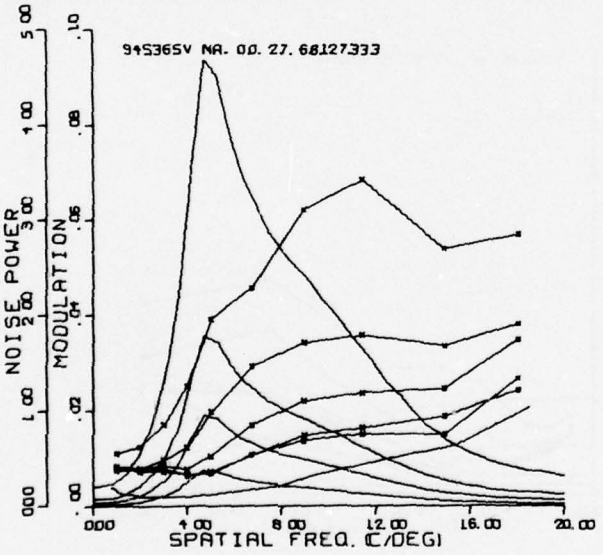

Figure 20. Modulation detectability threshold means (with x's) and noise power curves (without x's) for the line rate (945), noise passband (3.6-5.0 MHz), target orientation (V), and noise amplitudes (0.0, 2.7, 6.8, 12.7, 33.3 mV, rms) given in the legend in the upper left. Both sets of curves are generally in ascending order of noise amplitude with zero noise at the bottom. A modulation threshold function from DePalma and Lowry (1962) is also shown. Noise is in mV as a function of spatial frequency.

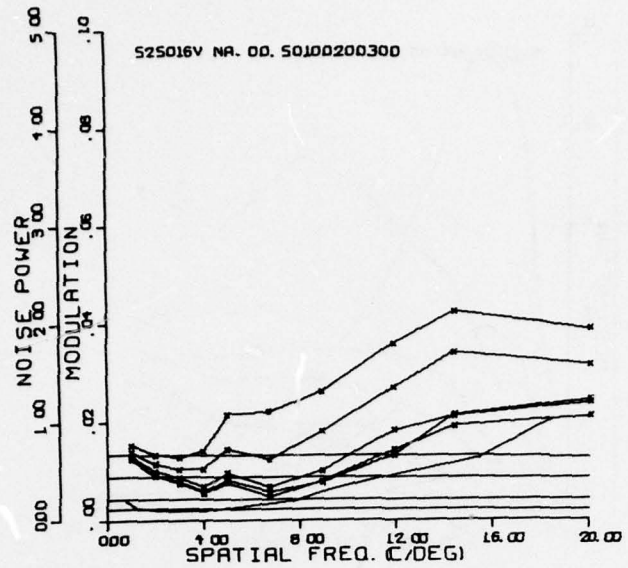

Figure 21. Modulation detectability threshold means (with x's) and noise power curves (without x's) for the line rate (525), noise passband (0.0-16.0 MHz), target orientation (V), and noise amplitudes (0.0, 5.0, 10.0, 20.0, 30.0 mV, rms) given in the legend in the upper left. Both sets of curves are generally in ascending order of noise amplitude with zero noise at the bottom. A modulation threshold function from DePalma and Lowry (1962) is also shown. Noise is in mV as a function of spatial frequency.

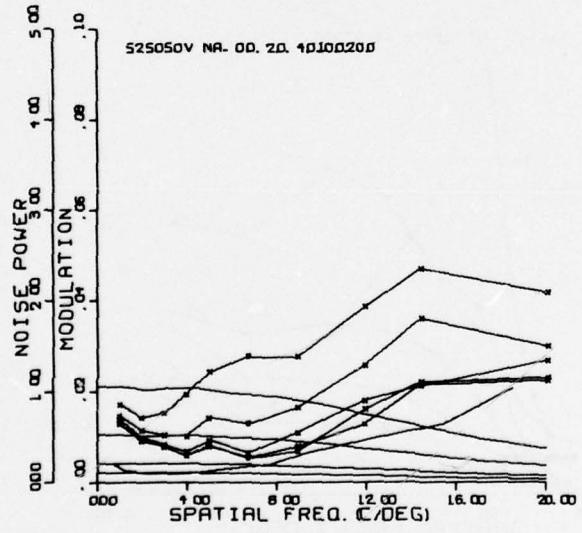

Figure 22. Modulation detectability threshold means (with x's) and noise power curves (without x's) for the line rate (525), noise passband (0.0-5.0 MHz), target orientation (V), and noise amplitudes (0.0, 2.0, 4.0, 10.0, 20.0 mV, rms) given in the legend in the upper left. Both sets of curves are generally in ascending order of noise amplitude with zero noise at the bottom. A modulation threshold function from DePalma and Lowry (1962) is also shown. Noise is in mV as a function of spatial frequency.

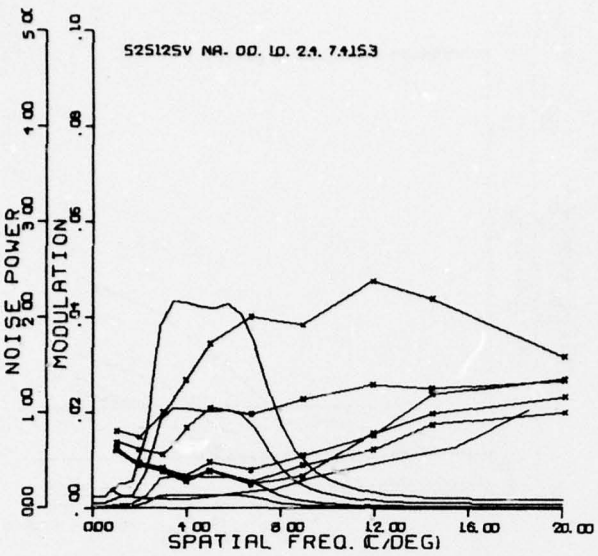

Figure 23. Modulation detectability threshold means (with x's) and noise power curves (without x's) for the line rate (525), noise passband (1.0-2.5 MHz), target orientation (V), and noise amplitudes (0.0, 1.0, 2.4, 7.4, 15.3 mV, rms) given in the legend in the upper left. Both sets of curves are generally in ascending order of noise amplitude with zero noise at the bottom. A modulation threshold function from DePalma and Lowry (1962) is also shown. Noise is in mV as a function of spatial frequency.

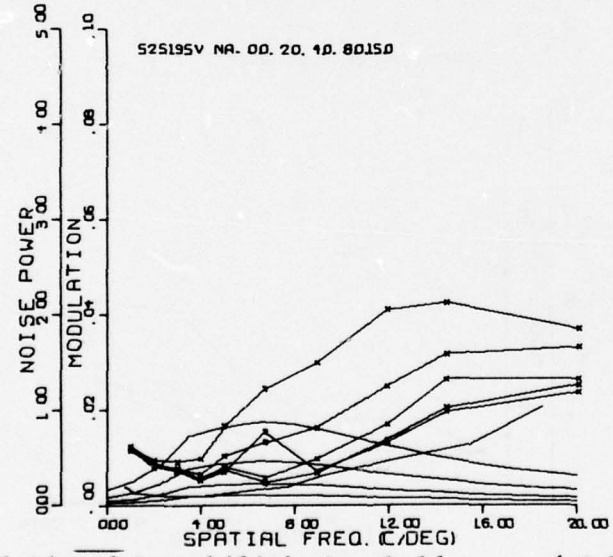

Figure 24. Modulation detectability threshold means (with x's) and noise power curves (without x's) for the line rate (525), noise passband (1.9-5.0 MHz), target orientation (V), and noise amplitudes (0.0, 2.0, 4.0, 8.0, 15.0 mV, rms) given in the legend in the upper left. Both sets of curves are generally in ascending order of noise amplitude with zero noise at the bottom. A modulation threshold function from DePalma and Lowry (1962) is also shown. Noise is in mV as a function of spatial frequency.

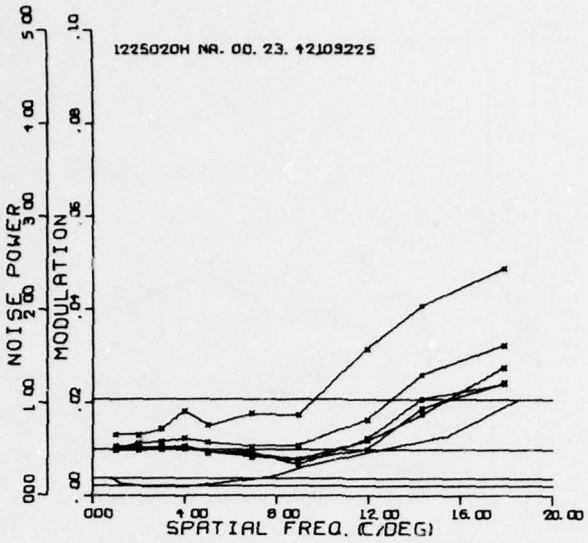

Figure 25. Modulation detectability threshold means (with x's) and noise power curves (without x's) for the line rate (1225), noise passband (0.0-20.0 MHz), target orientation (H), and noise amplitudes (0.0, 2.3, 4.2, 10.9, 22.5 mV, rms) given in the legend in the upper left. Both sets of curves are generally in ascending order of noise amplitude with zero noise at the bottom. A modulation threshold function from DePalma and Lowry (1962) is also shown. Noise is in mV as a function of spatial frequency.

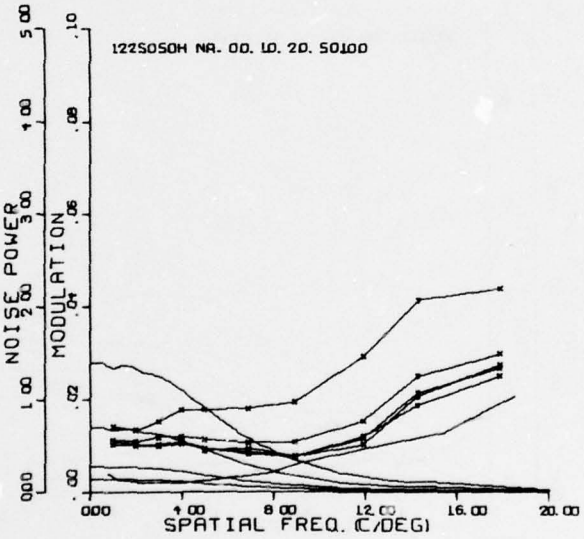

Figure 26. Modulation detectability threshold means (with x's) and noise power curves (without x's) for the line rate (1225), noise passband (0.0-5.0 MHz), target orientation (H), and noise amplitudes (0.0, 1.0, 2.0, 5.0, 10.0 mV, rms) given in the legend in the upper left. Both sets of curves are generally in ascending order of noise amplitude with zero noise at the bottom. A modulation threshold function from DePalma and Lowry (1962) is also shown. Noise is in mV as a function of spatial frequency.

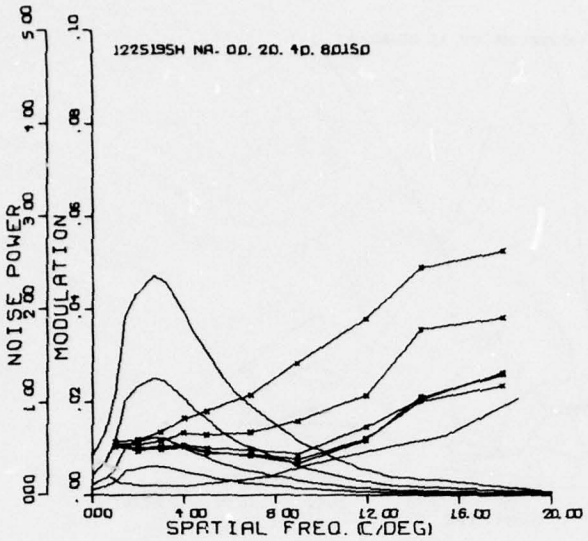

Figure 27. Modulation detectability threshold means (with x's) and noise power curves (without x's) for the line rate (1225), noise passband (1.9-5.0 MHz), target orientation (H), and noise amplitudes (0.0, 2.0, 4.0, 8.0, 15.0 mV, rms) given in the legend in the upper left. Both sets of curves are generally in ascending order of noise amplitude with zero noise at the bottom. A modulation threshold function from DePalma and Lowry (1962) is also shown. Noise is in mV as a function of spatial frequency.

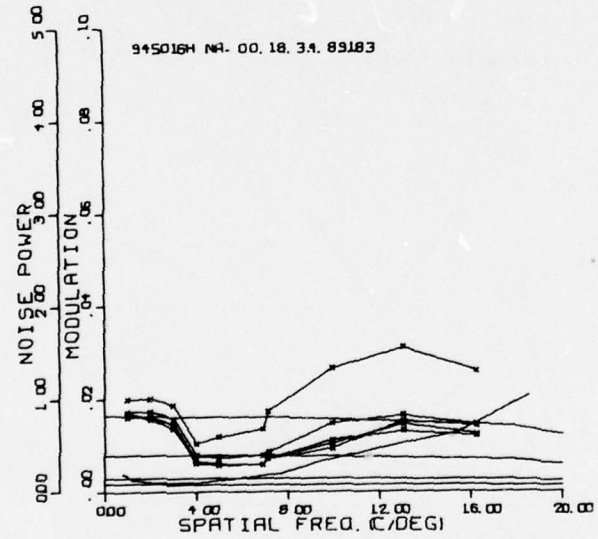

Figure 28. Modulation detectability threshold means (with x's) and noise power curves (without x's) for the line rate (945), noise passband (0.0-16.0 MHz), target orientation (H), and noise amplitudes (0.0, 1.8, 3.4, 8.9, 18.3 mV, rms) given in the legend in the upper left. Both sets of curves are generally in ascending order of noise amplitude with zero noise at the bottom. A modulation threshold function from DePalma and Lowry (1962) is also shown. Noise is in mV as a function of spatial frequency.

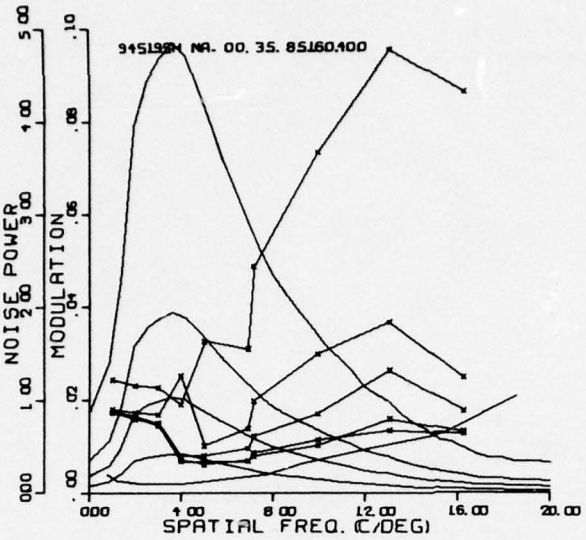

Figure 29. Modulation detectability threshold means (with x's) and noise power curves (without x's) for the line rate (945), noise passband (1.9-5.0 MHz), target orientation (H), and noise amplitudes (0.0, 3.5, 8.5, 16.0, 40.0 mV, rms) given in the legend in the upper left. Both sets of curves are generally in ascending order of noise amplitude with zero noise at the bottom. A modulation threshold function from DePalma and Lowry (1962) is also shown. Noise is in mV as a function of spatial frequency.

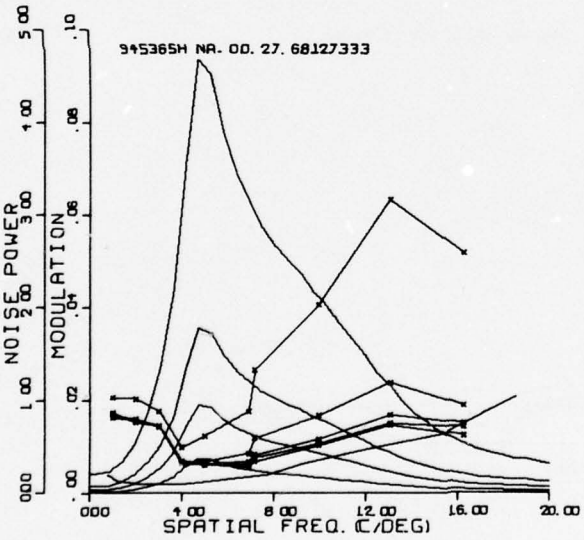

Figure 30. Modulation detectability threshold means (with x's) and noise power curves (without x's) for the line rate (945), noise passband (3.6-5.0 MHz), target orientation (H), and noise amplitudes (0.0, 2.7, 6.8, 12.7, 33.3 mV rms) given in the legend in the upper left. Both sets of curves are generally in ascending order of noise amplitude with zero noise at the bottom. A modulation threshold function from DePalma and Lowry (1962) is also shown. Noise is in mV as a function of spatial frequency.

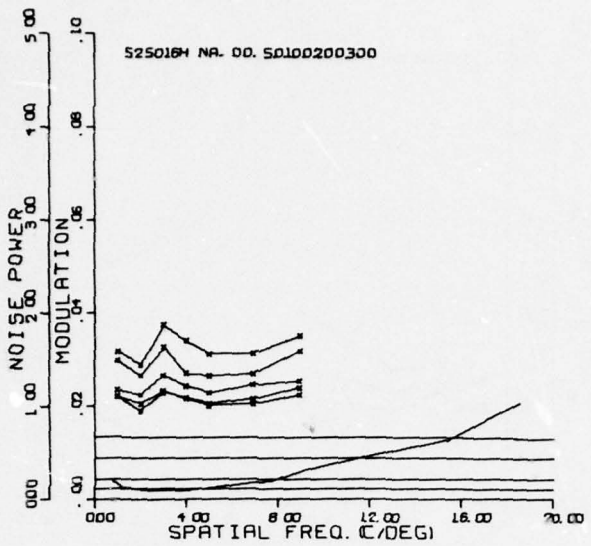

Figure 31. Modulation detectability threshold means (with x's) and noise power curves (without x's) for the line rate (525), noise passband (0.0-16.0 MHz), target orientation (H), and noise amplitudes (0.0, 5.0, 10.0, 20.0, 30.0 mV, rms) given in the legend in the upper left. Both sets of curves are generally in ascending order of noise amplitude with zero noise at the bottom. A modulation threshold function from DePalma and Lowry (1962) is also shown. Noise is in mV as a function of spatial frequency.

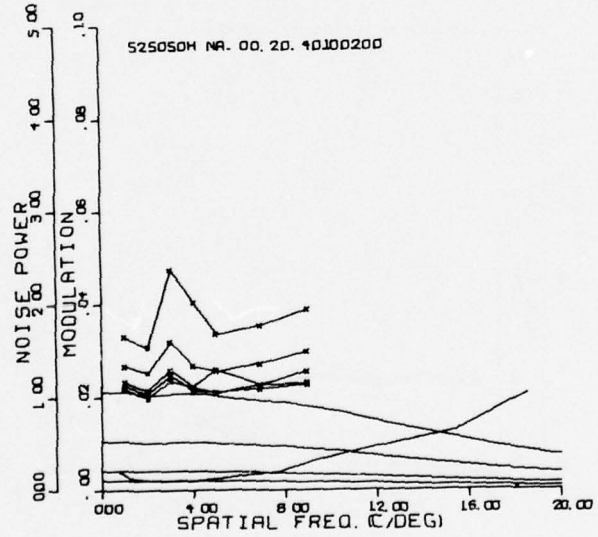

Figure 32. Modulation detectability threshold means (with x's) and noise power curves (without x's) for the line rate (525), noise passband (0.0-5.0 MHz), target orientation (H), and noise amplitudes (0.0, 2.0, 4.0, 10.0, 20.0 mV, rms) given in the legend in the upper left. Both sets of curves are generally in ascending order of noise amplitude with zero noise at the bottom. A modulation threshold function from DePalma and Lowry (1962) is also shown. Noise is in mV as a function of spatial frequency.

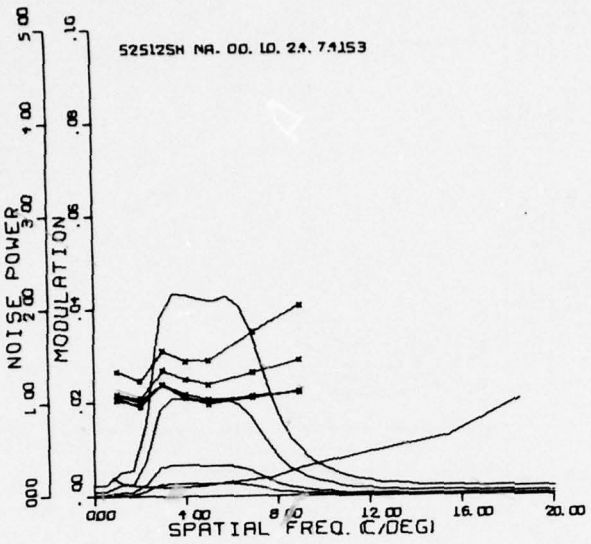

Figure 33. Modulation detectability threshold means (with x's) and noise power curves (without x's) for the line rate (525), noise passband (1.0-2.5 MHz), target orientation (H), and noise amplitudes (0.0, 1.0, 2.4, 7.4, 15.3 mV, rms) given in the legend in the upper left. Both sets of curves are generally in ascending order of noise amplitude with zero noise at the bottom. A modulation threshold function from DePalma and Lowry (1962) is also shown. Noise is in mV as a function of spatial frequency.

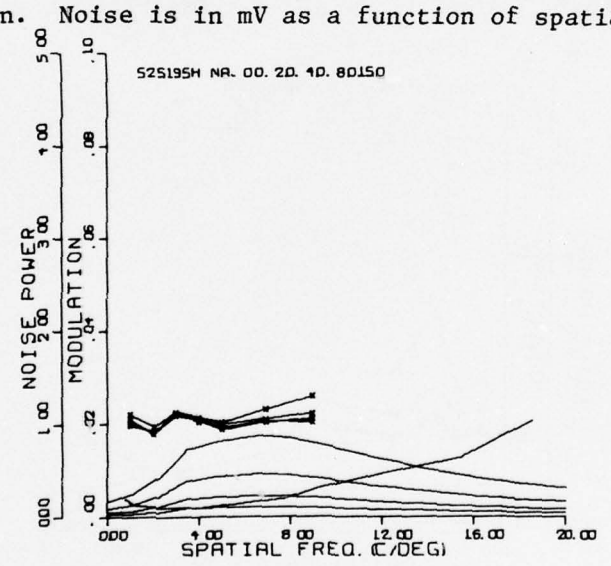

Figure 34. Modulation detectability threshold means (with x's) and noise power curves (without x's) for the line rate (525), noise passband (1.9-5.0 MHz), target orientation (H), and noise amplitudes (0.0, 2.0, 4.0, 8.0, 15.0 mV, rms) given in the legend in the upper left. Both sets of curves are generally in ascending order of noise amplitude with zero noise at the bottom. A modulation threshold function from DePalma and Lowry (1962) is also shown. Noise is in mV as a function of spatial frequency.

945. This is a target with a nominal spatial frequency of 9 c/deg, but given by the PWRSPC program as slightly above 7 c/deg.

And lastly, the 3 c/deg modulation detectability thresholds have an unreasonable elevation within the 525 line rate horizontal results (figures 31-34).

The only explanation for these anomalies is that errors or misadjustments in the photometry or unusual transients in the display equipment during the photometry caused incorrect conversion of modulation detectability thresholds from the original voltage gain values.

After determining that, within line rate and target orientation, the thresholds are equivalent at zero noise amplitude, the thresholds with noise can be compared with the confidence that differences are due to the character of the noise and that there is a common base to these comparisons. Using factorial comparisons based upon t-tests, there were very few significant differences ($p<.05$) among zero noise functions found for different noise passbands within each line rate. For example, in the vertical orientation condition, there was no difference among the zero noise amplitude means for the 0.0-20.0 MHz, 0.0-5.0 MHz, and 1.9-5.0 MHz noise passbands at the 1225 line rate. Results were similar at the other target orientation and line rate combinations. As would be expected, the zero noise means were generally different among combinations of target orientations and line rate.

Cursory investigation of the plotted means to determine the noise passband effects are stymied by the use of different sets of noise amplitudes within different noise passbands. Choice of the sets was discussed under Section II

above. To place the data in a comparable but simple form, simple regressions were applied. These regressions had the form:

$$m(\nu) = A + Bn^2 \qquad (11)$$

where $m(\nu)$ = modulation detectability threshold at spatial frequency ν for some line rate, noise passband, and target orientation,

A = constant of the regression (intercept),

B = regression coefficient, and

n = noise amplitude, rms mV.

One regression equation was computed for each target, *i.e.*, one computation of A and B for each grating spatial frequency, at each target orientation, and for each line rate-noise passband. Thus, there are 188 such equations and they are listed in Appendix D. Other forms of the noise amplitude variable were tried, but the n^2 form resulted in the best overall fit.

To aid visualization of the noise passband effects, these sample regression equations have been exercised at noise amplitudes of 0.0 and 20.0 mV rms with the predicted modulation detectability thresholds plotted as a function of spatial frequency with noise amplitude as a parameter. The noise power curve for 20 mV noise amplitude is also shown. These graphs are in figures 35 through 54.

A detailed examination of the results as they relate to noise passband effects using these figures will be segregated into vertical and horizontal sections since one would expect the effects of noise in general to be quite different for the two grating orientations.

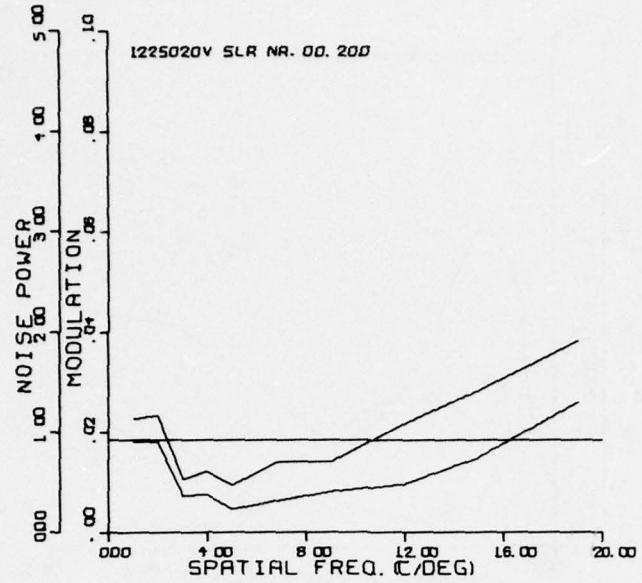

Figure 35. Modulation detectability functions predicted from simple regression and noise power curve for line rate (1225), noise passband (0.0-20.0), target orientation (V), and noise amplitude (0 and 20mV, rms) given in the legend at the upper left. Noise is mV as a function of spatial frequency.

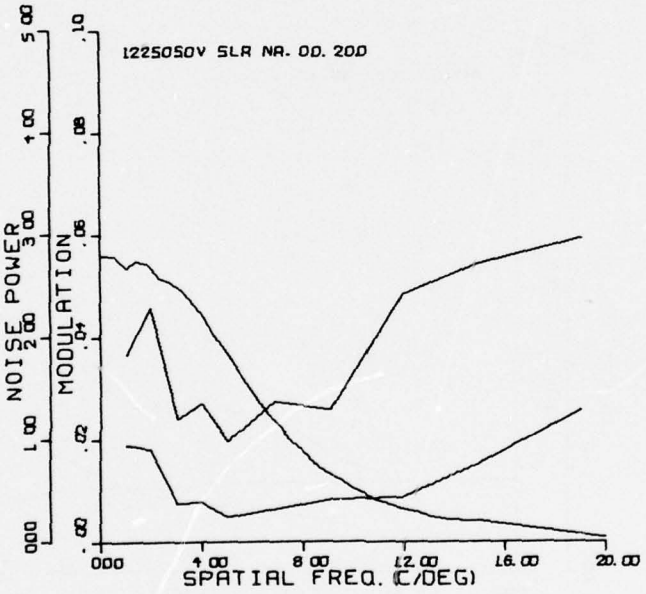

Figure 36. Modulation detectability functions predicted from simple regression and noise power curve for line rate (1225), noise passband (0.0-5.0), target orientation (V), and noise amplitude (0 and 20mV, rms) given in the legend at the upper left. Noise is mV as a function of spatial frequency.

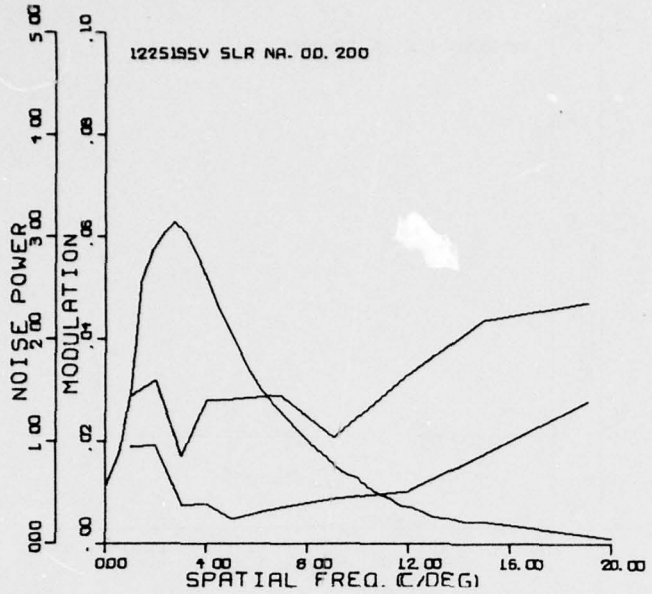

Figure 37. Modulation detectability functions predicted from simple regression and noise power curve for line rate (1225), noise passband (1.9-5.0), target orientation (V), and noise amplitude (0 and 20 mV, rms) given in the legend at the upper left. Noise is mV as a function of spatial frequency.

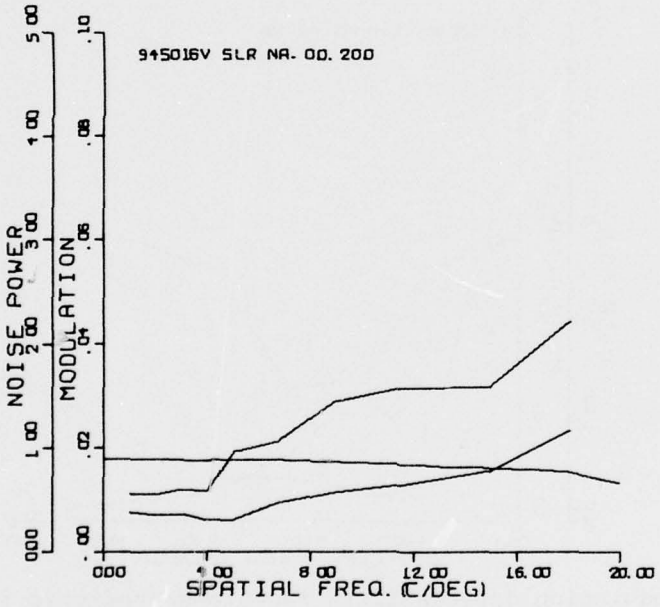

Figure 38. Modulation detectability functions predicted from simple regression and noise power curve for line rate (945), noise passband (0.0-16.0), target orientation (V), and noise amplitude (0 and 20 mV, rms) given in the legend at the upper left. Noise is mV as a function of spatial frequency.

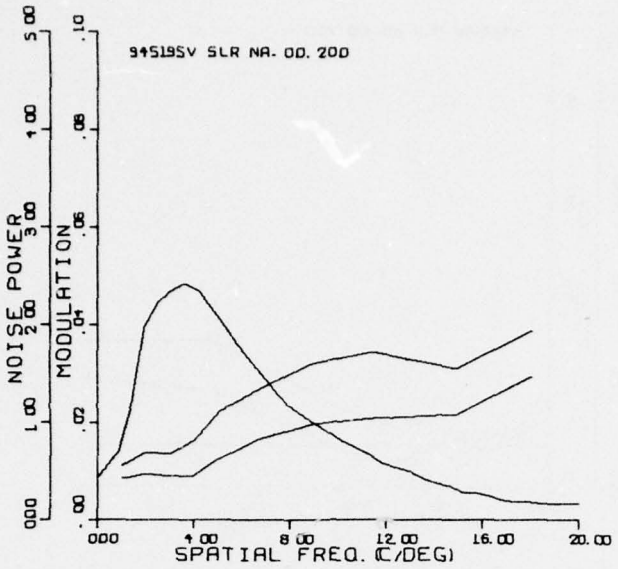

Figure 39. Modulation detectability functions predicted from simple regression and noise power curve for line rate (945), noise passband (1.9-5.0), target orientation (V), and noise amplitude (0 and 20 mV, rms) given in the legend at the upper left. Noise is mV as a function of spatial frequency.

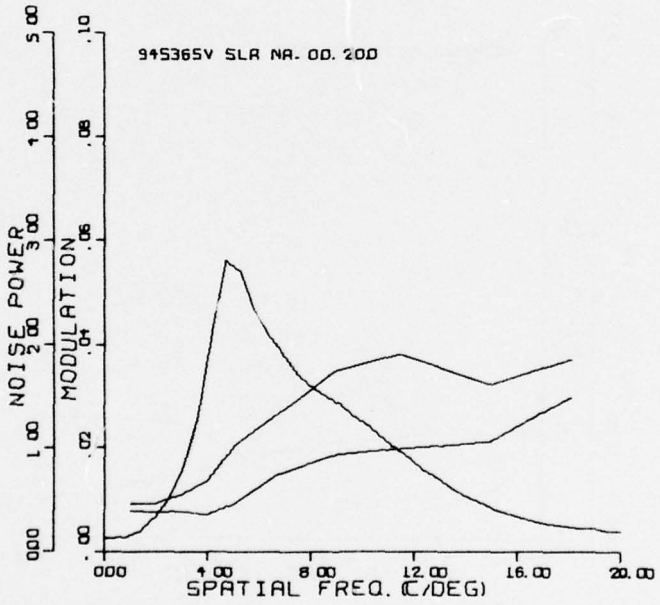

Figure 40. Modulation detectability functions predicted from simple regression and noise power curve for line rate (945), noise passband (3.6-5.0), target orientation (V), and noise amplitude (0 and 20 mV, rms) given in the legend at the upper left. Noise is mV as a function of spatial frequency.

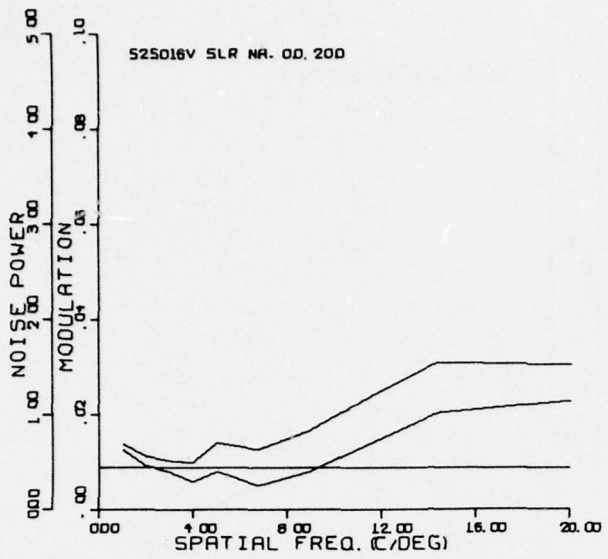

Figure 41. Modulation detectability functions predicted from simple regression and noise power curve for line rate (525), noise passband (0.0-16.0), target orientation (V), and noise amplitude (0 and 20 mV, rms) given in the legend at the upper left. Noise is mV as a function of spatial frequency.

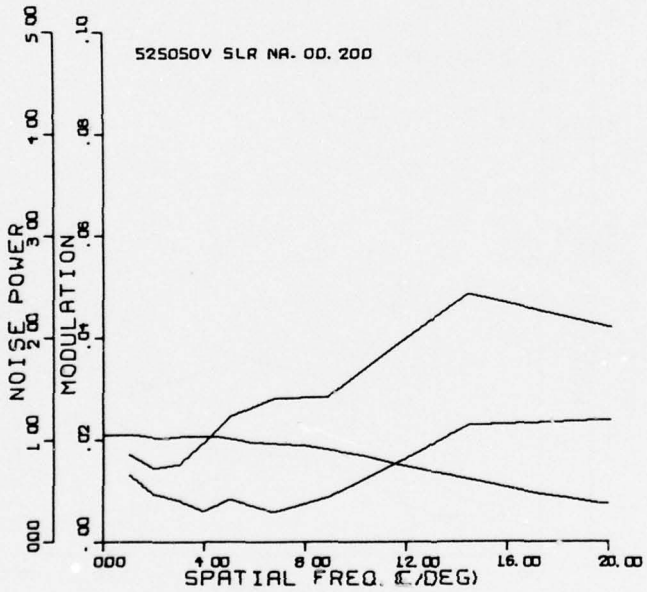

Figure 42. Modulation detectability functions predicted from simple regression and noise power curve for line rate (525), noise passband (0.0-5.0), target orientation (V), and noise amplitude (0 and 20 mV, rms) given in the legend at the upper left. Noise is mV as a function of spatial frequency.

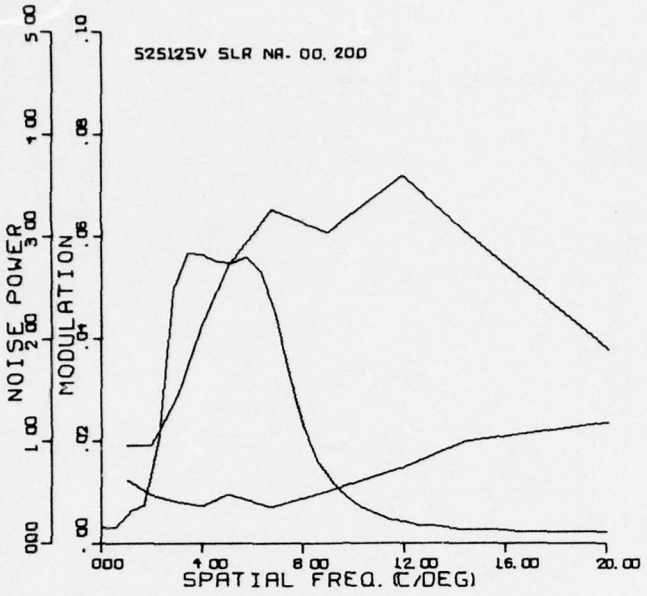

Figure 43. Modulation detectability functions predicted from simple regression and noise power curve for line rate (525), noise passband (1.0-2.5), target orientation (V), and noise amplitude (0 and 20 mV, rms) given in the legend at the upper left. Noise is mV as a function of spatial frequency.

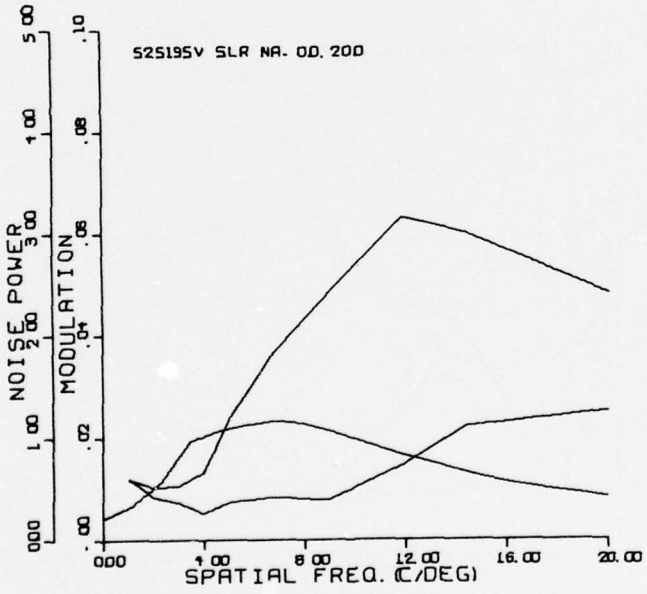

Figure 44. Modulation detectability functions predicted from simple regression and noise power curve for line rate (525), noise passband (1.9-5.0), target orientation (V), and noise amplitude (0 and 20 mV, rms) given in the legend at the upper left. Noise is mV as a function of spatial frequency.

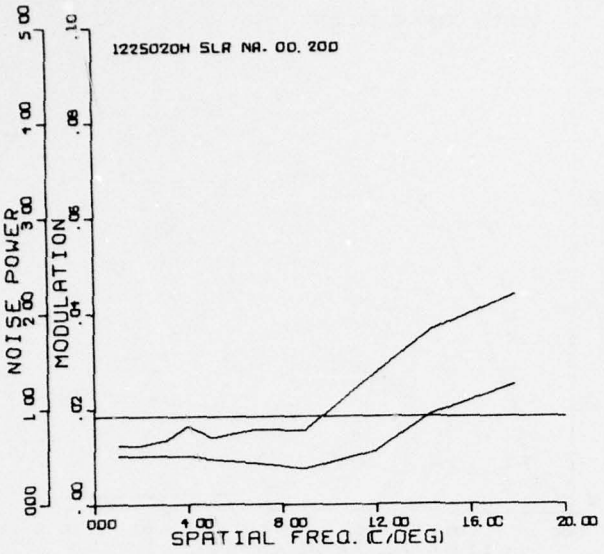

Figure 45. Modulation detectability functions predicted from simple regression and noise power curve for line rate (1225), noise passband (0.0-20.0), target orientation (H), and noise amplitude (0 and 20 mV, rms) given in the legend at the upper left. Noise is mV as a function of spatial frequency.

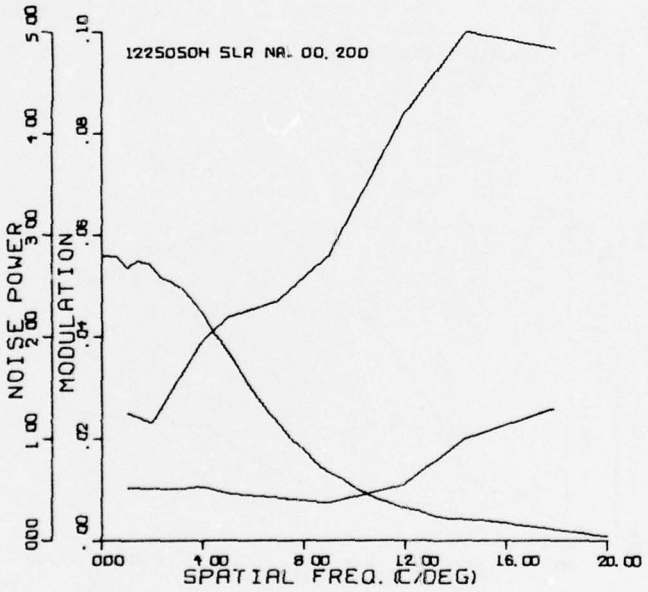

Figure 46. Modulation detectability functions predicted from simple regression and noise power curve for line rate (1225), noise passband (0.0-5.0), target orientation (H), and noise amplitude (0 and 20 mV, rms) given in the legend at the upper left. Noise is mV as a function of spatial frequency.

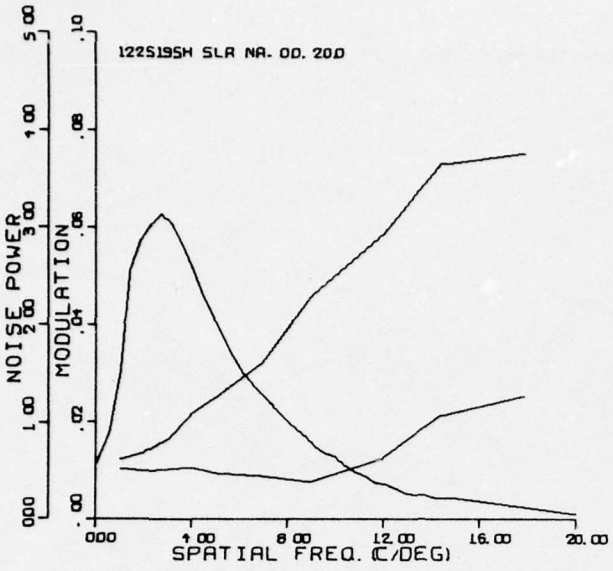

Figure 47. Modulation detectability functions predicted from simple regression and noise power curve for line rate (1225), noise passband (1.9-5.0), target orientation (H), and noise amplitude (0 and 20 mV, rms) given in the legend at the upper left. Noise is mV as a function of spatial frequency.

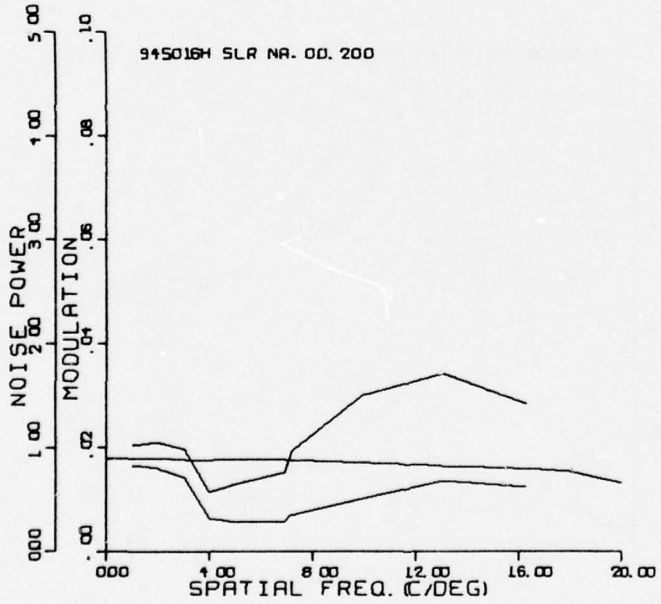

Figure 48. Modulation detectability functions predicted from simple regression and noise power curve for line rate (945), noise passband (0.0-16.0), target orientation (H), and noise amplitude (0 and 20 mV, rms) given in the legend at the upper left. Noise is mV as a function of spatial frequency.

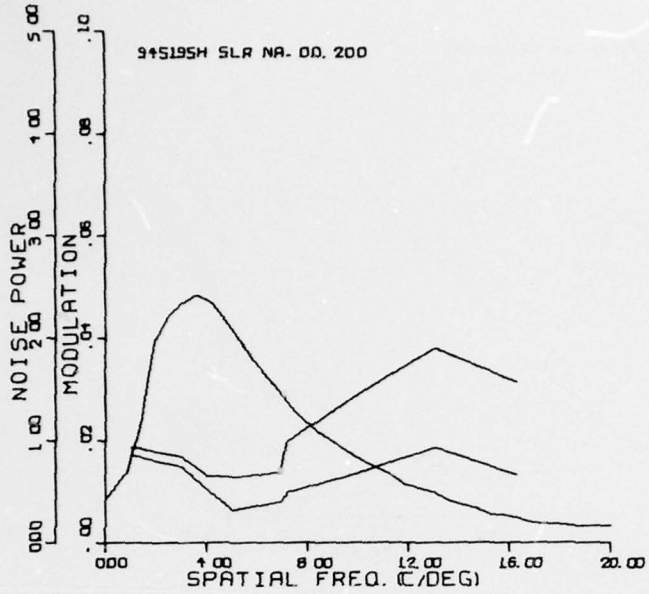

Figure 49. Modulation detectability functions predicted from simple regression and noise power curve for line rate (945), noise passband (1.9-5.0), target orientation (H), and noise amplitude (0 and 20 mV, rms) given in the legend at the upper left. Noise is mV as a function of spatial frequency.

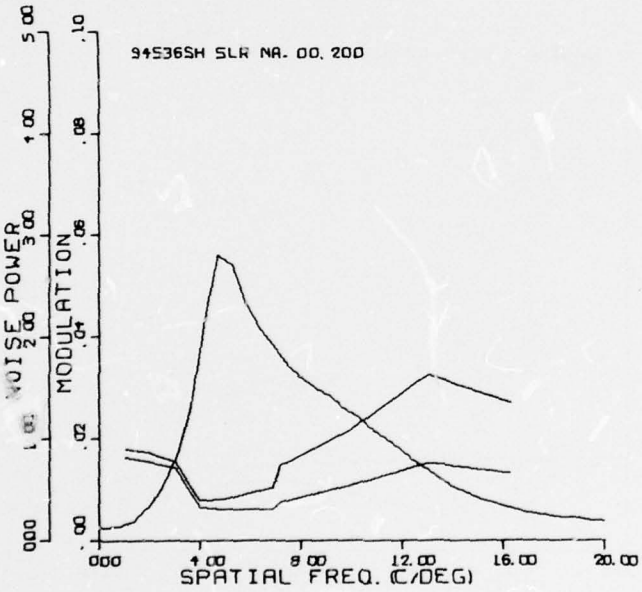

Figure 50. Modulation detectability functions predicted from simple regression and noise power curve for line rate (945), noise passband (3.6-5.0), target orientation (H), and noise amplitude (0 and 20 mV, rms) given in the legend at the upper left. Noise is mV as a function of spatial frequency.

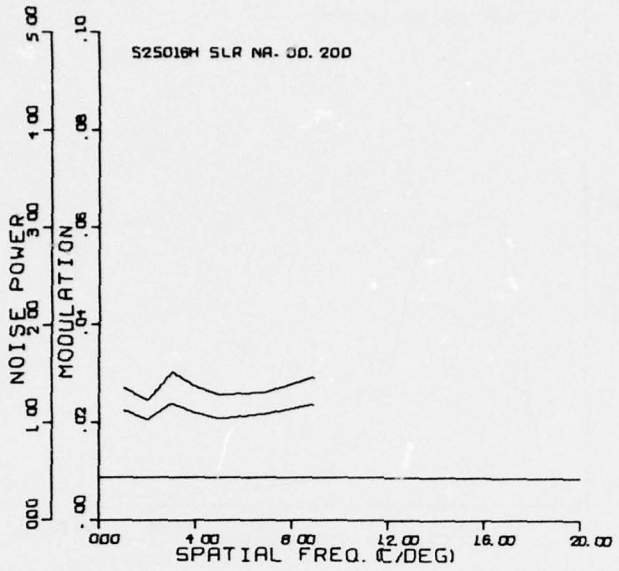

Figure 51. Modulation detectability functions predicted from simple regression and noise power curve for line rate (525), noise passband (0.0-16.0), target orientation (H), and noise amplitude (0 and 20 mV, rms) given in the legend at the upper left. Noise is mV as a function of spatial frequency.

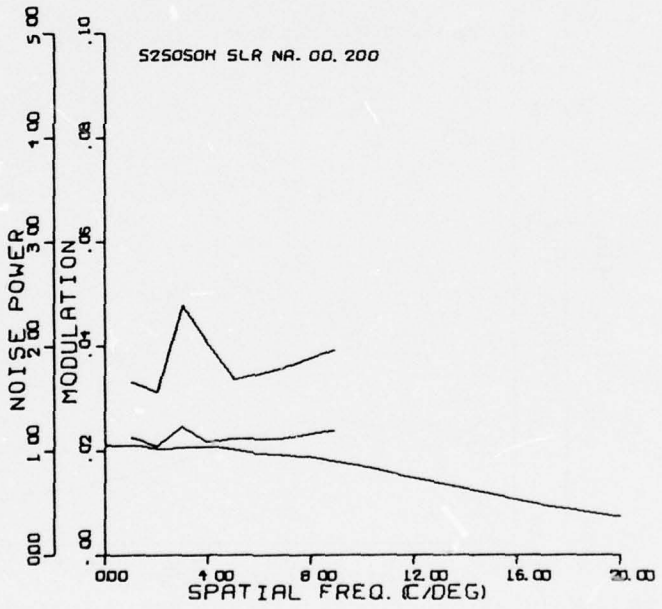

Figure 52. Modulation detectability functions predicted from simple regression and noise power curve for line rate (525), noise passband (0.0-5.0), target orientation (H), and noise amplitude (0 and 20 mV, rms) given in the legend at the upper left. Noise is mV as a function of spatial frequency.

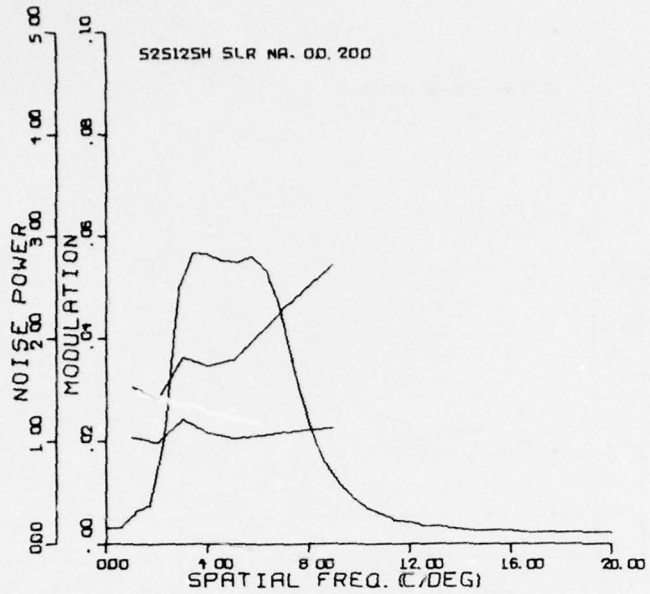

Figure 53. Modulation detectability functions predicted from simple regression and noise power curve for line rate (525), noise passband (1.0-2.5), target orientation (H), and noise amplitude (0 and 20 mV, rms) given in the legend at the upper left. Noise is mV as a function of spatial frequency.

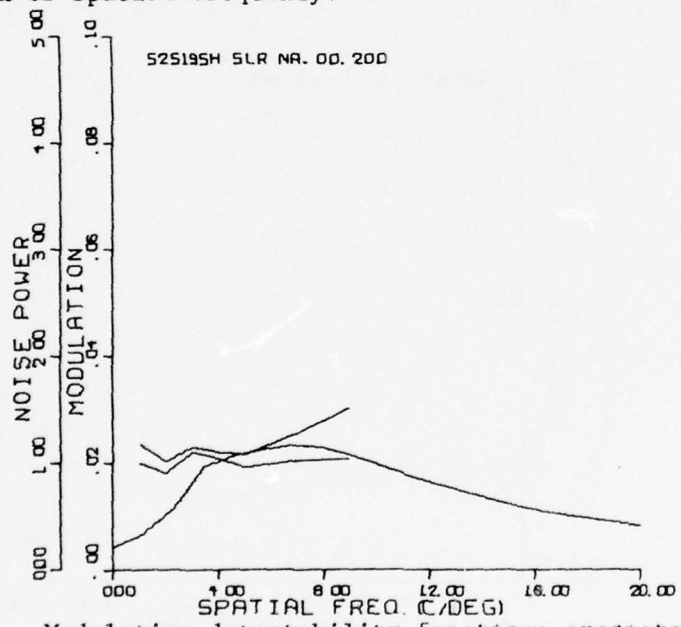

Figure 54. Modulation detectability functions predicted from simple regression and noise power curve for line rate (525), noise passband (1.9-5.0), target orientation (H), and noise amplitude (0 and 20 mV, rms) given in the legend at the upper left. Noise is mV as a function of spatial frequency.

Vertical

It seems that the difference between the 0.0 and 20.0 mV curves at 1225 0.0-20.0 MHz increases with spatial frequency. This is reasonable because it indicates that the broadband noise raises the threshold modulation proportionately rather than absolutely. Curves are similar for the other line rates at the broad noise passbands.

In the figures for 1225 0.0-20.0 MHz and 0.0-5.0MHz (figures 35 and 36), the zero noise amplitude curves are virtually identical. Also, the 20 mV curve for the 0.0-5.0 MHz passband has a two to three times greater difference from the zero curve than the 0.0-20.0 MHz curve. In the plot for 1225 V, 1.9-5.0 MHz (figure 37), the 20 mV curve also has a greater elevation above the zero noise curve than that of the 0.0-20.0 noise passband, but it is not the same as the elevation for the 0.0-5.0 MHz band.

The 0.0-5.0 curve for 20 mV generally exceeds that for 1.9-5.0 except for the spatial frequency region just above the vicinity of the peak of the 1.9-5.0 noise power spectrum.

Although similar, but only faintly discernable, trends may be spotted in the 945 V plots (figures 38-40), the 525 V plots (figures 41-44) are more instructive. The narrow, 0.0-5.0 MHz, noise passband (figure 42) is uniformly higher than the broadband 0.0-16.0 (figure 41) with allowance for greater noise effect at higher spatial frequencies. The very narrow 1.0-2.5 (figure 43) MHz band produces a startlingly high threshold for spatial frequencies at and above the peak of the noise spectra. While there is threshold elevation at

the lowest and the highest target grating spatial frequencies, it is very small compared with elevation in the mid-range.

The noise spectrum of the 1.9-5.0 MHz noise passband (figure 44) is much broader than that of the 1.0-2.5 MHz noise passband (figure 43) although both would be called narrow with reference to the 0.0-16.0 MHz noise passband (figure 41). They also produce different results. The modulation detectability threshold for the 1.9-5.0 MHz noise passband (figure 44) at 20 mV noise amplitude is no different than that at zero noise at 1 c/deg. The elevation of the modulation threshold for 1.9-5.0 MHz (figure 44) over the broad noise passband (figure 41) is greatest at spatial frequencies slightly above the peak of the noise spectra. The threshold elevation is reduced somewhat at the highest spatial frequencies, but is still substantially higher than the broadband curve.

There would appear to be four influences on modulation detectability thresholds identified in this examination of the data for vertical target gratings:

(1) In both comparisons of a 0.0-5.0 MHz noise passband with a broad noise passband, thresholds were generally higher over all spatial frequencies. This implies that the noise-limited modulation detectability threshold is more sensitive to the noise power in the low spatial frequencies. A variable that might represent this sensitivity is the integration of noise power below 2 c/deg.

(2) It is evident from the data for vertical targets at the narrower noise passbands, especially at the 1.0-2.5 MHz noise passband at 525 line rate (figure 23), that the concentration of the noise power over a small spatial frequency band tends to raise modulation detectability thresholds over all

spatial frequencies.

(3) It further follows from a review of the narrow noise passband data that the modulation detectability threshold at a particular spatial frequency is raised by noise power concentrated within the same spatial frequency region. Most plots for narrow noise passbands showed a weighted integral effect; that is, threshold elevation was greatest at spatial frequencies slightly higher than the spatial frequency of the peak noise power.

(4) There is some indication from the medium-width noise passbands that the effect of noise power is cumulative toward higher spatial frequency. For example, the differences in modulation detectability threshold for a grating of 5 c/deg for a broad and a narrow noise passband might be predicted, in part, by the noise power integrated up to 5 c/deg.

Horizontal

A review of the data for the horizontally oriented gratings shows evidence of the same trends that stand out for the vertical gratings. The single addition is that the zero noise modulation detectability thresholds are considerably higher for the 525 line rate than for either of the higher line rates. Differences between 1225 and 945 are uncertain.

MODEL DEVELOPMENT

Development of a predictive model from the experimental data required that variables be improvised that would represent the trends identified above as well as other pertinent parameters. These improvised and adapted variables became candidates for the model. Selection from among these candidates was

by multiple iteration and adjustment of a step-wise multiple regression digital computer program.

Description of the quantification of these variables follows.

The first trend listed above was the implication that the amount of noise power at low spatial frequencies, probably less than 2 c/deg, increased the modulation detectability threshold at all spatial frequencies. The implied variable, called LFINT for "low frequency integration", was defined as:

$$\text{LFINT} = n \int_0^2 N(\nu)\, d\nu \tag{12}$$

where n = noise amplitude in rms mV,

ν = spatial frequency in c/deg, and

$N(\nu)$ = noise power as a function of spatial frequency for a noise amplitude of 1 mV rms.

Values of LFINT were principally computed for each noise amplitude at each noise passband.

The second improvised variable was an attempt to represent the concentration of noise power in a narrow spatial frequency. This was accomplished by taking a second moment about the mean noise power. The variable, CONNP, is computed as:

$$\text{CONNP} = \frac{n}{\nu_o} \int_0^\infty (N(\nu) - \bar{N})^2\, d\nu \tag{13}$$

where $\bar{N}$ = mean noise power, and

ν_o = spatial frequency at which noise power declines to zero.

It seemed apparent above, and was suggested by Stromeyer and Julesz (1972), that the modulation detectability threshold at a given spatial frequency is affected by noise in the surrounding spatial frequency region. The thresholds for narrow noise passbands gave the appearance that this influence had unequal weighting of the noise power with noise at frequencies slightly above the target frequency having the greatest effect. The variable, NPSFT, is defined to be:

$$\text{NPSFT} = n \int_{\nu_T - 3}^{\nu_T + 1} (\nu - (\nu_T - 3))N(\nu)\, d\nu \tag{14}$$

where ν_T = target grating spatial frequency.

The last of the noise power related improvised variables represents the effect of the integrated noise power of frequencies below that of the target spatial frequency. This variable, CUMNP, partially shares the constituency of LFINT and NPSFT and is defined to be:

$$\text{CUMNP} = \frac{n}{\nu_T} \int_0^{\nu_T} N(\nu)\, d\nu. \tag{15}$$

Four variables were generated to include the interference effect of the raster. The first was the inverse of the raster frequency, a variable that would be higher for the more detrimental 525 line rate:

$$\text{ORSF} = \frac{1}{\nu_R} \tag{16}$$

where ν_R = spatial frequency of the fundamental raster frequency.

The second raster variable was like the first but weighted by the raster modulation:

$$\text{RASMOD} = \frac{M_R}{\nu_R} \tag{17}$$

where M_R = modulation of the raster.

Two other variables were constructed to compare the raster frequency to the target grating frequency. These were:

$$\text{OR-TSF} = \frac{1}{\nu_R - \nu_T} \tag{18}$$

and

$$\text{MORTSF} = \frac{M_R}{\nu_R - \nu_T}. \tag{19}$$

These variables, along with offspring of these and basic parameters of the experiment trials such as noise amplitude and grating spatial frequency, were input to the step-wise regression. The candidate variables with descriptions are listed in Appendix E.

The step-wise regression program used was BMD02R (revised March 27, 1973) written by Health Sciences Computing Facility, UCLA (Dixon, 1973). This regression procedure admits one variable at a time to the regression equation, beginning with the variable that contributes the most reduction to the error sum of squares. This criterion is measured by the *F*-ratio for the variable's regression coefficient. At each successive step, a variable is entered or removed, and then new *F*-ratios are computed for evaluating the potential reduction in remaining error sum of squares of each variable not in the equation. A variable may be entered only if its *F*-ratio is the greatest of any not in the equation and if it is greater than some preset value. A variable is removed from the equation if its *F*-ratio falls below a preset value. The

minimum *F*-ratio to enter and the *F*-ratio to remove were both set equal to the very liberal 1.0. The procedure continues until no variable has an *F*-ratio great enough to enter. The facility exists for forcing one or more variables into the regression equation. A forced variable is entered in steps before non-forced variables provided its *F*-ratio is greater than the minimum *F*-ratio to enter.

Development of the models, one for vertical target gratings and one for horizontal, progressed through many repeated applications of the regression program to the complete experiment data set, followed by modification and adjustment of promising variables and addition of new variable combinations where warranted. Each of these two data sets, one for each target orientation, consisted of 14 replications (2 per subject, 7 subjects) at each combination of line rate-noise passband, spatial frequency, and noise amplitude. Thus, there were 7000 degrees of freedom for the vertical orientation and 6160 for the horizontal.

Vertical Model

There are two resulting equations for each target grating orientation. The first is the result of allowing the program to choose variables solely on their contributions to reduced error. A summary table for this freely run step-wise regression on the vertical targets across all conditions is in table 4. Although the program executed 31 steps, only the first five are given in the table. The regression showed that the first variable entered, CUMNP, had an R^2 = 0.4963, which indicates that the equation at the first step accounted for more than 49% of the variance in modulation detectability

Table 4. Summary of Results from Step-Wise Regression on Modulation Thresholds for Vertical Gratings.

Step	R	R^2	ΔR^2	Variable Entered	Equation: Modulation x 10^3 =
1	.7045	.4963	.4963	CUMNP	= 11.0 + 0.000177 CUMNP
2	.7479	.5593	.0630	$(SF-7)^2$	= 9.25 + 0.000161 CUMNP + 0.0493 $(SF-7)^2$
3	.7658	.5863	.0271	NPSFT	= 7.81 + 0.000133 CUMNP + 0.0622 $(SF-7)^2$ + 0.000440 NPSFT
4	.7803	.6089	.0225	$(SF-10)^2SF$	= 6.28 + 0.000123 CUMNP + 0.184 $(SF-7)^2$ + 0.000542 NPSFT - 0.00841 $(SF-10)^2$
5	.7877	.6205	.0116	LFINT	= 6.68 + 0.000140 CUMNP + 0.190 $(SF-7)^2$ + 0.000719 NPSFT - 0.00886 $(SF-10)^2$ - 0.000245 LFINT

Asymptotes: R = .8142

R^2 = .6628

Steps to End: 31

Number of Variables Entered at End: 23

Total Degrees of Freedom: 7000

thresholds. The inclusion of just two more variables yielded an equation that accounted for almost 59% of the total variance, less than 8% short of the asymptotic value, 66%. This asymptote is significant because it shows that even with a very large equation, containing 23 variables, 34% of the variance is not accounted for. It must be assumed, then, that this 34% is within- and between-subject and other random error, and that prediction of 66% of the variance may be the best that can reasonably be expected.

Because the step-wise regression permits one to judge the importance to prediction accuracy of each additional variable, one can compromise accuracy for simplicity. In this vertical model, it was decided to retain the first three variables in the predictive equation. At that point, 59% of the variance is predicted.

However, the second variable, $(SF - 7)^2$, is one that represents only the general shape of the threshold function. There is suspicion that this variable, centered at one spatial frequency as it is, may be excessively peculiar to this experimental situation. Further, a review of the *F*-ratios of other variables at the first step shows several variables having *F*-ratios clustered with $(SF - 7)^2$. Two of these were $(SF - 9)^2$ and the modulation detectability threshold function from DePalma and Lowry (1962) at the 89 cm viewing distance. Of the clustered variables, the DePalma and Lowry function has the most generality. Therefore, the decision was made to force the DEPALM variable into the equation.

The result, summarized for the first three variables in table 5, demonstrated a quirk of the step-wise regression. The procedure's consideration of one variable at a time often ignores the advantages of some combinations. In

Table 5. Summary of Results from Step-Wise Regression on Modulation Thresholds for Vertical Gratings with DEPALM Forced.

Step	R	R^2	ΔR	Variable Entered	Equation: Modulation x 10^3 =
1	.7045	.4963	.4963	CUMNP	= 11.0 + .000177 CUMNP
2	.7453	.5555	.0592	DEPALM	= 8.24 + .000156 CUMNP + 521 DEPALM
3	.7665	.5875	.0321	NPSFT	= 6.21 + .000124 CUMNP + 698 DEPALM + .000489 NPSFT

Asymptotes: R = .8172

R^2 = .6678

Steps to End: 43

Number of Variables Entered at End: 25

Total Degrees of Freedom: 7000

this case, the entrance at the second step of a less-than-optimum variable led to an overall improved R^2 after the third step.

Horizontal Model

The results of the freely running regression for horizontal targets shown in table 6 are similar to those for the vertical. In both cases, the first variable admitted is one that, to some degree, represents the increased sensitivity to noise at higher spatial frequencies. The second horizontal variable deals with raster effects and is not unexpected. $(SF - 9)^2$, the third variable, represents the general threshold function shape, as did the second variable in the vertical results.

That NASF, the product of the noise amplitude and grating spatial frequency, and CUMNP, the cumulative noise power, predict essentially the same variance is indicated by the facts that their correlation coefficient is 0.943 and the *F*-ratio to remove for NASF drops from about 4600 in the first three steps to 20 at the fourth step entrance of CUMNP to the equation. Since CUMNP seems to be the stronger variable, it is reasonable to force it into the equation, as was done in the vertical model. However, the correlation between $(SF - 9)^2$ and DEPALM is sufficiently low to make the forcing of DEPALM unwarranted.

Table 7 shows that the predicted variance, with CUMNP forced, at the end of the third step, 54.95%, is 2.5% greater than the predicted variance at the third step in the free choice results in table 6.

Table 6. Summary of Results from Step-Wise Regression on Modulation Thresholds for Horizontal Gratings.

Step	R	R^2	ΔR^2	Variable Entered	Equation: Modulation x 10^3 =
1	.5893	.3473	.3473	NASF	= 14.0 + .0801 NASF
2	.6907	.4771	.1298	ORSF	= .826 + .0846 NASF + 555 ORSF
3	.7244	.5247	.0477	$(SF-9)^2$	= -3.24 + .0822 NASF + 614 ORSF + .0901 $(SF-9)^2$
4	.7423	.5509	.0262	CUMNP	= -5.37 + .0164 NASF + 689 ORSF + .104 $(SF-9)^2$ + .000130 CUMNP
5	.7478	.5593	.0083	LFINT	= -6.42 + .0200 NASF + 707 ORSF + .103 $(SF-9)^2$ + .000104 CUMNP + .000168 LFINT
6	.7618	.5803	.0210	NPSFT	= -6.05 + .0176 NASF + 726 ORSF + .0883 $(SF-9)^2$ + .000117 CUMNP + .000327 LFINT - .000406 NPSFT

Asymptotes: R = .8144

R^2 = .6632

Steps to End: 40

Number of Variables Entered at End: 26

Total Degrees of Freedom: 6160

Table 7. Summary of Results from Step-Wise Regression on Modulation Thresholds for Horizontal Gratings with CUMNP Forced.

Step	R	R^2	ΔR^2	Variable Entered	Equation: Modulation x 10^3 =
1	.5628	.3167	.3167	CUMNP	= 14.5 + .000142 CUMNP
2	.6941	.4818	.1651	ORSF	= -.708 + .000160 CUMNP + 632 ORSF
3	.7413	.5495	.0677	$(SF-9)^2$	= -5.73 + .000159 CUMNP + 705 ORST + .107 $(SF-9)^2$

Asymptotes: R = .8143

R^2 = .6632

Steps to End: 38

Number of Variables Entered at End: 26

Total Degrees of Freedom: 6160

SECTION IV

DISCUSSION

it is obvious from an inspection of figures 15-34, the plots of mean modulation detectability thresholds, noise power curves, and the DePalma and Lowry (1962) threshold, that even at zero noise, the line-scan threshold functions found here are greater than the flat-field, non-raster threshold. The line-scan thresholds are greater than the DePalma and Lowry function by a factor of 2 or 3 for 1225V to greater than 10 for 525H. The single surprising outcome in this is that a raster effect was not very significant in the vertical equation. In the step-wise regression for vertical gratings without any forced variables, the raster variable ORSF entered sixth, adding just 0.41% to the predicted variance. With some variables forced into the equation, the first raster variable to enter was RASMOD, at step 10, with an R^2 increase of only 0.0081.

There are several studies that have investigated the relationship between detectability thresholds and noise amplitude or between detectability threshold and noise passband. Rosell and Willson (1973) investigated the effect on threshold signal-to-noise ratio at the display (SNR_D) of noise amplitude, but their strictly electrical measurements are very much equipment dependent and not comparable.

Rosell (1975)[1] recommends work by Mertz (1950) and Coltman and Anderson (1960). These papers both assert that noise effects are dependent on the noise power per unit bandwidth. Neither paper systematically evaluated this conclusion as

---

[1]Rosell, F. A. Personal telecommunication to H. L. Snyder (1975).

a prediction for modulation thresholds at specific spatial frequencies. Coltman and Anderson clearly stated that their research was not well controlled and not meant to be definitive. The very general statement that a threshold signal-to-noise ratio is dependent on noise power per unit bandwidth could possible be supported by this present research. However, a step-wise regression computed early in the model development included a variable defined to be the mean cumulative noise power for a particular target spatial frequency. This variable never entered significantly into the prediction equations, a result which tends to contradict the Mertz (1950) and Coltman and Anderson (1960) views.

Barstow and Christopher (1962), Eckhardt (1969), and Snyder, *et al.* (1974) studied aspects of noise passband effects. Although none of these papers analyzed the influence of noise spectrum shape on visibility of specific spatial frequencies, all concluded that low-frequency noise was more detrimental than high-frequency noise. The importance of the cumulative noise power variable in both the vertical and horizontal models substantiates this general conclusion.

SECTION V

CONCLUSIONS AND RECOMMENDATIONS

Two models have been empirically developed which predict the modulation detectability threshold functions for vertical and horizontal gratings displayed perpendicular and parallel, respectively, to the raster of a line scan display. The two equations,

$$m_V(\nu) = (6.21 + .000124\ \text{CUMNP} + 698\ \text{DEPALM} + .000489\ \text{NPSFT}) \times 10^{-3}, \text{ and} \quad (20)$$

$$m_H(\nu) = (-5.73 + .000159\ \text{CUMNP} + 705\ \text{ORSF} + .107\ (\text{SF}-9)^2) \times 10^{-3}, \quad (21)$$

have correlation coefficients of .77 and .74, respectively, with the experimentally determined threshold data. These coefficients measure the correlation of the models with the experimental data, which were data that included replications both within and between subjects. As the models make no attempt to predict either specific subject bias or effect, or replication effects within subjects, these correlations may be conservative estimates of the correlations of the models with population means.

These models predict the modulation detectability function for medium- and high-resolution line-scan displays and thus permit the application of MTFA to these systems as an image quality measure early in the system development. Limitations of the models are that they should be applied to systems having characteristics within the range of the systems simulated in this experiment: line rate greater than 500, frame rate of 30 per second, noise levels less

than 20 mV rms, and a display luminance of 31.2 to 62.3 cd/m^2 viewed in a darkened environment.

The vertical and horizontal models developed in this research meet most of the assigned objectives, and permit further evaluation of the spatial frequency analysis of line-scan image quality outlined by Snyder, *et al.* (1974).

Further research should be undertaken to develop a photometric procedure for measuring noise spectra as displayed on line-scan monitors. This would not only greatly enhance the generalizability of results such as those obtained here but would permit the evaluation of the displayed threshold signal-to-noise ratio as a useful image quality parameter.

Because line-scan displays are only occasionally installed in dark environments, a thorough, but not necessarily factorial, study should be made of display surround luminance influences.

The greatest need found in the course of this research, other than for reliable experimental and measurement equipment, was for a comprehensive base of data on modulation detectability thresholds for sinusoidal gratings displayed on a flat field. Such data would have been a firm basis for comparison with raster and noise affected thresholds.

Brown and Mueller (1965, p. 238) plot the results of four studies using sinusoidal gratings (figure 55). The functions are so disparate as to make the whole, or any part, nearly useless. Clearly, a factorial investigation of modulation detectability functions for sinusoidal gratings dependent on mean

luminance, grating spatial frequency, grating orientation, and viewing distance, conducted with appreciation for psychophysical and inferential statistics principles, would be a great service to all doing vision-connected research and engineering.

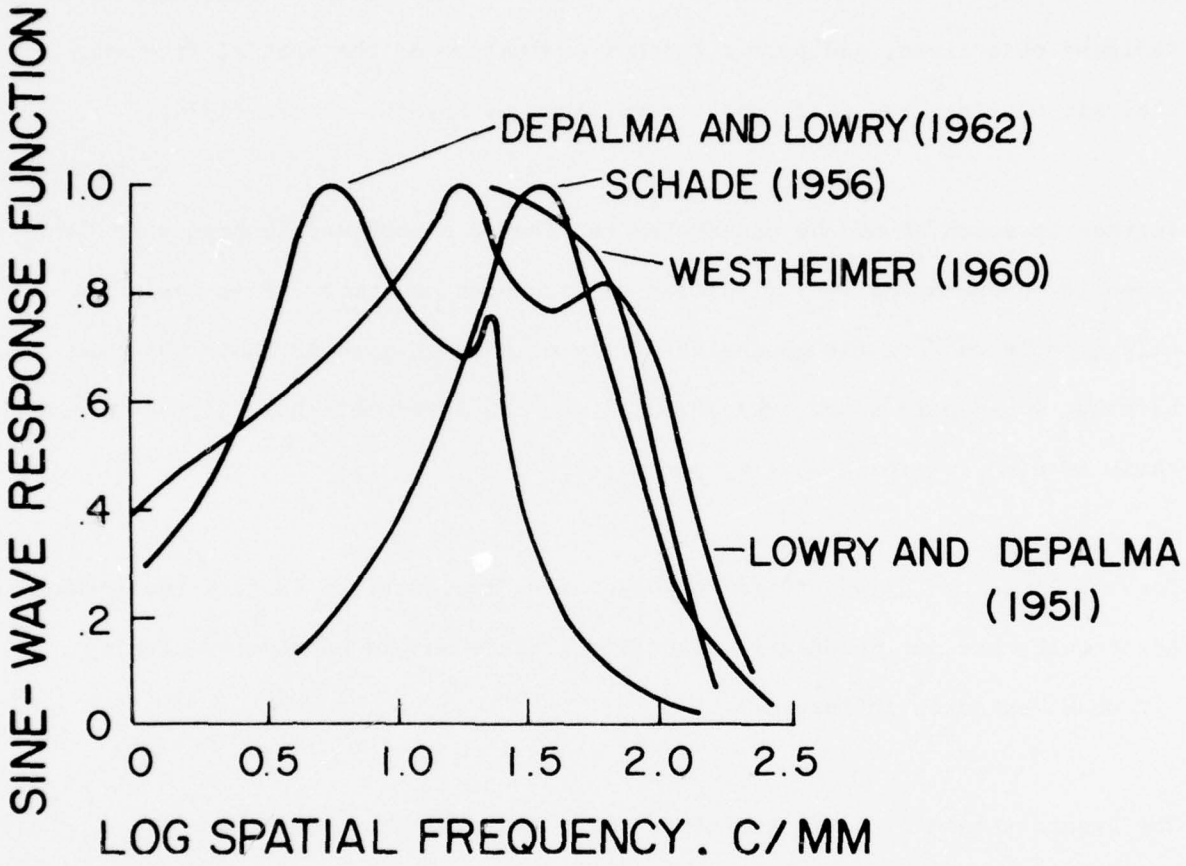

Figure 55. Results of Several Studies Undertaken to Determine the Human Visual Sine-Wave Response Function, after Brown and Mueller (1969).

APPENDIX A. EQUIPMENT DESCRIPTIONS

Digital Counter: John Fluke Mfg. Co., Ltd., Scarborough, Ontario, Canada. Model 1941A.

Digital Voltmeter: Heath Company, Benton Harbor, Michigan. Model IM-102.

Filters: Hope Electronics, Clifton, New Jersey. Various custom specified high and low pass RF filters.

Image Generator: Designed and constructed in the Human Factors Laboratory, Department of Industrial Engineering and Operations Research, Virginia Polytechnic Institute and State University, Blacksburg, Virginia.

Mixer: Designed and constructed in the Human Factors Laboratory, IEOR Dept., VPI & SU .

Monitor: Conrac Corporation, Covina, California. Model RQA-17.

Noise Generator: General Radio Company, West Concord, Massachusetts. Model 1383.

Photometer and Accessory Equipment: Gamma Scientific, Incorporated, San Diego, California. Photometer, Model 2400. Photomultiplier, Model 2400-1A. Scanning Micrometer Eyepiece, Model 700-10-65. Calibration Source, Model 220, and Luminance Head, Model 220-1.

Sine-Wave Generator: Wavetek, San Diego, California. Model 164.

True RMS Voltmeter: Ballantine Laboratories, Inc., Boonton, New Jersey. Model 323-01.

X-Y Plotter: Hewlett-Packard Company, San Diego, California. Model 7004B.

APPENDIX B. NOISE FILTER PASSBANDS

Figures on the following pages show the noise filter passband shapes for the filters used in this experiment.

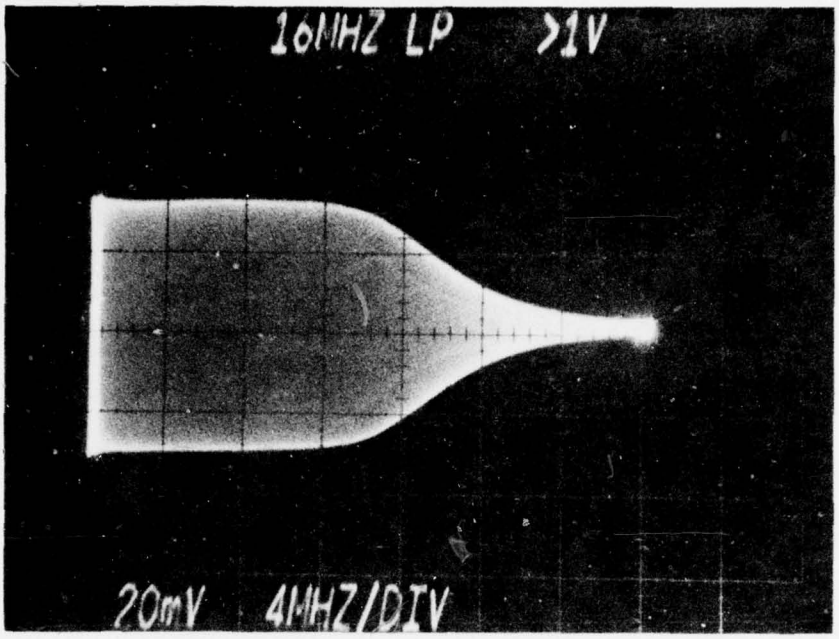

Figure B-1. Oscilloscope Image of Sweep Generator Output for 16 MHz Low Pass Filter. Vertical Scale: 20 mV/Major Division. Horizontal: 4 MHz/Major Division.

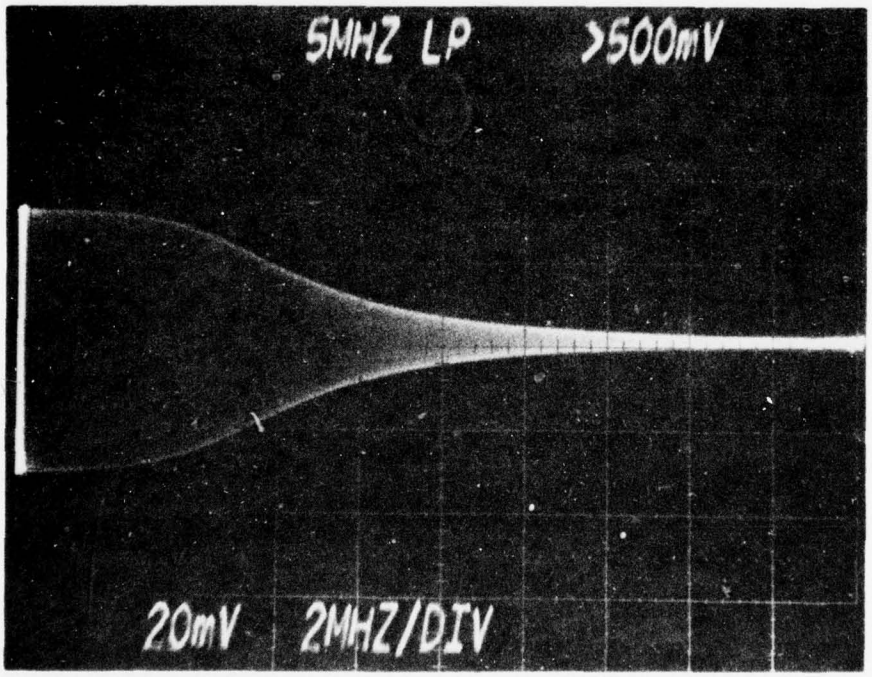

Figure B-2. Oscilloscope Image of Sweep Generator Output for 5 MHz Low Pass Filter. Vertical Scale: 20 mV/Major Division. Horizontal: 2 MHz/Major Division.

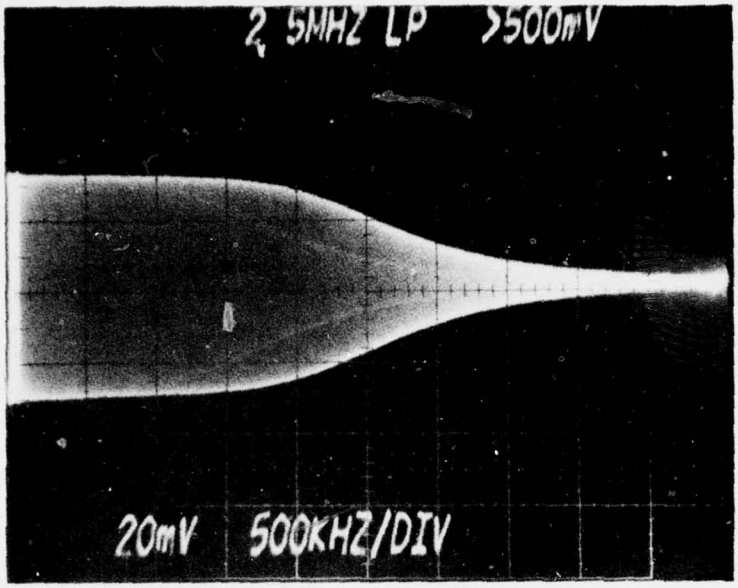

Figure B-3. Oscilloscope Image of Sweep Generator Output for 2.5 MHz Low Pass Filter. Vertical Scale: 20 mV/Major Division. Horizontal: 500 KHz/Major Division.

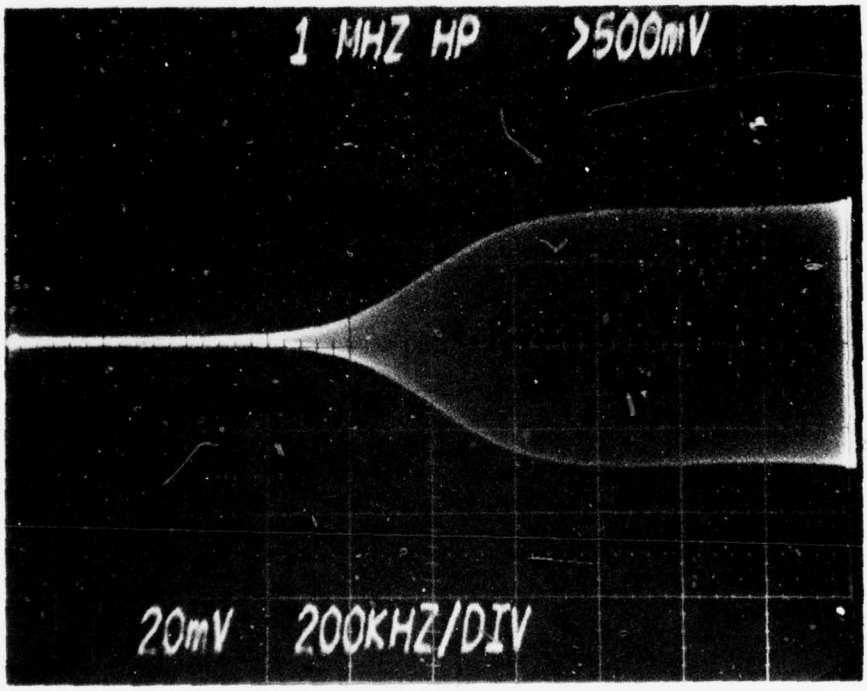

Figure B-4. Oscilloscope Image of Sweep Generator Output for 1.0 MHz High Pass Filter. Vertical Scale: 20 mV/Major Division. Horizontal: 200 KHz/Major Division.

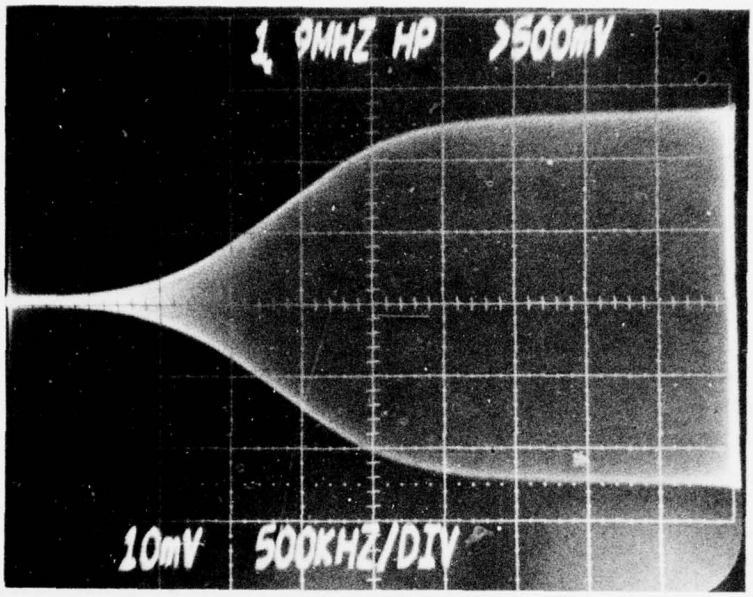

Figure B-5. Oscilloscope Image of Sweep Generator Output for 1.9 MHz High Pass Filter. Vertical Scale: 10 mV/Major Division. Horizontal: 500 KHz/Major Division.

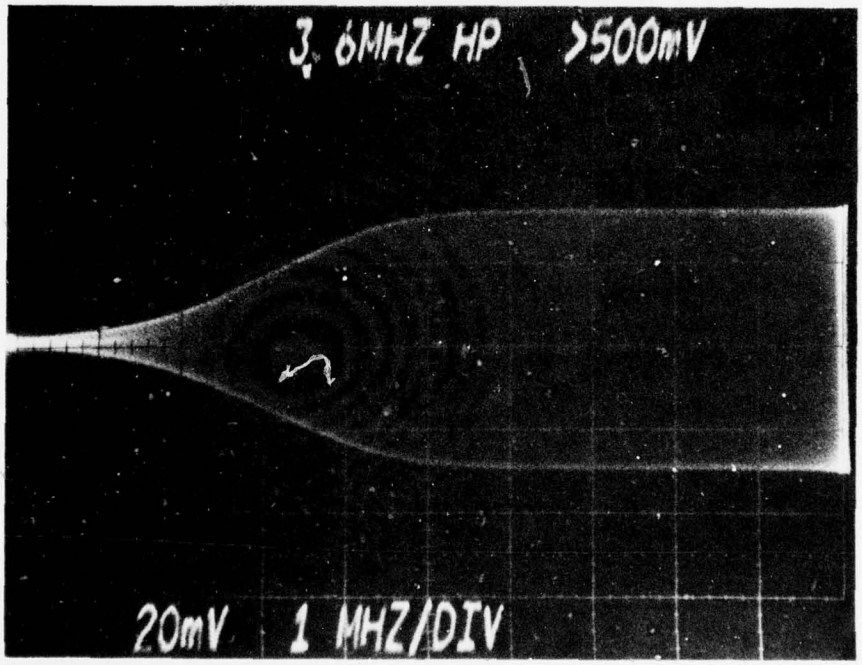

Figure B-6. Oscilloscope Image of Sweep Generator Output for 3.6 MHz High Pass Filter. Vertical Scale: 20 mV/Major Division. Horizontal: 1 MHz/Major Division.

APPENDIX C. TABULATION OF THE MODULATION DETECTABILITY THRESHOLD MEANS.

Means across subjects and replications are given in the following tables.

Table C-1. Summary Table of Mean Modulation Detectability Thresholds for 1225 Line Rate, 0-20 Noise Passband, Vertical.

Noise Amplitude, mV rms		0.0	2.3	4.2	10.9	22.5
Tgt No	Spatial Freq., c/deg					
1	1.00	0.01810	0.01805	0.01830	0.01996	0.02379
2	1.99	0.01767	0.01877	0.01814	0.02036	0.02482
3	3.01	0.00707	0.00722	0.00731	0.00852	0.01145
4	3.99	0.00749	0.00787	0.00793	0.00895	0.01364
5	5.00	0.00465	0.00480	0.00492	0.00613	0.01069
6	6.91	0.00650	0.00691	0.00666	0.00897	0.01626
7	9.05	0.00848	0.00803	0.00878	0.00979	0.01587
8	11.96	0.00863	0.00945	0.01118	0.01399	0.02471
9	14.94	0.01441	0.01459	0.01633	0.01946	0.03171
10	19.08	0.02664	0.02605	0.02671	0.02944	0.04170

Table C-2. Summary Table of Mean Modulation Detectability Thresholds for 1225 Line Rate, 0-5 Noise Passband, Vertical.

Noise Amplitude, mV rms		0.0	1.0	2.0	5.0	10.0
Tgt No	Spatial Freq., c/deg					
1	1.00	0.01842	0.01817	0.02091	0.02028	0.02344
2	1.99	0.01857	0.01706	0.01814	0.02121	0.02478
3	3.01	0.00726	0.00737	0.00772	0.00867	0.01154
4	3.99	0.00798	0.00775	0.00825	0.00911	0.01272
5	5.00	0.00483	0.00490	0.00542	0.00568	0.00867
6	6.91	0.00597	0.00661	0.00699	0.00805	0.01167
7	9.05	0.00859	0.00782	0.00895	0.00953	0.01272
8	11.96	0.00938	0.00832	0.00977	0.01118	0.01888
9	14.94	0.01694	0.01416	0.01456	0.01838	0.02495
10	19.08	0.02280	0.02821	0.02738	0.02803	0.03428

Table C-3. Summary Table of Mean Modulation Detectability Thresholds for 1225 Line Rate, 1.9-5 Noise Passband, Vertical.

Noise Amplitude, mV rms		0.0	2.0	4.0	8.0	15.0
Tgt No	Spatial Freq., c/deg					
1	1.00	0.01868	0.01903	0.01955	0.02053	0.02456
2	1.99	0.01953	0.01897	0.01899	0.02235	0.02613
3	3.01	0.00755	0.00726	0.00774	0.00943	0.01274
4	3.99	0.00745	0.00793	0.00865	0.01158	0.01896
5	5.00	0.00490	0.00495	0.00592	0.00854	0.01809
6	6.91	0.00603	0.00686	0.00832	0.01246	0.01891
7	9.05	0.00827	0.00885	0.00993	0.01166	0.01532
8	11.96	0.00932	0.00951	0.01115	0.01669	0.02215
9	14.94	0.01632	0.01704	0.01846	0.02419	0.03146
10	19.08	0.02768	0.02616	0.03044	0.03173	0.03844

AD-A035 735 VIRGINIA POLYTECHNIC INST AND STATE UNIV BLACKSBURG --ETC F/G 6/16
PREDICTION OF MODULATION DETECTABILITY THRESHOLDS FOR LINE-SCAN--ETC(U)
DEC 76 R L KEESEE F33615-71-C-1739

UNCLASSIFIED AMRL-TR-76-38 NL

2 OF 2
AD-A
035 735

END
DATE
FILMED
3-25-77
NTIS

Table C-4. Summary Table of Mean Modulation Detectability Thresholds for 945 Line Rate, 0-16 Noise Passband, Vertical.

Noise Amplitude, mV rms		0.0	1.8	3.4	8.9	18.3
Tgt No	Spatial Freq., c/deg					
1	1.00	0.00750	0.00796	0.00795	0.00861	0.01069
2	1.99	0.00731	0.00699	0.00737	0.00776	0.01041
3	3.01	0.00738	0.00743	0.00772	0.00797	0.01137
4	3.99	0.00607	0.00629	0.00622	0.00744	0.01077
5	5.00	0.00658	0.00652	0.00670	0.00859	0.01721
6	6.74	0.00929	0.00968	0.00977	0.01225	0.01926
7	8.96	0.01072	0.01117	0.01215	0.01614	0.02582
8	11.45	0.01254	0.01231	0.01447	0.01692	0.02834
9	14.94	0.01526	0.01607	0.01530	0.02009	0.02901
10	18.10	0.02354	0.02284	0.02336	0.02984	0.04069

Table C-5. Summary Table of Mean Modulation Detectability Thresholds for 945 Line Rate, 1.9-5 Noise Passband, Vertical.

Noise Amplitude, mV rms		0.0	3.5	8.5	16.0	40.0
Tgt No	Spatial Freq., c/deg					
1	1.00	0.00846	0.00833	0.00871	0.01085	0.01913
2	1.99	0.00786	0.00815	0.00995	0.01627	0.02680
3	3.01	0.00811	0.00815	0.01036	0.01334	0.02691
4	3.99	0.00682	0.00683	0.01148	0.01820	0.03666
5	5.00	0.00714	0.00742	0.01782	0.02757	0.04909
6	6.74	0.01051	0.01306	0.02155	0.03206	0.05611
7	8.96	0.01285	0.01819	0.02602	0.03363	0.06804
8	11.45	0.01628	0.01812	0.02797	0.03381	0.07445
9	14.94	0.01836	0.01828	0.02718	0.03198	0.05829
10	18.10	0.02644	0.02825	0.03274	0.03901	0.06699

Table C-6. Summary Table of Mean Modulation Detectability Thresholds for 945 Line Rate, 3.6-5 Noise Passband, Vertical.

Noise Amplitude, mV rms		0.0	2.7	6.8	12.7	33.3
Tgt No	Spatial Freq., c/deg					
1	1.00	0.00839	0.00751	0.00822	0.00792	0.01111
2	1.99	0.00728	0.00743	0.00792	0.00796	0.01249
3	3.01	0.00744	0.00787	0.00849	0.00978	0.01720
4	3.99	0.00642	0.00660	0.00780	0.01235	0.02525
5	5.00	0.00693	0.00734	0.01066	0.01995	0.03932
6	6.74	0.01088	0.01078	0.01706	0.02935	0.04585
7	8.96	0.01381	0.01494	0.02214	0.03437	0.06229
8	11.45	0.01525	0.01654	0.02381	0.03594	0.06877
9	14.94	0.01518	0.01896	0.02479	0.03371	0.05407
10	18.10	0.02693	0.02442	0.03504	0.03830	0.05717

Table C-7. Summary Table of Mean Modulation Detectability Thresholds for 525 Line Rate, 0-16 Noise Passband, Vertical.

Noise Amplitude, mV rms		0.0	5.0	10.0	20.0	30.0
Tgt No	Spatial Freq., c/deg					
1	1.00	0.01256	0.01276	0.01308	0.01396	0.01541
2	1.99	0.00908	0.00923	0.01001	0.01159	0.01343
3	3.01	0.00765	0.00792	0.00879	0.01052	0.01295
4	3.99	0.00565	0.00582	0.00698	0.01062	0.01433
5	5.00	0.00775	0.00826	0.00976	0.01464	0.02166
6	6.74	0.00496	0.00598	0.00695	0.01247	0.02236
7	8.96	0.00812	0.00786	0.01024	0.01829	0.02646
8	11.96	0.01455	0.01343	0.01859	0.02727	0.03624
9	14.48	0.01943	0.02176	0.02145	0.03442	0.04285
10	20.12	0.02139	0.02479	0.02420	0.03184	0.03916

Table C-8. Summary Table of Mean Modulation Detectability Thresholds for 525 Line Rate, 0-5 Noise Passband, Vertical.

Noise Amplitude, mV rms		0.0	2.0	4.0	10.0	20.0
Tgt No	Spatial Freq., c/deg					
1	1.00	0.01315	0.01291	0.01386	0.01471	0.01722
2	1.99	0.00931	0.00910	0.00984	0.01152	0.01427
3	3.01	0.00786	0.00788	0.00833	0.01036	0.01528
4	3.99	0.00587	0.00588	0.00670	0.01021	0.01941
5	5.00	0.00806	0.00792	0.00925	0.01426	0.02435
6	6.74	0.00527	0.00555	0.00651	0.01295	0.02779
7	8.96	0.00691	0.00799	0.01101	0.01657	0.02776
8	11.96	0.01620	0.01290	0.01805	0.02581	0.03874
9	14.48	0.02216	0.02155	0.02134	0.03619	0.04711
10	20.12	0.02310	0.02243	0.02681	0.02995	0.04174

Table C-9. Summary Table of Mean Modulation Detectability Thresholds for 525 Line Rate, 1.0-2.5 Noise Passband, Vertical.

Noise Amplitude, mV rms		0.0	1.0	2.4	7.4	15.3
Tgt No	Spatial Freq., c/deg					
1	1.00	0.01264	0.01218	0.01214	0.01384	0.01626
2	1.99	0.00911	0.00895	0.00950	0.01233	0.01488
3	3.01	0.00770	0.00793	0.00838	0.01133	0.02014
4	3.99	0.00573	0.00603	0.00686	0.01695	0.02698
5	5.00	0.00782	0.00804	0.00977	0.02109	0.03466
6	6.74	0.00502	0.00545	0.00801	0.01975	0.04016
7	8.96	0.00681	0.00914	0.01119	0.02297	0.03849
8	11.96	0.01575	0.01235	0.01537	0.02597	0.04771
9	14.48	0.01989	0.01762	0.02394	0.02517	0.04399
10	20.12	0.02356	0.02032	0.02729	0.02694	0.03195

Table C-10. Summary Table of Mean Modulation Detectability Thresholds for 525 Line Rate, 1.9-5 Noise Passband, Vertical.

Noise Amplitude, mV rms		0.0	2.0	4.0	8.0	15.0
Tgt No	Spatial Freq., c/deg					
1	1.00	0.01251	0.01197	0.01187	0.01156	0.01206
2	1.99	0.00880	0.00805	0.00852	0.00873	0.00950
3	3.01	0.00722	0.00736	0.00742	0.00774	0.00921
4	3.99	0.00540	0.00550	0.00571	0.00655	0.00988
5	5.00	0.00725	0.00759	0.00818	0.01049	0.01677
6	6.74	0.01556	0.00485	0.00586	0.01335	0.02459
7	8.96	0.00723	0.00695	0.00990	0.01644	0.03013
8	11.96	0.01332	0.01391	0.01713	0.02513	0.04116
9	14.48	0.01974	0.02060	0.02647	0.03184	0.04266
10	20.12	0.02389	0.02541	0.02667	0.03336	0.03720

Table C-11. Summary Table of Mean Modulation Detectability Thresholds for 1225 Line Rate, 0-20 Noise Passband, Horizontal.

Noise Amplitude, mV rms		0.0	2.3	4.2	10.9	22.5
Tgt No	Spatial Freq., c/deg					
1	1.00	0.01069	0.01062	0.00978	0.01006	0.01308
2	1.99	0.01043	0.01038	0.00967	0.01125	0.01306
3	3.01	0.01036	0.00996	0.01025	0.01165	0.01439
4	3.99	0.01045	0.01017	0.01072	0.01234	0.01822
5	5.00	0.00943	0.00947	0.00924	0.01148	0.01518
6	6.91	0.00842	0.00890	0.00921	0.01066	0.01777
7	8.96	0.00774	0.00782	0.00669	0.01085	0.01737
8	11.96	0.01010	0.01195	0.01239	0.01643	0.03164
9	14.34	0.01884	0.01757	0.02081	0.02612	0.04093
10	17.92	0.02440	0.02762	0.02408	0.03241	0.04887

Table C-12. Summary Table of Mean Modulation Detectability Thresholds for 1225 Line Rate, 0-5 Noise Passband, Horizontal.

Noise Amplitude, mV rms		0.0	1.0	2.0	5.0	10.0
Tgt No	Spatial Freq., c/deg					
1	1.00	0.01088	0.01039	0.01040	0.01126	0.01419
2	1.99	0.01029	0.01005	0.01014	0.01090	0.01334
3	3.01	0.00994	0.00987	0.01023	0.01184	0.01533
4	3.99	0.01095	0.01060	0.01097	0.01207	0.01791
5	5.00	0.00951	0.00947	0.00902	0.01142	0.01789
6	6.91	0.00868	0.00831	0.00944	0.01079	0.01821
7	8.96	0.00762	0.00765	0.00780	0.01091	0.01959
8	11.96	0.01037	0.01217	0.01173	0.01552	0.02937
9	14.34	0.02086	0.01893	0.02157	0.02514	0.04143
10	17.92	0.02759	0.02519	0.02692	0.02995	0.04391

Table C-13. Summary Table of Mean Modulation Detectability Thresholds for 1225 Line Rate, 1.9-5 Noise Passband, Horizontal.

Noise Amplitude, mV rms		0.0	2.0	4.0	8.0	15.0
Tgt No	Spatial Freq., c/deg					
1	1.00	0.01074	0.01056	0.01056	0.01081	0.01154
2	1.99	0.01007	0.00963	0.01009	0.01084	0.01200
3	3.01	0.00996	0.01022	0.01049	0.01170	0.01367
4	3.99	0.01059	0.01049	0.01088	0.01352	0.01658
5	5.00	0.00922	0.00910	0.01002	0.01296	0.01802
6	6.91	0.00860	0.00873	0.00961	0.01357	0.02162
7	8.96	0.00695	0.00763	0.00882	0.01608	0.02847
8	11.96	0.01186	0.01219	0.01467	0.02144	0.03790
9	14.34	0.02118	0.02038	0.02062	0.03566	0.04899
10	17.92	0.02595	0.02348	0.02632	0.03809	0.05248

Table C-14. Summary Table of Mean Modulation Detectability Thresholds for 945 Line Rate, 0-16 Noise Passband, Horizontal.

Noise Amplitude, mV rms		0.0	1.8	3.4	8.9	18.3
Tgt No	Spatial Freq., c/deg					
1	1.00	0.01686	0.01626	0.01711	0.01729	0.01996
2	1.99	0.01600	0.01624	0.01575	0.01743	0.02025
3	3.01	0.01468	0.01447	0.01378	0.01583	0.01875
4	3.99	0.00646	0.00667	0.00629	0.00795	0.01051
5	5.00	0.00601	0.00584	0.00575	0.00725	0.01191
6	6.91	0.00590	0.00602	0.00605	0.00805	0.01368
7	7.17	0.00734	0.00745	0.00723	0.00870	0.01745
8	9.96	0.01125	0.01049	0.00946	0.01491	0.02676
9	13.07	0.01315	0.01465	0.01531	0.01656	0.03119
10	16.29	0.01216	0.01244	0.01430	0.01455	0.02609

Table C-15. Summary Table of Mean Modulation Detectability Thresholds for 945 Line Rate, 1.9-5 Noise Passband, Horizontal.

Noise Amplitude, mV rms		0.0	3.5	8.5	16.0	40.0
Tgt No	Spatial Freq., c/deg					
1	1.00	0.01742	0.01737	0.01750	0.01799	0.02434
2	1.99	0.01647	0.01624	0.01588	0.01730	0.02313
3	3.01	0.01497	0.01454	0.01511	0.01691	0.02267
4	3.99	0.00708	0.00691	0.00791	0.02533	0.01909
5	5.00	0.00622	0.00664	0.00809	0.01025	0.03261
6	6.91	0.00701	0.00687	0.00972	0.01387	0.03099
7	7.17	0.00870	0.00805	0.01230	0.01984	0.04867
8	9.96	0.01147	0.01033	0.01709	0.02992	0.07331
9	13.07	0.01350	0.01599	0.02635	0.03671	0.09530
10	16.29	0.01280	0.01316	0.01764	0.02479	0.08609

Table C-16. Summary Table of Mean Modulation Detectability Thresholds for 945 Line Rate, 3.6-5 Noise Passband, Horizontal.

Noise Amplitude, mV rms		0.0	2.7	6.8	12.7	33.3
Tgt No	Spatial Freq., c/deg					
1	1.00	0.01636	0.01698	0.01643	0.01736	0.02070
2	1.99	0.01563	0.01584	0.01610	0.01540	0.02044
3	3.01	0.01466	0.01441	0.01438	0.01443	0.01767
4	3.99	0.00669	0.00701	0.00657	0.00678	0.00997
5	5.00	0.00625	0.00609	0.00622	0.00699	0.01242
6	6.91	0.00571	0.00626	0.00693	0.00862	0.01772
7	7.17	0.00775	0.00689	0.00837	0.01198	0.02666
8	9.96	0.01075	0.01038	0.01164	0.01675	0.04073
9	13.07	0.01508	0.01476	0.01691	0.02384	0.06341
10	16.29	0.01429	0.01244	0.01504	0.01890	0.05168

Table C-17. Summary Table of Mean Modulation Detectability Thresholds for 525 Line Rate, 0-16 Noise Passband, Horizontal.

Noise Amplitude, mV rms		0.0	5.0	10.0	20.0	30.0
Tgt No	Spatial Freq., c/deg					
1	1.00	0.02217	0.02209	0.02358	0.02990	0.03183
2	2.02	0.02065	0.01904	0.02251	0.02668	0.02902
3	3.01	0.02335	0.02304	0.02670	0.03280	0.03759
4	3.99	0.02169	0.02189	0.02441	0.02715	0.03414
5	5.00	0.02021	0.02065	0.02287	0.02656	0.03130
6	6.91	0.02065	0.02163	0.02471	0.02701	0.03141
7	8.96	0.02252	0.02403	0.02551	0.03187	0.03516

Table C-18. Summary Table of Mean Modulation Detectability Thresholds for 525 Line Rate, 0-5 Noise Passband, Horizontal.

Noise Amplitude, mV rms		0.0	2.0	4.0	10.0	20.0
Tgt No	Spatial Freq., c/deg					
1	1.00	0.02241	0.02176	0.02319	0.02661	0.03298
2	2.02	0.02065	0.01986	0.02150	0.02530	0.03079
3	3.01	0.02464	0.02348	0.02582	0.03189	0.04749
4	3.99	0.02142	0.02207	0.02233	0.02671	0.04043
5	5.00	0.02105	0.02082	0.02583	0.02560	0.03353
6	6.91	0.02186	0.02268	0.02271	0.02725	0.03553
7	8.96	0.02281	0.02320	0.02561	0.02992	0.03900

Table C-19. Summary Table of Mean Modulation Detectability Thresholds for 525 Line Rate, 1.0-2.5 Noise Passband, Horizontal.

Noise Amplitude, mV rms		0.0	1.0	2.4	7.4	15.3
Tgt No	Spatial Freq., c/deg					
1	1.00	0.02156	0.02082	0.02056	0.02175	0.02672
2	2.02	0.02027	0.01926	0.01946	0.02099	0.02474
3	3.01	0.02402	0.02403	0.02408	0.02713	0.03121
4	3.99	0.02116	0.02134	0.02193	0.02509	0.02901
5	5.00	0.02029	0.01983	0.02079	0.02401	0.02919
6	6.91	0.02151	0.02130	0.02108	0.02657	0.03520
7	8.96	0.02235	0.02226	0.02245	0.02909	0.04085

Table C-20. Summary Table of Mean Modulation Detectability Thresholds for 525 Line Rate, 1.9-5 Noise Passband, Horizontal.

Noise Amplitude, mV rms		0.0	2.0	4.0	8.0	15.0
Tgt No	Spatial Freq., c/deg					
1	1.00	0.02026	0.02043	0.01975	0.02100	0.02216
2	2.02	0.01821	0.01804	0.01841	0.01787	0.01944
3	3.01	0.02242	0.02211	0.02193	0.02255	0.02264
4	3.99	0.02061	0.02081	0.02090	0.02128	0.02150
5	5.00	0.01947	0.01923	0.01898	0.02011	0.02051
6	6.91	0.02054	0.02086	0.02072	0.02122	0.02340
7	8.96	0.02138	0.02050	0.02118	0.02245	0.02615

APPENDIX D. TABULATION OF THE SIMPLE LINEAR REGRESSION EQUATIONS.

These tables contain the regression constants and coefficients for simple linear regression equations that predict modulation detectability thresholds as a function of the squared noise amplitude at each spatial frequency within each block of target orientation, line rate, and noise passband.

Table D-1. Summary of Simple Linear Regression Equations, Vertical Orientation, for the 1225 Line Rate, 0-20.0 Noise Passband. Intercepts and coefficients for simple regressions that predict threshold modulation as a function of the noise amplitude (in mV, rms) squared at each spatial frequency are given below.

Spatial Frequency	1000 · Modulation =	+	$(NA)^2$
1.00	18.17824	0.01129	
1.99	18.23630	0.01324	
3.01	7.21311	0.00851	
3.99	7.64527	0.01181	
5.00	4.70195	0.01185	
6.91	6.57619	0.01916	
9.05	8.25294	0.01495	
11.96	9.70031	0.03003	
14.94	14.97942	0.03333	
19.08	26.14766	0.03057	

Table D-2. Summary of Simple Linear Regression Equations, Vertical Orientation, for the 1225 Line Rate, 0-5.0 Noise Passband. Intercepts and coefficients for simple regressions that predict threshold modulation as a function of the noise amplitude (in mV, rms) squared at each spatial frequency are given below.

Spatial Frequency	1000 · Modulation =	+	$(NA)^2$
1.00	19.09456	0.04420	
1.99	18.14644	0.06940	
3.01	7.42683	0.04167	
3.99	7.91229	0.04809	
5.00	4.93872	0.03703	
6.91	6.49233	0.05250	
9.05	8.39046	0.04356	
11.96	8.92987	0.09902	
14.94	15.24588	0.09819	
19.08	25.96123	0.08376	

Table D-3. Summary of Simple Linear Regression Equations, Vertical Orientation, for the 1225 Line Rate, 1.9-5.0 Noise Passband. Intercepts and coefficients for simple regressions that predict threshold modulation as a function of the noise amplitude (in mV, rms) squared at each spatial frequency are given below.

Spatial Frequency	1000 · Modulation =	+ $(NA)^2$
1.00	18.91451	0.02517
1.99	19.23140	0.03176
3.01	7.46653	0.02393
3.99	7.80774	0.05030
5.00	4.84385	0.05883
6.91	7.13681	0.05469
9.05	8.99892	0.02920
11.96	10.29189	0.05615
14.94	17.44826	0.06545
19.08	27.91669	0.04811

Table D-4. Summary of Simple Linear Regression Equations, Vertical Orientation, for the 945 Line Rate, 0-16.0 Noise Passband. Intercepts and coefficients for simple regressions that predict threshold modulation as a function of the noise amplitude (in mV, rms) squared at each spatial frequency are given below.

Spatial Frequency	1000 · Modulation =	+ $(NA)^2$
1.00	7.79014	0.00875
1.99	7.13826	0.00966
3.01	7.36847	0.01174
3.99	6.17068	0.01385
5.00	6.36114	0.03216
6.74	9.53664	0.02929
8.96	11.44312	0.04380
11.45	12.94660	0.04625
14.94	15.66046	0.04063
18.10	23.54102	0.05261

Table D-5. Summary of Simple Linear Regression Equations, Vertical Orientation, for the 945 Line Rate, 1.9-5.0 Noise Passband. Intercepts and coefficients for simple regressions that predict threshold modulation as a function of the noise amplitude (in mV, rms) squared at each spatial frequency are given below.

Spatial Frequency	1000 · Modulation =	+	$(NA)^2$
1.00		8.49622	0.00670
1.99		9.44954	0.01122
3.01		8.95856	0.01138
3.99		9.13952	0.01767
5.00		12.57701	0.02379
6.74		16.74376	0.02555
8.96		19.76381	0.03087
11.45		20.94246	0.03397
14.94		21.75586	0.02335
18.10		29.42589	0.02386

Table D-6. Summary of Simple Linear Regression Equations, Vertical Orientation, for the 945 Line Rate, 3.6-5.0 Noise Passband. Intercepts and coefficients for simple regressions that predict threshold modulation as a function of the noise amplitude (in mV, rms) squared at each spatial frequency are given below.

Spatial Frequency	1000 · Modulation =	+	$(NA)^2$
1.00		7.86903	0.00288
1.99		7.40950	0.00457
3.01		7.92198	0.00844
3.99		7.33030	0.01645
5.00		9.52547	0.02763
6.74		15.11439	0.02897
8.96		18.80698	0.04043
11.45		20.14722	0.04500
14.94		21.39525	0.02709
18.10		29.97432	0.01800

Table D-7. Summary of Simple Linear Regression Equations, Vertical Orientation, for the 525 Line Rate, 0-16.0 Noise Passband. Intercepts and coefficients for simple regressions that predict threshold modulation as a function of the noise amplitude (in mV, rms) squared at each spatial frequency are given below.

Spatial Frequency	1000 · Modulation =	+	$(NA)^2$
1.00	12.67705	0.00307	
1.99	9.30207	0.00479	
3.01	7.92475	0.00576	
3.99	5.89331	0.00978	
5.00	8.02950	0.01539	
6.74	5.12127	0.01903	
8.96	8.17898	0.02110	
11.96	14.90120	0.02497	
14.48	20.46608	0.02637	
20.12	22.95647	0.01867	

Table D-8. Summary of Simple Linear Regression Equations, Vertical Orientation, for the 525 Line Rate, 0-5.0 Noise Passband. Intercepts and coefficients for simple regressions that predict threshold modulation as a function of the noise amplitude (in mV, rms) squared at each spatial frequency are given below.

Spatial Frequency	1000 · Modulation =	+	$(NA)^2$
1.00	13.33250	0.00999	
1.99	9.52479	0.01234	
3.01	8.02341	0.01844	
3.99	6.12498	0.03366	
5.00	8.55653	0.04050	
6.74	5.80069	0.05593	
8.96	8.97708	0.04876	
11.96	16.25336	0.05853	
14.48	22.99097	0.06423	
20.12	24.12276	0.04503	

Table D-9. Summary of Simple Linear Regression Equations, Vertical Orientation, for the 525 Line Rate, 1.0-2.5 Noise Passband. Intercepts and coefficients for simple regressions that predict threshold modulation as a function of the noise amplitude (in mV, rms) squared at each spatial frequency are given below.

Spatial Frequency	1000 · Modulation =	+	$(NA)^2$
1.00	12.41395	0.01691	
1.99	9.51119	0.02438	
3.01	8.00207	0.05233	
3.99	7.25079	0.08899	
5.00	9.64984	0.11205	
6.74	7.03737	0.14620	
8.96	10.24499	0.12645	
11.96	14.98461	0.14287	
14.48	20.10361	0.10181	
20.12	23.89742	0.03575	

Table D-10. Summary of Simple Linear Regression Equations, Vertical Orientation, for the 525 Line Rate, 1.9-5.0 Noise Passband. Intercepts and coefficients for simple regressions that predict threshold modulation as a function of the noise amplitude (in mV, rms) squared at each spatial frequency are given below.

Spatial Frequency	1000 · Modulation =	+	$(NA)^2$
1.00	12.02147	- 0.00040	
1.99	8.42687	0.00474	
3.01	7.25698	0.00861	
3.99	5.38215	0.01985	
5.00	7.47696	0.04176	
6.74	8.48462	0.07054	
8.96	7.84370	0.10172	
11.96	14.62361	0.12147	
14.48	22.39104	0.09496	
20.12	25.36879	0.05753	

Table D-11. Summary of Simple Linear Regression Equations, Horizontal Orientation, for the 1225 Line Rate, 0-20.0 Noise Passband. Intercepts and coefficients for simple regressions that predict threshold modulation as a function of the noise amplitude (in mV, rms) squared at each spatial frequency are given below.

Spatial Frequency	1000 · Modulation =	+ $(NA)^2$
1.00	10.13981	0.00546
1.99	10.21621	0.00573
3.01	10.23517	0.00838
3.99	10.36119	0.01558
5.00	9.46223	0.01157
6.91	8.66772	0.01794
8.96	7.52498	0.01983
11.96	11.26072	0.04047
14.34	19.17844	0.04379
17.92	25.39499	0.04694

Table D-12. Summary of Simple Linear Regression Equations, Horizontal Orientation, for the 1225 Line Rate, 0-5.0 Noise Passband. Intercepts and coefficients for simple regressions that predict threshold modulation as a function of the noise amplitude (in mV, rms) squared at each spatial frequency are given below.

Spatial Frequency	1000 · Modulation =	+ $(NA)^2$
1.00	10.46382	0.03682
1.99	10.10657	0.03229
3.01	10.03571	0.05406
3.99	10.63157	0.07191
5.00	9.20818	0.08676
6.91	8.59799	0.09575
8.96	7.57150	0.12087
11.96	11.08576	0.18263
14.34	20.03441	0.21353
17.92	26.12926	0.17630

Table D-13. Summary of Simple Linear Regression Equations, Horizontal Orientation, for the 1225 Line Rate, 1.9-5.0 Noise Passband. Intercepts and coefficients for simple regressions that predict threshold modulation as a function of the noise amplitude (in mV, rms) squared at each spatial frequency are given below.

Spatial Frequency	1000 · Modulation =	+	$(NA)^2$
1.00		10.58728	0.00414
1.99		9.93938	0.00952
3.01		10.22663	0.01590
3.99		10.73135	0.02722
5.00		9.42809	0.03941
6.91		8.84033	0.05803
8.96		7.72465	0.09492
11.96		12.51642	0.11485
14.34		21.37595	0.12933
17.92		25.54654	0.12486

Table D-14. Summary of Simple Linear Regression Equations, Horizontal Orientation, for the 945 Line Rate, 0-16.0 Noise Passband. Intercepts and coefficients for simple regressions that predict threshold modulation as a function of the noise amplitude (in mV, rms) squared at each spatial frequency are given below.

Spatial Frequency	1000 · Modulation =	+	$(NA)^2$
1.00		16.65363	0.00981
1.99		16.03490	0.01283
3.01		14.35987	0.01334
3.99		6.53283	0.01217
5.00		5.78533	0.01827
6.91		5.94366	0.02326
7.17		7.00213	0.03068
9.96		10.34430	0.04933
13.07		13.77820	0.05120
16.29		12.47764	0.04000

Table D-15. Summary of Simple Linear Regression Equations, Horizontal Orientation, for the 945 Line Rate, 1.9-5.0 Noise Passband. Intercepts and coefficients for simple regressions that predict threshold modulation as a function of the noise amplitude (in mV, rms) squared at each spatial frequency are given below.

Spatial Frequency	1000 · Modulation =	+ $(NA)^2$
1.00	17.20508	0.00443
1.99	16.10349	0.00438
3.01	14.94097	0.00490
3.99	10.79376	0.00637
5.00	6.41472	0.01635
6.91	8.03726	0.01457
7.17	9.98803	0.02454
9.96	13.71795	0.03789
13.07	18.74672	0.04850
16.29	13.20677	0.04557

Table D-16. Summary of Simple Linear Regression Equations, Horizontal Orientation, for the 945 Line Rate, 3.6-5.0 Noise Passband. Intercepts and coefficients for simple regressions that predict threshold modulation as a function of the noise amplitude (in mV, rms) squared at each spatial frequency are given below.

Spatial Frequency	1000 · Modulation =	+ $(NA)^2$
1.00	16.57448	0.00374
1.99	15.53597	0.00433
3.01	14.32376	0.00296
3.99	6.61698	0.00297
5.00	6.08212	0.00571
6.91	6.29523	0.01040
7.17	7.77604	0.01720
9.96	10.87379	0.02710
13.07	15.25556	0.04361
16.29	13.30957	0.03460

Table D-17. Summary of Simple Linear Regression Equations, Horizontal Orientation, for the 525 Line Rate, 0-16.0 Noise Passband. Intercepts and coefficients for simple regressions that predict threshold modulation as a function of the noise amplitude (in mV, rms) squared at each spatial frequency are given below.

Spatial Frequency	1000 · Modulation =	+	$(NA)^2$
1.00	22.64609	0.01147	
2.02	20.64499	0.01030	
3.01	24.07903	0.01620	
3.99	22.02065	0.01345	
5.00	20.87433	0.01209	
6.91	21.93439	0.01104	
8.96	23.90015	0.01376	

Table D-18. Summary of Simple Linear Regression Equations, Horizontal Orientation, for the 525 Line Rate, 0-5.0 Noise Passband. Intercepts and coefficients for simple regressions that predict threshold modulation as a function of the noise amplitude (in mV, rms) squared at each spatial frequency are given below.

Spatial Frequency	1000 · Modulation =	+	$(NA)^2$
1.00	22.60724	0.02675	
2.02	20.94521	0.02572	
3.01	24.62752	0.05805	
3.99	21.70595	0.04699	
5.00	22.43256	0.02820	
6.91	22.54326	0.03329	
8.96	24.09903	0.03855	

Table D-19. Summary of Simple Linear Regression Equations, Horizontal Orientation, for the 525 Line Rate, 1.0-2.5 Noise Passband. Intercepts and coefficients for simple regressions that predict threshold modulation as a function of the noise amplitude (in mV, rms) squared at each spatial frequency are given below.

Spatial Frequency	1000 · Modulation =	+	$(NA)^2$
1.00		20.82103	0.02472
2.02		19.65337	0.02181
3.01		24.27988	0.03074
3.99		21.79358	0.03234
5.00		20.56400	0.03820
6.91		21.60201	0.05969
8.96		22.69893	0.07948

Table D-20. Summary of Simple Linear Regression Equations, Horizontal Orientation, for the 525 Line Rate, 1.9-5.0 Noise Passband. Intercepts and coefficients for simple regressions that predict threshold modulation as a function of the noise amplitude (in mV, rms) squared at each spatial frequency are given below.

Spatial Frequency	1000 · Modulation =	+	$(NA)^2$
1.00		20.15929	0.00906
2.02		18.05179	0.00559
3.01		22.19637	0.00216
3.99		20.81084	0.00340
5.00		19.30396	0.00576
6.91		20.58635	0.01231
8.96		20.88344	0.02344

APPENDIX E. LIST OF CANDIDATE VARIABLES FOR THE STEP-WISE REGRESSION

Variable	*Description*
NA	Noise amplitude in RMS millivolts measured at the output of the filters.
SF	Spatial frequency in c/deg measured with reference to the position of the subjects' eyes.
NA2	$(NA)^2$
SF2	$(SF)^2$
SF3	$(SF)^3$
NASF	$(NA)(SF)$
NA2SF	$(NA)^2(SF)$
NASF2	$(NA)(SF)^2$
NASF3	$(NA)(SF)^3$
NA2SF2	$(NA)^2(SF)^2$
ESF	e^{SF}
LOGSF	$Log_{10}(SF)$
DEPALM	Value of the modulation detectability threshold determined by DePalma and Lowry (1962) for the spatial frequency of the target grating.
LFINT	Variable representing integration of the noise power at low frequencies as described on p. 70.
CONNP	Variable representing the degree of concentration of the noise power; described on p. 70.
NPSFT	Variable representing the noise power in the spatial frequency region of the target grating; described on p. 71
CUMNP	Variable integrating noise power from zero spatial frequency to the spatial frequency of the target grating; described on p. 71.

LFINT2	LFINT computed with NA2 rather than NA.
CONNP2	CONNP computed with NA2 rather than NA.
NPSFT2	NPSFT computed with NA2 rather than NA.
CUMNP2	CUMNP computed with NA2 rather than NA.
LFINTS	$(LFINT)^2$
CONNPS	$(CONNP)^2$
NPSFTS	$(NPSFT)^2$
CUMNPS	$(CUMNP)^2$
NASF.9	$(NA)(SF)^{0.9}$
SF-9)2	$(SF-9)^2$
SF92SF	$(SF-9)^2(SF)$
SF-7)2	$(SF-7)^2$
SF02SF	$(SF-10)^2(SF)$
ORSF	The inverse of the raster spatial frequency.
RASMOD	The raster modulation divided by the raster spatial frequency.
OR-TSF	The inverse of the difference between the spatial frequency of the raster and the target grating.
MORTSF	Product of OR-TSF and the raster modulation.

REFERENCES

Barstow, J. M. and Christopher, H. N., "The Measurement of Random Video Interference to Monochrome and Color Television Pictures," *AIEE Transactions on Communications and Electronics*, 1962, *63*, 313-320.

Blakemore, C. and Campbell, F. W., "On the Existence of Neurones in the Human Visual System Selectively Sensitive to the Orientation and Size of Retinal Images," *Journal of Physiology*, 1969, *203*, 237-260.

Brown, J. L. and Mueller, C. G., "Brightness Discrimination and Brightness Contrast," In C. H. Graham (Ed.) *Vision and Visual Perception*, Wiley, New York, 1965.

Charman, W. N. and Olin, A., "Tutorial - Image Quality Criteria for Aerial Camera Systems," *Photographic Science and Engineering*, 1965, *9*, 385-397.

Coltman, J. W. and Anderson, A. E., "Noise Limitations to Resolving Power in Electronic Imaging," *Proceedings of the IRE*, 1960, 858-865.

Cornsweet, T. N., *Visual Perception*, Academic Press, New York, 1970.

DePalma J. J. and Lowry, E. M., "Sine-Wave Response of the Visual System. II. Sine-Wave and Square-Wave Contrast Sensitivity," *Journal of the Optical Society of America*, 1962, *52*, 328-335.

Dixon, W. J. (Ed.), *BMD: Biomedical Computer Programs*, University of California Press, Berkeley, 1973.

Eckhardt, B. M. H. "The Visual Discrimination of Electro-Optically Formed Images in the Presence of Noise," Unpublished doctoral dissertation, Tufts University, 1969.

General Radio Co., "Instruction Manual - Type 1383 Random-Noise Generator," West Concord, Massachusetts, February, 1969.

Keesee, R. L., "Prediction of Modulation Detectability Thresholds for Line-Scan Displays," Unpublished doctoral dissertation, Virginia Polytechnic Institute and State University, 1976.

Lowry, E. M. and DePalma, J. J., "Sine-Wave Response of the Visual System. The Mach Phenomenon," *Journal of the Optical Society of America*, 1961, *51*, 740-746.

Mertz, P., "Perception of Television Random Noise," *Society of Motion Picture and Television Engineers*, 1950, *54*, 8-34.

Rosell, F. A. and Willson, R. H., "Recent Psychophysical Experiments and the Display Signal-to-Noise Concept," In L. M. Biberman (Ed.), *Perception of Displayed Information*, Plenum Press, New York, 1973.

Schober, H. A. W. and Hilz, R., "Contrast Sensitivity of the Human Eye for Square-Wave Gratings," *Journal of the Optical Society of America*, 1965, *55*, 1086-1091.

Scott, F. and Frauenhofer, D., "The Modulation Transfer Function and Methods

of Measurement," In L. M. Biberman and S. Nudelman (Ed.) *Photoelectronic Imaging Devices*, Vol. 1. Plenum Press, New York, 1971, 291-306.

Snyder, H. L., "Image Quality and Observer Performance," In L. M. Biberman (Ed.) *Perception of Displayed Information*, Pleneum Press, New York, 1973, 87-118.

Snyder, H. L., Keesee, R. L., Beamon, W. S. and Aschenbach, J. R., *Visual Search and Image Quality*, AMRL-TR-73-114 (AD A-007375), Aerospace Medical Research Laboratories, Wright-Patterson AFB, Ohio, October 1974.

Stromeyer, C. F., III, and Julesz, B., "Critical Bands in Spatial-Frequency Masking," *Journal of the Optical Society of America*, 1972, *62*, 1221-1232.

☆ U. S. GOVERNMENT PRINTING OFFICE: 1977 — 757-001/179